

# Queue Spillover Detection at Urban Signalised Intersections using Floating Car Data

Roeland Vandenberghe

Thesis submitted for the degree of  
Master of Engineering: Logistics and  
Traffic

**Thesis supervisor:**  
Prof. dr. ir. Chris Tampère

**Assessors:**  
Prof. dr. ir. H. Bruyninckx  
Prof. dr. ir. G. De Ceuster

**Mentors:**  
Ir. I. Abuamer  
Ir. J. Devriese  
Ir. J. Landtmeters

© Copyright KU Leuven

Without written permission of the thesis supervisor and the author it is forbidden to reproduce or adapt in any form or by any means any part of this publication. Requests for obtaining the right to reproduce or utilize parts of this publication should be addressed to Centre for Industrial Management, Celestijnenlaan 300A Bus 2422, B-3001 Heverlee, +32-16-322567.

A written permission of the thesis supervisor is also required to use the methods, products, schematics and programmes described in this work for industrial or commercial use, and for submitting this publication in scientific contests.

# Preface

This thesis is the capstone project of my master's degree in Logistics and Traffic at KU Leuven. It has been a very challenging but gratifying experience to start working on a problem from scratch and see it evolve step-by-step. It has taught me many invaluable skills and insights in terms of theoretical knowledge, coding skills and developing a hands-on approach to tackle new problems.

I would like to thank everyone who contributed and helped me with completing this thesis. Especially, I am grateful to Prof. Chris Tampère for his support and his crucial insights. Furthermore, this project would not have been possible without the help and motivation of Ismail Abuamer and Joachim Landtmeters, my mentors for this thesis. Furthermore, I would express my gratitude to Be-Mobile and in particular Jan Devriese for the proposal of the project, the provision of the data, and the vital inputs in the methodology.

Lastly, I am very lucky to have amazing friends and family who were always there for me when I needed a listening ear or a break filled with laughter. I would like to especially thank my parents who helped me proofread the thesis and were able to shed a light on the topic from another perspective, and my fellow students who were always there to answer any question I had.

*Roeland Vandenberghe*

# Contents

<b>Preface</b>	i
<b>Abstract</b>	iv
<b>List of Figures and Tables</b>	v
<b>List of Abbreviations and Symbols</b>	viii
<b>1 Introduction</b>	1
1.1 Problem Description . . . . .	1
1.2 Aim of the Thesis . . . . .	3
1.3 Structure of the Thesis . . . . .	5
<b>2 Problem Analysis</b>	7
2.1 Traffic State Estimation . . . . .	7
2.2 Data Sources . . . . .	16
2.3 Data Analysis . . . . .	18
2.4 Summary . . . . .	22
<b>3 Literature Review</b>	23
3.1 Methods using Loop Detectors . . . . .	23
3.2 Methods using Floating Car Data . . . . .	25
3.3 Other Methods . . . . .	27
3.4 Summary . . . . .	27
3.5 Originality of the Proposed Method . . . . .	30
<b>4 Methodology</b>	31
4.1 Model Selection . . . . .	31
4.2 General Overview of the Model . . . . .	32
4.3 Markov Model . . . . .	34
4.4 Logistic Regression Model . . . . .	37
4.5 Evaluation of Results . . . . .	39
4.6 Summary . . . . .	40
<b>5 Model Implementation</b>	41
5.1 Case Study . . . . .	41
5.2 Implementation . . . . .	44
5.3 Results . . . . .	53
5.4 Summary . . . . .	63

<b>6 Discussion</b>	<b>65</b>
6.1 Assumptions and Limitations . . . . .	65
6.2 Application to a Real-life Setting . . . . .	70
6.3 Validity of Floating Car Data . . . . .	72
6.4 Summary . . . . .	72
<b>7 Conclusion</b>	<b>75</b>
<b>Bibliography</b>	<b>77</b>
<b>The Lighthill-Whitham-Richard Model</b>	<b>89</b>
<b>Proof of Concept</b>	<b>90</b>
Methodology . . . . .	90
Case study . . . . .	90
<b>The Coefficients of the Logistic Regression Models</b>	<b>93</b>
The Logistic Regression Model from State $U$ . . . . .	94
The Logistic Regression Model from State $O_1$ . . . . .	95
The Logistic Regression Model from State $O_2$ . . . . .	96
The Logistic Regression Model from State $O_3$ . . . . .	97
The Logistic Regression Model from State $Sp$ . . . . .	98

# Abstract

This thesis proposes a method to detect queue spillovers on urban signalised intersections. These spillovers occur when a queue on a downstream link spills back and blocks an upstream intersection, preventing vehicles from entering the intersection even though the traffic signal is green. In order to minimise the incurred delays for all travellers on the network, these blockages need to be detected and resolved as soon as possible.

Due to the increasing popularity of smartphones as a data source, new opportunities for better traffic management arise. Floating Car Data (FCD), which consists of a vehicle's location on the network, has recently attracted the attention of many researchers. However, its main limitations are that the current penetration rate is low and that the measurement of the location is unreliable. Consequently, the aim of this thesis is to assess the validity of this data source for detecting queue spillovers.

The proposed method consists of a two-stage Hidden Markov Model (HMM) where a discrete-time finite-state Markov model is complemented by a multinomial logistic regression model (MLR). This latter model estimates the transition probabilities at each time step based on observations of incoming vehicles and other circumstantial evidence. The method is compared to a MLR without the addition of the Markov model. Apart from spillover detection, both methods are capable of distinguishing between different saturation levels.

The methods are tested on a microsimulation in *VISSIM* to limit the problem's complexity. Under varying conditions, both models show clear surges in the probability of spillover during the correct cycles. In the simulated setting, the logistic regression model predicts the short-lived spillovers better, but the Hidden Markov Model is more robust and is superior when estimating the overall traffic state.

The promising results suggest that FCD can be used for spillover detection and state estimation at signalised intersections. Even without additional efforts to reach higher penetration rates, the proposed methods can contribute significantly to better traffic management systems for urban networks.

# List of Figures and Tables

## List of Figures

1.1	Illustration of a traffic spillover where the downstream link is full and the vehicles on the approaching links of the upstream intersection are blocked. Vehicle 1 represents a vehicle that does not intend to go to the blocked link but is affected by the resulting queue, whereas vehicle 2 is affected by the red vehicles that entered the intersection while they cannot leave it.	2
1.2	Overview of the four successive intersections along the N344. The red markers indicate the location and IDs of the intersections. . . . .	5
2.1	Trajectories as proposed in the microscopic approach, where the blue lines represent the location of the vehicles in space and time. . . . .	8
2.2	Pairwise relationships according to the triangular fundamental diagram, where $k$ is the density, $q$ is the flow rate and $u$ is the speed. The free-flow branch is indicated in green, whereas the congested branch is indicated in red. The states A, C, and J represent the free-flow state, the capacity state and the jammed state, respectively. . . . .	10
2.3	Example of the shockwave analysis according to the LWR-model. . . . .	11
2.4	Shockwave profile of an undersaturated intersection where every vehicle has to stop at most once. . . . .	12
2.5	Shockwave profile of an oversaturated intersection where at least one vehicle has to stop more than once. . . . .	13
2.6	Shockwave profile of the four types of spillovers where a queue spills back from the downstream intersection at $x_{TL}^{down}$ until it reaches the upstream intersection at $x_{TL}^{up}$ . . . . .	14
2.7	Representation of the intersections and the respective sensors. . . . .	19
2.8	Smooth and inaccurate observed trajectory. The horizontal axis represents the timestamp of the observed trajectories in epoch-time, while the vertical axis shows the Euclidean distance to the stop line. . . . .	20
3.1	Queue length estimation method according to Liu et al. [2009]. Note the difference in notation: the driving direction is inverted and the shockwave speeds $v_1$ , $v_2$ , $v_3$ coincide with $\omega_{AJ}$ , $w$ , and $u_f$ , respectively. . . . .	25
4.1	Schematic overview of the Hidden Markov Model. . . . .	33

## LIST OF FIGURES AND TABLES

---

5.1	Schematic representation of the network. The four intersections are indicated with their respective IDs, the red lines represent the stop line where traffic signals are present, the lane labelled <i>Researched lane</i> is examined closer for the development of the tool, while the downstream lanes of this approach are labelled DL1, DL2 and DL3. . . . .	42
5.2	Two definitions of the effective spillover duration and the definition of later starts for spillovers that end near the end of the cycle. . . . .	46
5.3	Example of a trajectory with the start shockwaves for each of its four stops. Shockwave (1) perfectly coincides with a green signal, (2) does not coincide with a green signal due to a short spillover, (3) is faster than expected and causes a negative deviation from the green signal, (4) is slower than expected and causes a positive deviation from the green signal.	50
5.4	Example of a simplified intersection, where lane 1 is a directly connected downstream lane with respect to the researched lane, and lane 2, 3 and 4 are indirectly connected downstream lanes. . . . .	52
5.5	State distribution during peak-periods in the four regimes predicted by $M_1$ with one vehicle per cycle. Each bar represents the state distribution at every time step, while the strips underneath the plot represents the ground truth for the corresponding time step. The surges in the spillover probability correctly coincide with spillover time steps. . . . .	58
5.6	State distribution during peak-periods in the four regimes predicted by $M_2$ with one vehicle per cycle. Each bar represents the state distribution at every time step, while the strip underneath the plot represents the ground truth for the corresponding time step. The surges in the spillover probability correctly coincide with spillover time steps and change more smoothly compared to $M_1$ . . . . .	59
5.7	The state distribution of the 5-hour period in medium regime by $M_2$ with one vehicle per cycle. Each bar represents the state distribution at every time step, while the strip underneath the plot represents the ground truth for the corresponding time step. The traffic state is correctly approximated for all states. . . . .	60
5.8	Comparison of the $M_1$ (orange)- and $M_2$ (blue)-model's accuracy and log loss. . . . .	61
5.9	State estimation at 5% penetration rate for $M_1$ (left) and $M_2$ (right). Each bar represents the state distribution at every time step, while the strip underneath the plot represents the ground truth for the corresponding time step. . . . .	62
1	Framework of the Proof of Concept. . . . .	91

## List of Tables

3.1	A summary of the available literature, their aim, working principle and data sources. . . . .	29
-----	---	----

---

LIST OF FIGURES AND TABLES

---

4.1	Example of the transition probability matrix with categorical covariates.	36
5.1	Classification of the states in the model, where $n$ equals the average number of stops of the vehicles during the approach to the intersection.	45
5.2	Summary of the considered covariates. . . . .	48
5.3	Resulting coefficients and odd-ratios of the logistic regression model from state $O_3$ to all other states. . . . .	56
5.4	Accuracy (A) and log loss (LL) of $M_0$ . . . . .	57
5.5	Overview of the resulting accuracy (A) and log loss (LL) of M1 and M2 for different penetration rates $\rho$ . . . . .	63
1	Confusion matrix resulting from the proof of concept. . . . .	91
2	Resulting coefficients and odd-ratios of the logistic regression model from state $U$ to all other states. . . . .	94
3	Resulting coefficients and odd-ratios of the logistic regression model from state $O_1$ to all other states. . . . .	95
4	Resulting coefficients and odd-ratios of the logistic regression model from state $O_2$ to all other states. . . . .	96
5	Resulting coefficients and odd-ratios of the logistic regression model from state $O_3$ to all other states. . . . .	97
6	Resulting coefficients and odd-ratios of the logistic regression model from state $Sp$ to all other states. . . . .	98

# List of Abbreviations and Symbols

## Abbreviations

FCD	Floating Car Data
CCS	Channelized Section Spillover
HMM	Hidden Markov Model
ITF	Intersection Topology Format
LWR	Lighthill-Whitham-Richards model
CTM	Cell Transmission Model
SPM	Shockwave Profile Model
PDF	Probability Density Function
MLR	Multinomial Logistic Regression Model
$M_0$	Null-model with constant predictions equal to the ratio of occurrences
$M_1$	Logistic regression model only
$M_2$	Hidden Markov Model with
LL	Log loss
MLE	Maximum Likelihood Estimation
A0..	Intersection name in Deventer
HDOP	Horizontal Dilution of Precision

## Symbols

### Traffic Flow Variables & Traffic States

$x$	Position	m
$t$	Variable of continuous or discrete time	s
$q$	Flow	$\frac{\text{vehicles}}{\text{h}}$
$k$	Density	$\frac{\text{vehicles}}{\text{km}}$
$u$	Speed	$\frac{\text{m}}{\text{s}}$
$o$	Relative Occupancy	-
$d$	Length of a vehicle	m
$D$	Detector length	m
$A$	State under free-flow conditions	-
$C$	State under capacity conditions	-
$J$	State under jammed conditions	-
$Q_e$	Empirical formulation of the density-flow relation in the fundamental diagram	-
$c$	Characteristic speed	$\frac{\text{m}}{\text{s}}$
$\omega_{12}$	Shockwave speed between state 1 and state 2	$\frac{\text{m}}{\text{s}}$
$w$	Shockwave speed of the congested branch of the fundamental diagram	$\frac{\text{m}}{\text{s}}$
$v_f$	Shockwave speed of the free-flow branch	$\frac{\text{m}}{\text{s}}$
$n$	Average number of stops	-
$\sigma$	Smoothing factor for shockwave covariate	-
$g$	Length of a link	-
$C_{lane}$	Score for the saturation level on the downstream link	-
$\alpha_i$	Weight for the saturation level on the downstream link for state i	-
$\gamma_{lane}$	Influence of a lane on the upstream state	-
$U$	Undersaturated state	-
$O_1$	Oversaturation level 1	-
$O_2$	Oversaturation level 2	-
$O_3$	Oversaturation level 3	-
$Sp$	Spillover	-
$\rho$	Penetration rate	%

## LIST OF ABBREVIATIONS AND SYMBOLS

---

### Methodological Symbols

$P(t)$	Transition probability matrix at time t	-
$p_{ij}$	Probability of transitioning from state i to state j	-
$p_i$	Probability of being in state i	-
$P(A B)$	Probability of A given B	-
$I$	State set	-
$L$	Total number of states	-
$K$	Total number of covariates	-
$Y_t$	Dependent state variable	-
$i, j$	States indices	-
$X$	Set of K trajectory covariates at time t	-
$Z$	Set of M circumstantial covariates	-
$\beta_{ij}^k$	Regression coefficient of the covariate k for transition from state i to j	-
$\mu_{ij}$	Intercept for the transition from state i to j	-
$S_t$	State distribution at time t	-

# Chapter 1

## Introduction

Over the last decades, delays experienced by road traffic have drastically increased, especially on urban networks. The demand has risen, while the infrastructure capacity is saturated and cannot be expanded due to densely built-up city centres. This results in congestion in areas where it is least desirable: close to where people work and live. Moreover, the vehicular traffic mixes with other road users such as public transport and cyclists, whose safety and efficiency are severely impaired when the traffic breaks down.

As improvements to the network's layout are often difficult, the solution should be sought in more effective traffic management systems. By adjusting the traffic signals at signalised intersections to match the varying requirements of urban traffic, delays and their societal impacts can be reduced. Emerging vehicle-to-infrastructure communication techniques will play a major role in this advancement. Similarly, the increasing popularity of smartphones has introduced a new data source for traffic management, namely Floating Car Data (FCD), which measures the locations of vehicles on the network. Consequently, this thesis examines the utilisation of this new data source for the detection of one of the principle causes of delays at signalised intersections: queue spillovers.

### 1.1 Problem Description

#### 1.1.1 Spillover Definition

Traffic queues form when the inflow (demand) on a link exceeds the maximally allowed outflow. In urban networks, the outflow of a link is mostly regulated by traffic signals. When these are too restrictive or the demand is too high, the tail of the queue might extend further upstream, leading to a blockage of the upstream intersection, as shown in Figure 1.1. A spillover is defined as a situation where vehicles are unable to enter the intersection even though the traffic signal is green.

Spillovers severely impact the travel time of all vehicles on the network. Obviously, those travelling towards the congested link are unable to continue their path

## 1. INTRODUCTION

---

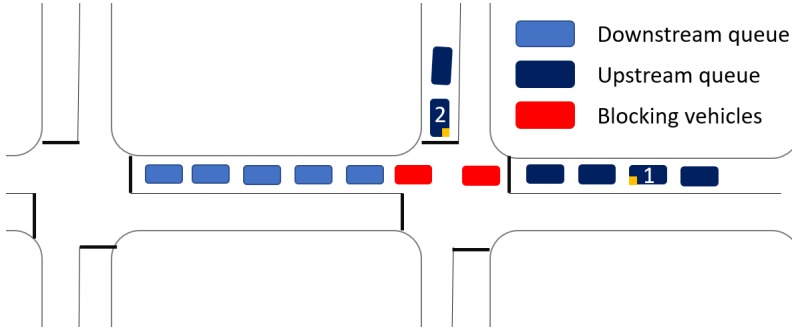


Figure 1.1: Illustration of a traffic spillover where the downstream link is full and the vehicles on the approaching links of the upstream intersection are blocked. Vehicle 1 represents a vehicle that does not intend to go to the blocked link but is affected by the resulting queue, whereas vehicle 2 is affected by the red vehicles that entered the intersection while they cannot leave it.

since the downstream link is full. This results in queues on the upstream links that influence vehicles regardless of their intended destination, as illustrated by vehicle 1 in Figure 1.1. Even worse delays are incurred when drivers disregard the traffic regulations and enter the intersection even though they cannot evacuate it, blocking the outflow of other directions (approaches) onto the intersection, as illustrated by vehicle 2 in Figure 1.1. Consequently, additional queues spill back on all approaches to the intersection, which is detrimental to the performance of the network. In the worst case, spillovers result in a network-wide gridlock that takes hours to clear.

### 1.1.2 Importance of Spillover Detection

It is crucial to detect spillovers, find out why they occurred and determine how they can be prevented. They result in major delays on urban networks and cause important externalities to other stakeholders, such as local residents and public transport operators. A study by [Skabardonis and Geroliminis \[2008\]](#) found that the travel time on short links between signalised intersections during spillovers can double compared to the travel time in free flow. Consequently, spillovers should be detected as soon as possible in order to adapt the control strategy swiftly and avoid delays.

Both in offline and online settings, spillover detection plays a pivotal role. In online settings, its main purpose is the adequate adaptation of the control strategy for the traffic signals. These are nowadays mostly regulated by an optimisation algorithm that minimises the total delay for the arriving traffic on all approaches to the intersection [\[Xu et al., 2019\]](#). When a spillover is identified, the control strategy needs to be modified: shorter green times at the upstream intersection ease the inflow into the congested downstream link, while longer green times at the downstream intersection dissolve the queue as soon as possible. Furthermore, the control system

needs to trade off the aforementioned strategy with the delays incurred by other drivers on the network. An additional purpose of spillover detection is the rerouting of vehicles in order to reduce the inflow of the congested links. This is made possible by the recent developments in vehicle-to-infrastructure communication technologies.

In offline settings, spillover detection is used as a performance measure to decide on the optimal control strategies and the most impactful infrastructure improvements. In the Netherlands, this data-driven evaluation of signalised intersections has been common practice for over 30 years with the development of applications such as *Kwaliteitscentrale* and more advanced applications recently [van der Brugt, 2000].

### 1.1.3 Current Practice

Current methods for spillover detection primarily use measurements from inductive loop detectors as their main input. These are presence detectors installed under the road pavement, making them costly and impractical in regions where they do not cover the network sufficiently. Therefore, FCD is proposed as a possible replacement for loop detectors. This data source collects the GPS-trajectories of some vehicles on the network, referred to as probe vehicles. It has benefited greatly from the surge in smartphone users over the last decade. However, the penetration rate of this new data source in the average traffic mix is still rather limited.

FCD is currently mainly applied for the real-time travel time estimations used by navigation services [Cohen and Christoforou, 2015]. Moreover, research has been conducted for its application to the traffic state estimation and incident detection [Sunderrajan et al., 2016], [Houbraken et al., 2017]. For the purpose of spillover detection, limited initial research has resulted in promising first steps, but no real-world applications have been found [Ramezani and Geroliminis, 2015].

## 1.2 Aim of the Thesis

This thesis aims to assess the validity of FCD as a data source for the detection of spillovers on urban signalised intersections. The objective is to develop a method that can handle the data source's limited penetration rate and accuracy. Therefore, two probabilistic methods are developed and validated on a simulated case study.

### 1.2.1 Product Specification

The proposed method for spillover detection using FCD needs to fulfill several criteria that have been put forward by Be-Mobile, who have proposed this thesis. As they gather an abundance of FCD through their navigation software, they are constantly on the lookout for additional usage opportunities.

As a first criterion, the method should be capable of identifying spillover situations at signalised intersections. Ideally, the non-spillover situations should be further

## 1. INTRODUCTION

---

classified into different saturation levels in order to use the model as a comprehensive tool for traffic state estimation.

As a second criterion, two types of data sources can be used for the method. The use of FCD is primordial, but inductive loop detector data can be included to complement the FCD if it is insufficient. This is not practical in reality as it restricts the use to networks where loop detectors are installed.

As a third criterion, the model should be applicable to different intersections with limited additional data gathering. This allows for a rapid rollout on a nationwide scale.

As a final criterion, there are two options for the time of data gathering. Ideally, the proposed model runs in an online setting where data is gathered and evaluated in real-time. Alternatively, the tool can also be developed for the offline case where all data is available at the time of analysis. However, this limits the use of the model to the evaluation of the traffic control strategy.

### 1.2.2 Proposed Methods

The proposed methods are probabilistic approaches that aim to predict the traffic state distribution for every time step. For this purpose, a Hidden Markov Model (HMM) with covariate-dependent transition probabilities is designed and implemented on a simulated case study. Its performance is compared to a second model, which uses a multinomial regression model without information on the state in the previous cycle.

They operate with only FCD as an input, while some additional data sources can be used to improve the models' performances. The model functions in a pseudo-online setting where a decision is made with a limited time lag compared to the real occurrence of the traffic state. This is mostly due to inaccuracies in the FCD, as is discussed in section 2.

### 1.2.3 Case Study

This thesis is made in collaboration with Be-Mobile, a Belgian company that provides software and data to road authorities and private individuals. Some examples of applications in their portfolio are the *Flitsmeister*-app, which is the most popular navigation app in the Netherlands, the *Touring Mobilis*-app for traffic information, and many more. Moreover, they are regularly involved in innovative projects with regards to smart vehicles and smart traffic infrastructure. For this thesis, they proposed the topic and provided three datasets for a case study: loop detector measurements, traffic signal states (red, green or amber) and high-resolution FCD.

The proposed models are tested on a network in Deventer, a city in the province of Overijssel, the Netherlands. Its population has increased to over 100,000 inhabitants and the city has several important cultural attractions and employment opportunities

[Staat van Deventer, 2021]. This results in high traffic intensities during large parts of the day which require a proper management strategy.

As shown in Figure 1.2, the network consists of four successive intersections along the important arterial road N344. Most intersections consist of three incoming and three outgoing links, where each one consists of up to four lanes including the turning bays. The network is prone to spillovers since the investigated intersections are located in proximity to each other. Consequently, proper management is needed to limit delays and ensure the safety of other road users such as cyclists, busses and pedestrians.

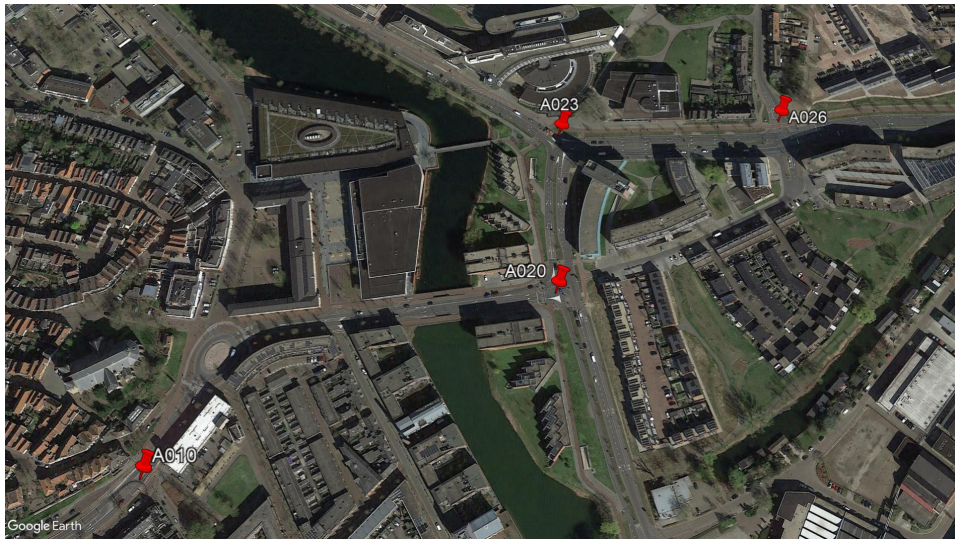


Figure 1.2: Overview of the four successive intersections along the N344. The red markers indicate the location and IDs of the intersections.

## 1.3 Structure of the Thesis

Chapter 2 briefly introduces traffic flow theory, analyses the problem and defines the distinguished traffic states. Furthermore, the working principles of the data sources are discussed and their strengths and weaknesses are summarised. Chapter 3 reviews the available literature on state estimation and spillover detection at signalised intersections. Chapter 4 discusses the theoretical framework of the proposed model. In Chapter 5, the model is applied to the simulated counterpart of the case study and the obtained results are presented. Finally, Chapter 6 discusses the model's main assumptions and shortcomings, as well as the required adaptations for an implementation in a real-world setting.



# Chapter 2

## Problem Analysis

In order to design a method for traffic state estimation, it is necessary to define the different traffic states and evaluate how they can be distinguished theoretically. Two equivalent perspectives are therefore introduced in this chapter: a microscopic and a macroscopic approach. Furthermore, the working principles, the strengths, and the weaknesses of the data sources need to be assessed in order to recognise the main constraints that need to be addressed by the proposed method.

### 2.1 Traffic State Estimation

The traffic state is typically evaluated by a microscopic or a macroscopic approach, where the former assesses vehicles as separate entities and the latter aggregates them to a continuous state-space field. This section briefly introduces these approaches and defines the main parameters for the state estimation. Furthermore, the traffic state at signalised intersections is defined and analysed in terms of the two approaches.

#### 2.1.1 Microscopic Approach

The microscopic traffic flow modelling approach describes the vehicles' position as trajectories in a position-time graph ( $x-t$ ), as shown in Figure 2.1. The speed and the acceleration of a vehicle can be determined as the derivative and the second derivative of these trajectories with respect to time, respectively. Obviously, two trajectories can never cross on a single-lane approach as this would result in a collision. Moreover, the later vehicle is generally assumed to decide on its driving speed according to the distance to its predecessor. Consequently, car-following models can be constructed to describe a vehicle's behaviour based on the leading vehicle's trajectory [Sherali, 2014]. They describe the traffic's wave-like behaviour, visualised in Figure 2.1 by the two periods of standstill that propagate over the link. The microscopic traffic data is collected by data sources that are able to capture the trajectory over space and time, such as FCD or image capturing devices.

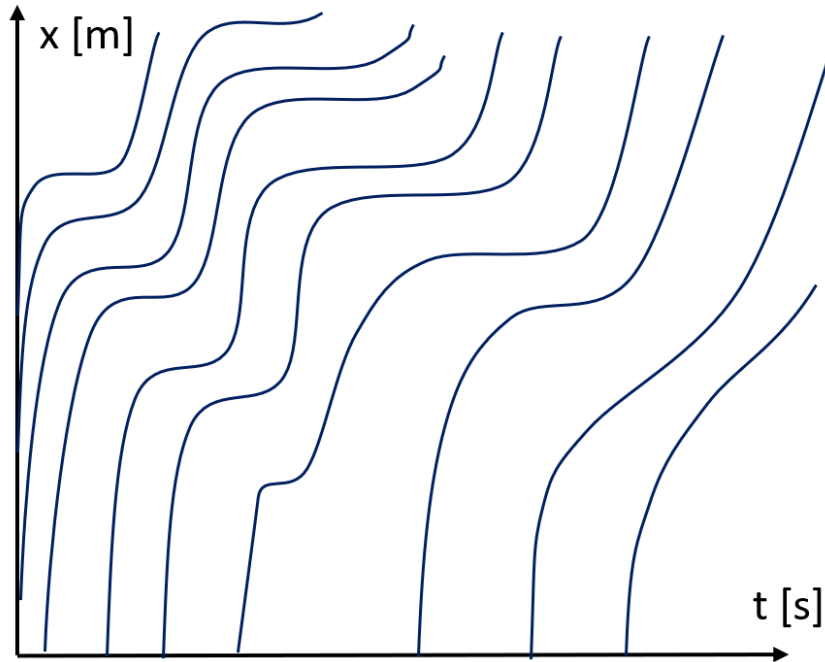


Figure 2.1: Trajectories as proposed in the microscopic approach, where the blue lines represent the location of the vehicles in space and time.

### 2.1.2 Macroscopic Approach

The macroscopic approach considers the traffic on the network as a continuum where a traffic state prevails in a space-time field. This state is characterised by three fundamental variables: density  $k$ , flow rate  $q$  and speed  $u$ . By definition they are related through the fundamental relation, leaving only two independent variables to be determined:

$$q = k \cdot u \quad (2.1)$$

The variables are obtained through aggregation of the microscopic trajectories but this requires that all trajectories are available. Consequently, they are often estimated using stationary detectors, such as loop detectors [Sherali, 2014].

#### Flow rate

The flow rate ( $q$ ) is the number of vehicles that pass a road segment during a certain time interval and is often expressed in vehicles per hour. The maximal flow rate that passes a road section is referred to as the road's capacity and depends on various conditions such as the geometric layout of the road, the weather conditions, the control strategy and other factors [Wu and Giuliani, 2016].

## Speed

The mean speed ( $u$ ) represents the speed of the vehicles that passed the road segment during the aggregation period. With non-stationary data sources, the mean speed can be determined by arithmetically averaging the instantaneous speeds of all vehicles on the road segment, which are determined by taking the derivative of the vehicles' position with respect to time. With stationary detectors, however, a vehicle's instantaneous speed can only be determined accurately when two adjacent loop detectors measure the time difference between the detections of the vehicle on each detector. Alternatively, an approximation of the average vehicle length can be used in combination with the duration of a detection by a single loop detector [Thamizh and Dhivya, 2009].

## Traffic Density

The density represents the number of vehicles per road length at a certain time, resulting in an indication of the proximity of other vehicles [Al-Sobky and Mousa, 2016]. A direct measurement of the density is not trivial, as it requires the trajectories of all vehicles on the network [Park et al., 2015]. Moreover, stationary detectors only measure the vehicle's presence at a fixed location and are consequently not able to measure the density at a certain time. However, an established alternative is the relative occupancy, which is the ratio between the time a detector is occupied by a vehicle and the aggregation time [Sherali, 2014]. The relation between the relative occupancy  $o$  and the density  $k$  is given by

$$o = (d + D) \cdot k \quad (2.2)$$

where  $d$  is the length of the vehicle and  $D$  is the length of the detector [Thamizh and Dhivya, 2009]. Again, two adjacent detectors are required to determine the vehicle's length.

## The Fundamental Diagram

The fundamental relationship (2.1) allows to calculate the third variable when the other two are known. If only one of the variables is known, the traffic state can only be determined if the fundamental diagram, which represents the relationship between each pair of variables, is known [Knoop and Daamen, 2017]. A relationship between flow and density that is often used due to its simplicity is a triangular relationship, which is illustrated in Figure 2.2. Other commonly used fundamental diagrams are presented in the Greenshields Model, the Greenberg Model and the Underwood Model [Greenshields et al., 1935], [Greenberg, 1958], [Underwood, 1961].

In homogeneous and stationary traffic, the traffic state at all spatio-temporal locations is expected to behave according to this fundamental diagram [Sherali, 2014]. The assumption of homogeneity states that all vehicles have the same behaviour, and thus that a homogeneous traffic mix is present where every driver has the same

## 2. PROBLEM ANALYSIS

---

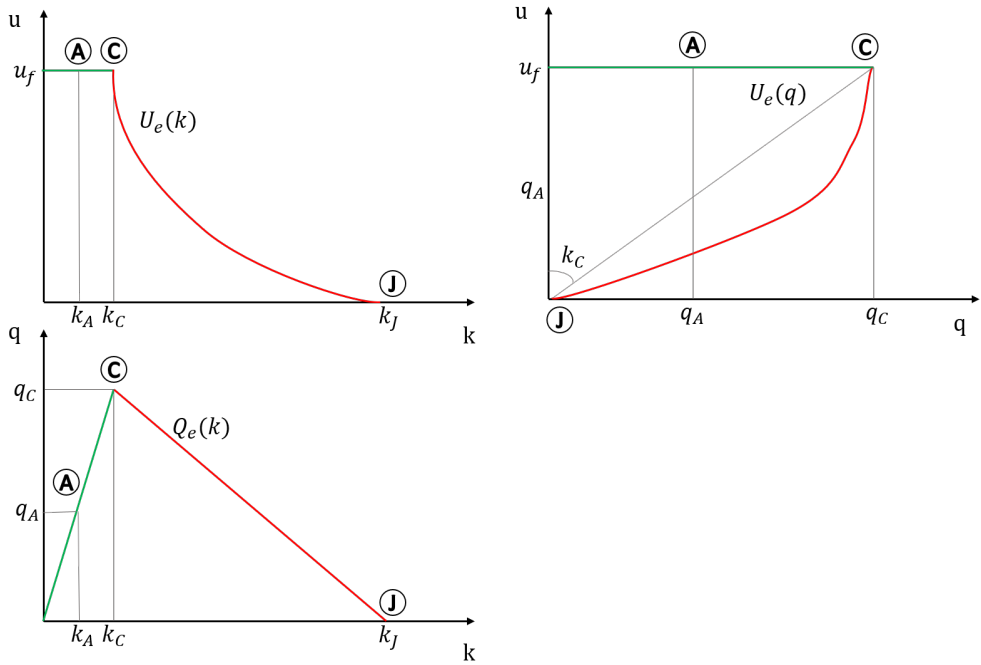


Figure 2.2: Pairwise relationships according to the triangular fundamental diagram, where  $k$  is the density,  $q$  is the flow rate and  $u$  is the speed. The free-flow branch is indicated in green, whereas the congested branch is indicated in red. The states A, C, and J represent the free-flow state, the capacity state and the jammed state, respectively.

reaction time, desired driving speed, and so on. The assumption of stationarity states that the traffic maintains a constant speed, flow and density [Immers and Logghe, 2002]. In reality these assumptions do not hold and the measurements of flow, density and speed are situated in a cloud of points around the assumed fundamental diagram.

In this fundamental diagram, three main states can be distinguished: free-flow state (A), capacity state (C), and jammed state (J), as shown in Figure 2.2. In state A vehicles are not influenced by other vehicles and travel at their maximal desired speed  $u_f$ . This state is situated on the free-flow branch of the fundamental diagram, which has a slope equal to  $u_f$ . State C is the critical edge between the free-flow and congested branches, where the maximal flow rate  $q_C$  is achieved. Traffic states with a higher density than the critical density  $k_C$  experience the influence by other drivers in their proximity. In the extreme case J, all vehicles are standing bumper to bumper with density  $k_J$ .

### 2.1.3 Shockwave Analysis

In the microscopic analysis, trajectories appeared to follow a wave-like behaviour. This behaviour can be modelled mathematically using the Lighthill-Whitham-Richard

## 2.1. Traffic State Estimation

(LWR) model, which is presented in Appendix 7 [Lighthill and Whitham, 1955]. When external constraints are imposed on the traffic flow, the a discontinuity originates since the stationarity assumption is violated. The LWR-model stipulates that these discontinuities propagate in time and space according to shockwaves with a wave speed  $\omega$  equal to

$$\omega_{12} = \frac{q_1 - q_2}{k_1 - k_2} \quad (2.3)$$

where index 1 indicates the initial upstream state and index 2 the resulting state after the shockwave has passed [Hoogendoorn, 2010]. These shockwave speeds can be read from the density-flow diagram as the slope of the connecting line between the respective states.

An illustration of the LWR-model is shown in Figure 2.3, where a traffic signal turns red at time  $t_0$ , resulting in a stop wave with speed  $\omega_{AJ}$ . This wave represents the tail of the queue, or equivalently the transition from the upstream state A to the jammed state J. Downstream, a shockwave propagates with speed  $u_f$  as the traffic state changes from the initial state A to a state 0 where no vehicles are present on the road. When the traffic signal turns green again at time  $t_1$ , the traffic can accelerate, leading to an expansion fan where the traffic changes from a congested state to a free-flow state. The LWR-model stipulates that this transition always passes the capacity regime [Immers and Logghe, 2002]. The wave travelling upstream, further referred to as the start wave, represents the head of the queue and has a speed equal to  $w$ , the slope of the congested branch of the fundamental diagram. Finally, when the stop and the start waves intersect, the queue has fully dissolved and a wave separating the capacity regime and the free-flow regime travels downstream with the free-flow speed  $u_f$ . The blue lines on the graph represent the trajectories of some vehicles on the network, in order to link this aggregated macroscopic approach with the microscopic approach.

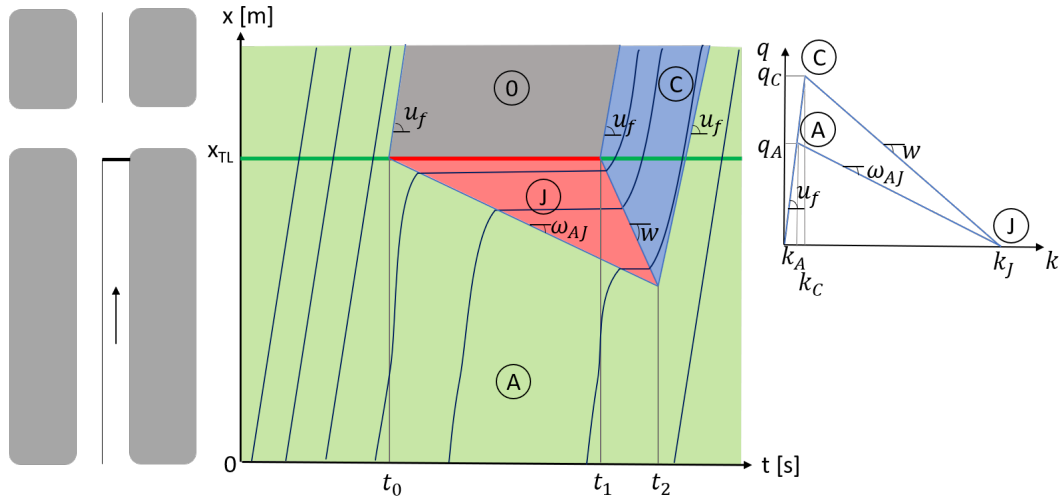


Figure 2.3: Example of the shockwave analysis according to the LWR-model.

## 2. PROBLEM ANALYSIS

---

### 2.1.4 State Classification on Urban Networks

So far, the traffic state is defined in terms of the fundamental parameters: speed, density, and flow. When describing the state at signalised intersections, however, the traffic state is commonly defined according to the number of stops the approaching vehicles make. This results in two main states, namely undersaturation and oversaturation. A third state can be distinguished as a special type of oversaturation: the spillover state.

#### Undersaturation

The lowest level of saturation that can occur on the approach to a signalised intersection is undersaturation, as illustrated for both the macro- and microscopic interpretations in Figure 2.4.

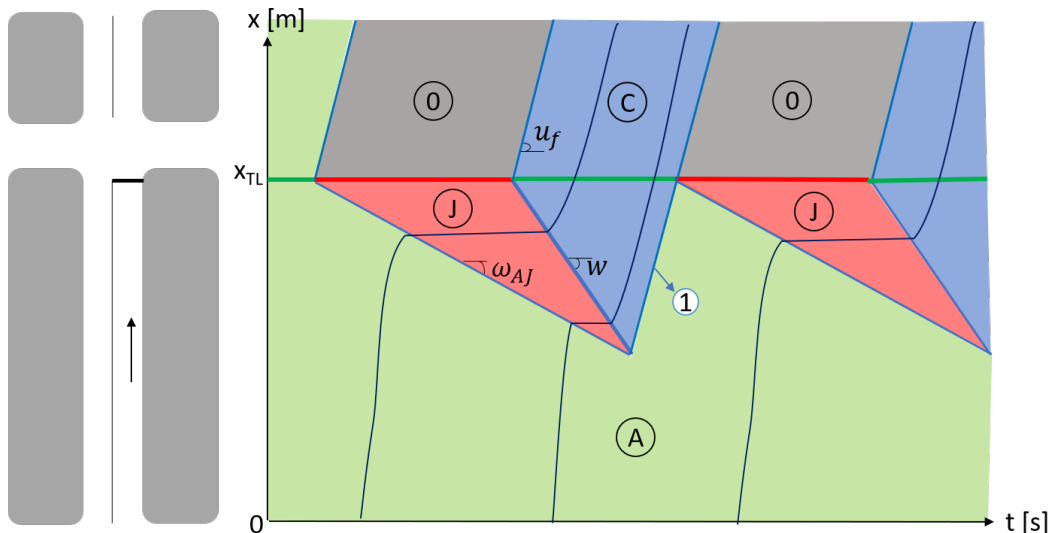


Figure 2.4: Shockwave profile of an undersaturated intersection where every vehicle has to stop at most once.

Microscopically, every vehicle has to stop at most once before passing the intersection when the flow is undersaturated. Consequently, the vehicles either arrive during a green cycle or at the back of a short queue where they can pass the intersection during the next green signal. Figure 2.4 depicts the boundary situation, as every vehicle on the approach has to stop once. The state can only occur when the demand is lower than the intersection's capacity.

Macroscopically, an equivalent definition of the undersaturated state can be found by examining the shockwave indicated as 1 in Figure 2.4. This shockwave has to cross the intersection before the traffic signal turns red again. At the boundary, the

shockwave reaches the intersection at the time of the signal change.

In the illustrated situation, the arrival state is assumed to be uninterrupted, resulting in a constant slope of the stop wave  $\omega_{AJ}$ . In general, this assumption is not satisfied as the state of the arriving traffic A depends on other constraints upstream. For example, if the intersection in Figure 2.4 is considered as an upstream intersection for an other intersection, the arriving traffic of that downstream intersection is not in state A, but varies between state A, state 0 and state C. This results in a variable arriving flow, and consequently in a piecewise linear stop wave. This shockwave is therefore not trivial to estimate without knowledge of the incoming traffic states.

## Oversaturation

Oversaturation is defined as the state where "traffic queues persist from cycle to cycle due to insufficient green splits or because of blockage" [Abu-Lebdeh and Benekohal, 2003, p. 110]. In that case, not all vehicles are able to pass the intersection with at most one stop and the shockwave, represented as shockwave 1 in Figure 2.5 intersects the next cycle's stop wave. The vehicles that were not able to pass the intersection during the green signal form a residual queue that is resolved in the next cycle. Later in this thesis, several levels of oversaturation are distinguished based on the number of stops the vehicles have to make during their approach.

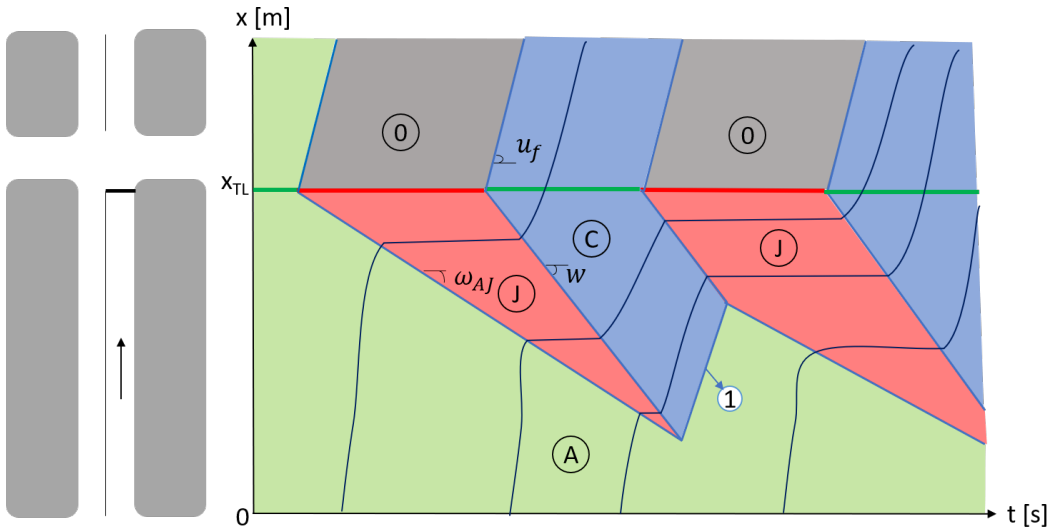


Figure 2.5: Shockwave profile of an oversaturated intersection where at least one vehicle has to stop more than once.

## 2. PROBLEM ANALYSIS

### Spillover

The aim of this thesis is to distinguish spillovers from the two previous states. A spillover is defined as a situation where a vehicle is unable to continue its path due to a queue spilling back from the downstream links, even though the traffic signal is green.

There are four different spillover situations that can be distinguished based on the timing of the blockage compared to the traffic signal cycle: (1) short spillovers, (2) early stops, (3) late departures and (4) long spillovers. They are visualised in Figure 2.6, where two successive intersections are shown.

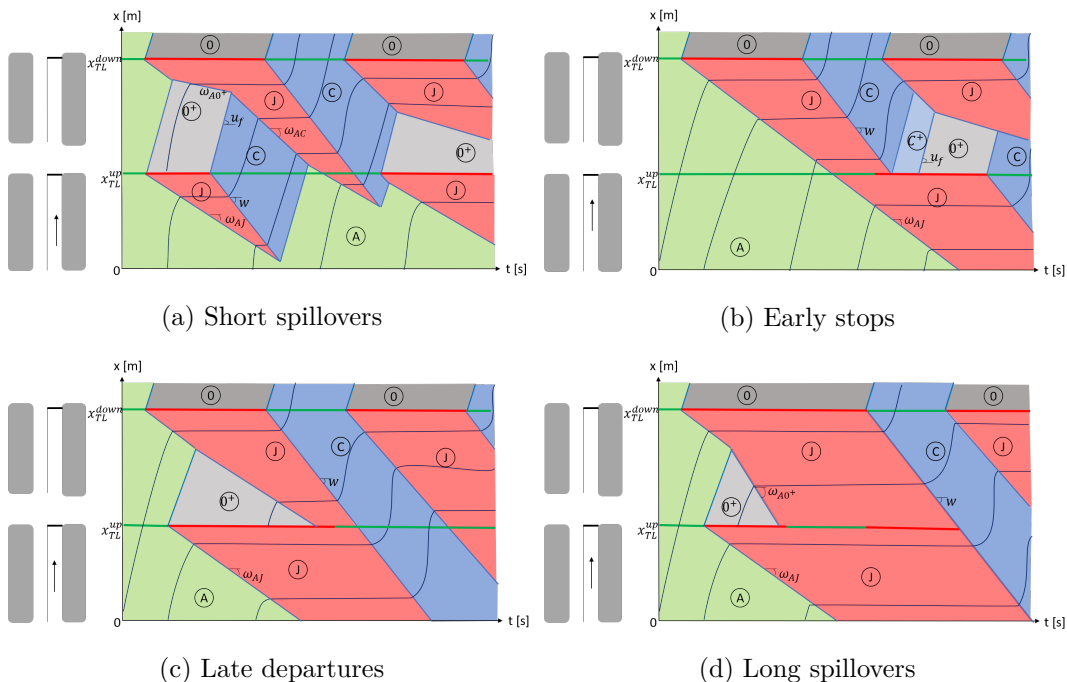


Figure 2.6: Shockwave profile of the four types of spillovers where a queue spills back from the downstream intersection at  $x_{TL}^{down}$  until it reaches the upstream intersection at  $x_{TL}^{up}$ .

Short spillovers occur when a queue spills back onto the intersection briefly during a green signal, as shown in Figure 2.6a. The vehicles in the front of the queue on the upstream link can accelerate when the traffic signal turns green, but this flow quickly joins the queue on the downstream link, causing it to spill back onto the upstream intersection. The blockage lasts until the downstream start wave reaches the upstream intersection. For short spillovers, this happens before the traffic signal turns red. Note that this does not mean that the queue caused by the spillover is completely dissolved, but the intersection itself is no longer blocked, i.e. the vehicle in the front of the queue is able to leave the link.

Early stops occur when the stop wave on the downstream link reaches the upstream intersection during the green time and the start wave only reaches the upstream intersection during the red signal cycle, as shown in Figure 2.6b. Microscopically, the vehicles experience a queue before the traffic signal turns red, but are able to leave when the signal turns green.

Inversely, late departures occur when the stop wave reaches the upstream intersection during a red traffic signal, and blocks the intersection until after the signal turns green, effectively extending the red cycle time, as shown in Figure 2.6c. This can for instance happen when the flow coming from the other approaches, indicated by  $0^+$ , is too intense and fills up the available space on the downstream link.

Long spillovers are the most severe spillover situations and last for the entire green cycle, as illustrated in Figure 2.6d. This situation can consequently be characterised by the lack of vehicles leaving the intersection during the green signal.

Macroscopically, a spillover is characterised by a stop or start wave on the downstream link propagating upstream until it reaches the upstream intersection. However, it is not very practical to look at the downstream link for spillover detection on the upstream link, as it requires a state estimation on the downstream link which is not always available when this link lacks the appropriate detectors or when it is not controlled by traffic signals.

On the downstream link, spillovers can be detected based on a shockwave profile that does not match the shockwaves caused by the traffic signals. The different types of spillover exhibit various shockwave profiles. During short spillovers both the stop and start waves propagate upstream from the upstream intersection. During early stops only the stop wave is visible, while during late departures only the start wave is visible. Long spillovers are characterised by the lack of a start wave when the traffic signal turns green.

Equivalently, spillovers can also be detected by analysing the vehicles' trajectories. If all trajectories on the network are available, spillovers can be detected by examining the first vehicle in the queue. When this vehicle stands still during a green signal, a spillover is present. However, as only a limited penetration rate is achieved, this is not possible. In that case, the shockwaves experienced by a vehicle need to be derived from the trajectory's acceleration and deceleration pattern, leading to a similar shockwave analysis as in the macroscopic approach.

An important problem for the microscopic analysis in a real-world setting is that some trajectories with extraordinary behaviour are present, whereas the macroscopic approach smooths anomalies out through aggregation. These anomalies might be an unexpected stop, e.g. due to a driver searching his directions or picking someone up. They cause unexpected shockwaves that might be misinterpreted as spillovers.

## 2. PROBLEM ANALYSIS

---

### 2.2 Data Sources

Several methods exist to distinguish between the aforementioned states on intersections. Mostly, they rely on the mature loop detector technology as their main data source. However, due to their limitations, methods using new data sources such as FCD are required. In this section, the working principle, the advantages and the limitations of both data sources are discussed.

#### 2.2.1 Loop detectors

Loop detectors are based on inductive properties of an insulated loop wire embedded in the road pavement. When a vehicle passes over the detector, eddy currents are induced in the loop which are measured by a road side detector [Klein et al., 2006].

Generally, two detector configurations are used: single loop detectors and double loop detectors. The former type consists of one loop and is only able to measure the presence of a vehicle, the traffic flow and the relative occupancy. Other parameters such as the vehicle's speed and the density can only be approximated after estimating the vehicle length, as discussed earlier [Thamizh and Dhivya, 2009]. The latter type consists of two adjacent loops. This allows for the speed measurement of a vehicle by examining the time difference between the detection on the first and last detector. Furthermore, the length of the vehicles can be estimated accurately with double loop detectors [Coifman and Kim, 2009].

#### Advantages

An advantage of loop detectors is that the technology is very mature and widely implemented. Therefore, extensive research has been done on the robust processing of the derived data, and reasonably accurate results for the traffic volume and relative occupancy can be expected, regardless of the weather circumstances [Fekpe et al., 2004]. Some even claim that loop detectors are the most reliable data source for traffic state measurements [Skszek, 2001].

#### Disadvantages

Despite its high reliability and maturity, loop detectors are not well-suited for every application. They are stationary detectors which can only detect vehicles passing over the installed sensor. Consequently, the spatial coverage of the output data is very limited and multiple detectors need to be installed on every lane for an adequate traffic state estimation [Cvetek et al., 2021].

The installation of these loop detectors is expensive due to the intrusive implementation in the road pavement which requires the traffic lane to be closed down, resulting in high externalities during installation and maintenance [Skszek, 2001]. When installed incorrectly, both the detector and the pavement can be irreversibly damaged, leading to additional costs [Skszek, 2001]. Moreover, the detectors have

a limited lifespan of 3 to 7 years [FLIR, 2020]. A comparative study in the USA found a total life cycle cost of \$14,000 for one intersection with only four detectors installed [Guerrero-Ibáñez et al., 2018].

### 2.2.2 Floating Car Data

FCD is one of the most recent data sources introduced in traffic management and is based on GPS-trajectories of the vehicles. The location and speed of a probe vehicle are recorded in every time step, resulting in a route choice, travel time, and travel speed measurement.

It is a non-intrusive method that does not require to be installed under the road pavement. Other examples of non-intrusive sensors are Bluetooth measurements, infra-red cameras, microwave radars and more [Klein et al., 2006]. Since FCD is recorded using a GPS-tracker in smartphones, it has become increasingly interesting for traffic data gathering due to the increasing popularity of these devices. Vehicles for which the GPS-data is available are referred to as probe vehicles or connected vehicles.

#### Current applications

FCD is currently mainly used to estimate the travel time over a road segment in real-time [Brockfeld et al., 2007]. Moreover, it is utilized to detect accidents on the motorway and gain insights in various traffic patterns [Talpe, 2016]. Consequently, it can also be used for the detection of traffic queues, which is the main contribution of this thesis.

Recently, several studies have shown how FCD can be implemented for other applications that were previously based on inductive loops and other sensing techniques. Sunderrajan et al. [2016] proposed a method to estimate the macroscopic traffic parameters on freeways using knowledge of the penetration rate. Torp and Lahrmann [2003] proposed an algorithm to assess the intensity of traffic flows on an urban network using GPS-data from taxis.

#### Advantages

One major advantage of FCD is that it is relatively cheap compared to inductive loops. Even though it requires investments to develop and maintain the appropriate software, the data acquisition happens at a limited cost to the data provider or the road authority. The cost for the sensor is borne by the road users when they buy their smartphone. As the FCD is not installed locally, the software can gather data at a multitude of intersections, reducing the cost per intersection drastically compared to loop detectors.

This non-locality of the data source results in a much broader image of the traffic state on the network. Due to this property, the real-time travel time and the speed

## 2. PROBLEM ANALYSIS

---

over a segment can be estimated much more accurately than with loop detectors [Cvetek et al., 2021].

### Disadvantages

The main disadvantage of FCD is that the data is only available for a limited number of the vehicles on the network. This means that it is difficult to make conclusions on the traffic state without knowledge on the exact penetration rate at that time. In the case of Be-Mobile, they claim an average penetration rate of 10% in the Netherlands. However, this is highly dependent on the location and the moment of the measurements. On local roads outside the metropolitan area of Amsterdam, this decreases to around 1% in the off-peak periods, whereas the penetration rate on freeways in the Amsterdam region approaches 20% in peak periods.

Furthermore, the measured trajectories only achieve a limited accuracy. The need for cheap production prevents the implementation of accurate clocks in the smartphone, resulting in the presence of small clock errors, which cause significant location errors. Merry and Bettinger [2019] found empirically that an average error of about 10 meters was present. In an urban setting, where the GPS-signals are reflected on the surrounding buildings, this error increases even further.

An important point of attention when using FCD is that strict privacy regulations need to be respected. The trajectories need to be anonymised in order to preserve the identity of the user. Furthermore, the starting and ending points of the trips need to be adapted in order to hide their exact location. These blurred locations are often in urban regions, where the penetration rate is already low.

## 2.3 Data Analysis

For this thesis, two datasets are available for 30-day period: V-Log data, which contains loop detector measurements and the traffic signal states, and FCD. In this section, these data sources are analysed and the aforementioned limitations are evaluated, as they dictate the methods that are viable for the development of a spillover detection method.

### 2.3.1 V-Log data

The first available data source is V-Log data, which is a protocol used in the Netherlands to register information such as the traffic signal state and the loop detector measurements [Vialis, 2020]. The data source is accompanied by a configuration file and an Intersection Topology Format (ITF) for each intersection. The former contains the reference names for all detectors and traffic signals. Furthermore, it clarifies the relationships between the intersection and the respective sensors, indicating which sensors and traffic signals are present at a certain approach to the intersection. The latter file contains the layout of each intersection and information on the different

lanes for each approach to the intersection, such as the location of the stop line, the speed limit, and the downstream lanes it connects to. Moreover, it also indicates the traffic signal group that regulates the outflow of this lane, and the location of the sensors. The intersections included in the case study and their respective sensors are shown in Figure 2.7, where the red dots represent the location of the loop detectors.

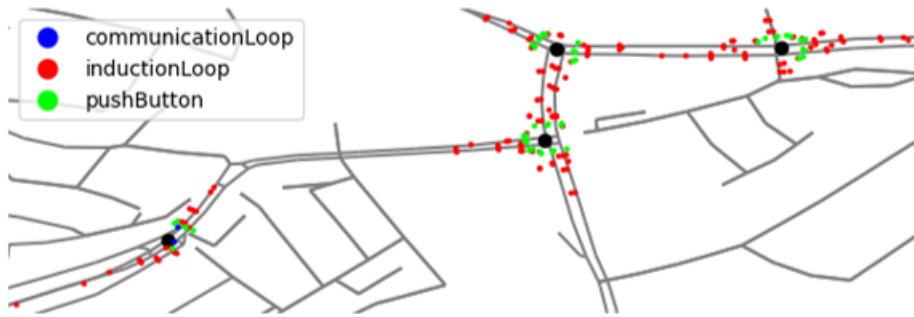


Figure 2.7: Representation of the intersections and the respective sensors.

### Calibration of the Fundamental Diagram

As discussed in Section 2.1.4, spillovers can be identified based on a macroscopic shockwave analysis using the LWR-model. This requires an estimation of a fundamental diagram for the approach to the intersection, as the shockwave speeds need to be known.

Using the V-Log data, it is possible to estimate the fundamental variables: speed, flow and density. However, this requires the estimation of an average vehicle length since single loop detectors are installed. In the Netherlands, the average car vehicle length is estimated to be 4.2 m, but this does not include other vehicles in the traffic mix and thus results in a coarse approximation of the speed and the density [Campestrini and Mock, 2011].

Next, it is possible to calibrate the fundamental diagram by fitting the chosen triangular relationship between the flow and the density through the cloud of loop detector measurements [Rompis, 2018]. However, the estimation proved highly sensitive to the average vehicle length.

Consequently, a different method to estimate the shockwave speeds is proposed where they are determined empirically by examining the experienced shockwaves of successive probe vehicles in historical data. For the start wave, this estimated shockwave speed is expected to remain constant, whereas the stop wave varies with the arrival pattern and can thus not be estimated easily. Only the speed of the start wave is consequently available for the further development of the model.

## 2. PROBLEM ANALYSIS

---

### 2.3.2 Floating Car Data

The second available data source is FCD whose aforementioned drawbacks are discussed and analysed. The accuracy of the data determines the methods that are viable for the real-time detection of spillovers.

#### Trajectory Measurements

The available data has a sampling frequency of 1 Hz. This is in general rather rare as it strongly influences the smartphone's battery usage. Therefore, providers typically set up a perimeter around monitored locations within which they gather the high-frequency samples. Outside this perimeter, lower-frequency samples are gathered, often at only one sample per minute.

The trajectories are preprocessed by Be-Mobile. This comprises of a map-matching of the trajectories to a base map, where the road segments that were most likely travelled by the vehicle are determined. This is necessary due to the limited accuracy of the FCD. After this preprocessing step, the data includes the vehicle's ID, the timestamp, the coordinates of the vehicle at that time, the travel speed and the road segment on which the vehicle was travelling.

Next, the trajectories are linked to the correct traffic signal group, using the information from the ITF-file. They are visualised in an xt-graph, where the Euclidean distance between the trajectory's location and the stop line of the approach is plotted against the timestamp, as illustrated in Figure 2.8.

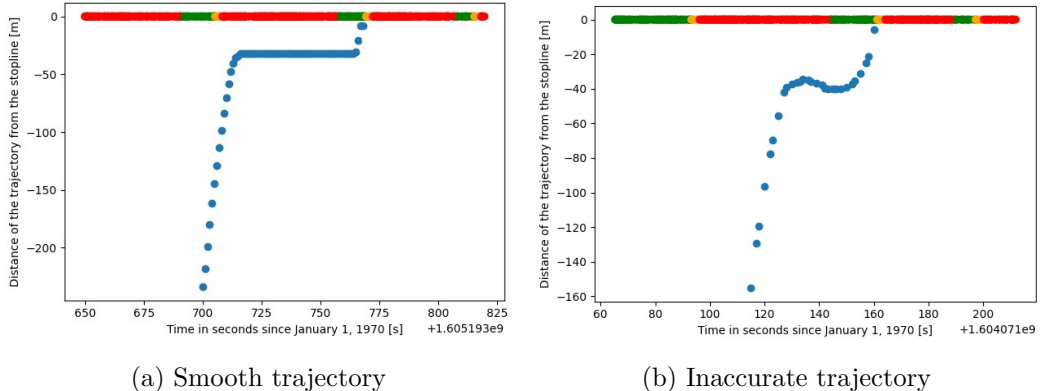


Figure 2.8: Smooth and inaccurate observed trajectory. The horizontal axis represents the timestamp of the observed trajectories in epoch-time, while the vertical axis shows the Euclidean distance to the stop line.

#### Penetration rate

The major problem with floating car data is the low penetration rate as only the available trajectories are for vehicles that have one of Be-Mobile's applications installed. By comparing the number of trajectories on each link with the loop detector's traffic counts, a penetration rate of about 6% is found for an average day, and this varies significantly during the day. Consequently, it cannot be assumed that a probe vehicle is present in every signal cycle and the proposed model needs to extrapolate the traffic state for these cycles.

#### Accuracy

Another drawback of the FCD is the limited accuracy of the location estimation due to the use of cheap sensors. This is also visible in the real data, as shown in Figure 2.8b. There is a significant error both in lateral and longitudinal positions along the road.

The accuracy is highly variable from one vehicle to another due to the wide variety of the quality and price of smartphones. Moreover, certain smartphones apply a filter to the recorded GPS-data, leading to smoother results, whereas others record the unfiltered data. Therefore, a trajectory might appear more realistic, but is less useful than those with a random noise on the location measurement.

The lateral error has important implications on the time setting of the proposed detection method. It is necessary to know the lane on which a vehicle was travelling in order to find where spillovers originated. Moreover, different lanes of the same link are not always controlled by the same traffic signal cycles. In an online real-time setting, it is nearly impossible to estimate the lane on which the vehicle was travelling.

A potential method in an online setting is to match the stop-pattern of a trajectory with the expected shockwave profile based on each lane's traffic signal cycles. In undersaturated conditions, this is expected to result in a reasonably accurate determination of the lane that was travelled. In oversaturation, however, residual queues are present which make the shockwave profile significantly harder to estimate. Furthermore, spillovers are by definition shockwaves that do not behave according to the expected shockwave profile. The method will thus not be reliable in these circumstances.

The alternative is to look at the trajectory only after it has passed the intersection. By looking at the chosen route, it is possible to determine with reasonable certitude on which lane the vehicle was driving earlier. This introduces a small time lag to the proposed method, as the trajectory is analysed when the probe vehicle passes the intersection rather than when it experienced the traffic state on the approach.

The longitudinal error has important implications on the measured characteris-

## 2. PROBLEM ANALYSIS

---

tics of the trajectory. To determine the number of stops and their exact locations, a filter needs to be included to correct for the measurement error on the stationary vehicle's location. As discussed before, some trajectories are already filtered with unknown techniques, which makes it hard to analyse the trajectories appropriately.

### 2.4 Summary

In conclusion, there are multiple difficulties that need to be considered when defining a method for the detection of spillovers. In general, spillovers can be detected through the estimation of the shockwaves on the upstream link. These shockwaves propagate upstream according to the fundamental diagram, as stipulated by the LWR-model. However, the shockwave profiles of the different types of spillover are vastly different, making it hard to define one detection strategy.

To find the fundamental diagram of each link on the network, single loop detector measurements are not sufficient as an accurate vehicle length estimation is required. Therefore, only an estimation of the wave at the head of the queue, the stop wave, is available.

The use of FCD as the main data source entails that an interpolation of the traffic state is necessary for periods where no probe vehicles pass the intersection. After all, only a limited penetration rate of about 6% is reached. Therefore, it cannot be assumed that a vehicle is present in every traffic signal cycle.

Moreover, the inaccuracies in the real-life trajectories need to be taken into account when deriving characteristics from them. The inaccuracies also limit the use of the methods to a pseudo-online setting, as it is necessary to distinguish the lane on which a vehicle was travelling. Due to a significant lateral error in the trajectory, it is not possible to locate the vehicle exactly, and the lane on which it travelled can only be determined after the vehicle has chosen its path.

# Chapter 3

## Literature Review

Even though spillover detection is an important issue for traffic control systems at signalised intersections, the research on it is rather scarce. Most research focuses on the estimation of the queue length or the travel time on urban links, which are the main control parameters for the traffic control system. As the general methodology for these estimations is similar to those for spillover detection, both methods are discussed in this chapter.

The available research uses different data sources as an input for the state estimation methods, namely loop detectors, FCD, and fusions of these deata sources. The methods using loop detectors are more plentiful than those using FCD, being a recent technology.

In general, the methods can be divided into three different categories [Ma et al., 2014]. Some techniques estimate the traffic state based on the cumulative input-output of vehicles, which results in an estimate of the queue length. Other techniques estimate the stop and start waves based on the LWR-model, allowing for queue length estimation and spillover detection. Recently, a third technique has emerged based on probabilistic models and deep learning approaches.

The methods discussed in this thesis focus on the state estimation of interrupted flows on urban networks. In the case of uninterrupted flows, on freeways for instance, the traffic state results from interactions between vehicles, whereas in interrupted flows, the states are dominated by external constraints such as traffic signals or stop signs [Sharma and Swami, 2016]. The latter situation is more complex due to the lack of homogeneity in the traffic mix and the presence of external constraints that change frequently [Sharma and Swami, 2012].

### 3.1 Methods using Loop Detectors

Traditionally, methods for traffic state estimation are based on the presence detections and relative occupancy measures of inductive loop detectors. The main limitation of

### 3. LITERATURE REVIEW

---

this data source is the local implementation, resulting in a severely restricted spatial resolution of the measurements.

#### 3.1.1 Queue Length Estimation

A first method is described by Webster [1958] and is based on the cumulative input and output of vehicles. Using vehicle counts from loop detectors upstream of the intersection and at the stop line, the method measures the cumulative inflow and outflow of vehicles, which gives the number of vehicles in the queue. One of the problems with this method is that the loop detector counts are prone to counting errors [Ramezani and Geroliminis, 2015]. Over time, these errors accumulate, especially since the noisy counts of both detectors are subtracted. Furthermore, the detection of the queue length is not possible when the queue extends past the location of the upstream loop detector. This method is further elaborated by Sharma et al. [2007] and Vigos et al. [2008] to increase its reliability using model-based approaches. However, the aforementioned limitations remain largely unsolved in their research.

A second method is based on the LWR-shockwave model. The shockwaves on the links are estimated in order to find the maximal queue length. Liu et al. [2009] propose a method that monitors the occupancy measured on an upstream loop detector. They define three breakpoints in the shockwave diagram, as visualised in Figure 3.1: breakpoint A where the stop wave reaches the location of the detector, breakpoint B where the start wave reaches that location and breakpoint C where the last vehicle that experienced the queue passes the detector. The time of occurrence of a breakpoint is determined based on the measured occupancy over the detector. Combining this time with the known traffic signal cycle and a fundamental diagram allows for an estimation of the shockwaves, resulting in the maximal queue length and the residual queue length. As the stop shockwave is dependent on the arrival pattern of the traffic, Liu et al. [2009] propose to use the intersection between the other two estimated shockwaves to determine the maximal queue length H. The main limitation of this model is that it requires very accurate occupancy measurements, which is not always possible in saturated traffic conditions [Yulianto, 2018]. Also, if the residual queue extends past the loop detector, no estimation of the maximal queue length can be made [Liu et al., 2009].

#### 3.1.2 Spillover Detection

For spillover detection, similar approaches can be taken. Implementations of methods based on the input and output of vehicles for the purpose of spillover detection have not been found. The method is expected to be inaccurate when estimating the short-lived queues caused by spillovers. Consequently, most techniques are based on the LWR-model.

Wu et al. [2010] proposed a method based on the time of the queue over the

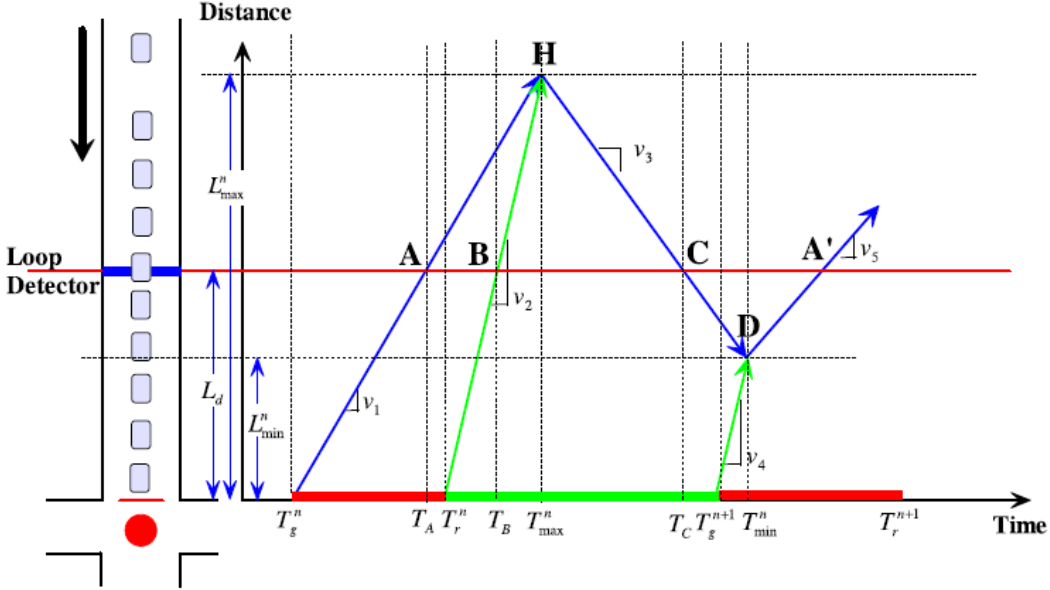


Figure 3.1: Queue length estimation method according to Liu et al. [2009]. Note the difference in notation: the driving direction is inverted and the shockwave speeds  $v_1$ ,  $v_2$ ,  $v_3$  coincide with  $\omega_{AJ}$ ,  $w$ , and  $u_f$ , respectively.

detector. The method defines a time interval within which a queue over the upstream detector can be caused by a red traffic signal, based on an estimation of the fundamental diagram of the approach and the LWR-model. If a queue is detected over the upstream detector outside this time interval, it has to be caused by a spillover.

Furthermore, a method proposed by Geroliminis [2009] defines a critical occupancy for the upstream loop detector, based on the LWR-model, a geometric analysis of the shockwaves under normal circumstances, and an assumption of the fundamental diagram. If the measured relative occupancy on the loop detector exceeds this critical occupancy, a spillover is present. Ma et al. [2014] extended this method in order to take into account the potential presence of residual queues.

## 3.2 Methods using Floating Car Data

The introduction of FCD is seen as a promising evolution that might replace loop detectors in the near future. Recently, some techniques have been developed that use FCD to estimate the queue length or the traffic state. Limited research has made the first steps towards spillover detection at signalized intersections. Due to the inaccuracies and limited availability of FCD, this research often resorts to probabilistic approaches rather than the analytical approaches discussed earlier.

### 3. LITERATURE REVIEW

---

#### 3.2.1 Queue Length Estimation

One of the first applications of GPS-data from probe vehicles for urban intersections was presented by Comert and Cetin [2009]. He proposed a method where the location of the last probe vehicle in the queue is used to determine a confidence interval on the maximal queue length. However, there are multiple problems with this method as the probability density function to determine the maximal queue length given the location of the last probe vehicle is not known in general. Moreover, he assumes that there is at least one vehicle in each traffic signal cycle and that the traffic is in steady-state, which are not valid assumptions with a limited penetration rate and in urban traffic [Comert and Cetin, 2009].

Wang et al. [2017] propose a method for the estimation of the maximal queue length based on the LWR-model. In this method, the time and location of a probe vehicle arriving in the queue and leaving it is recorded. Based on these coordinates, the method estimates the stop and start wave, which can be used in similar fashion to the methods described earlier. However, it assumes that there is one probe vehicle during each traffic signal cycle. Moreover, the study is limited to situations where no residual queue is present, but this limitation can be relaxed using the model by Wu et al. [2010].

Ramezani and Geroliminis [2015] propose a method that aims to estimate the queue length and the unknown red signal cycles. The probe vehicles are grouped into stopped vehicles and moving vehicles. Next, the  $(x,t)$ -coordinates of the stopped vehicles joining and leaving the queue can be used to estimate a polygonal shock-wave profile. For the stop wave, a profile is chosen based on an assumed arrival pattern, whereas the start wave is assumed to be linear. The robustness of the method is evaluated for different penetration rates and measurement errors on the GPS-trajectories. Similar studies have extended the method with Bayesian filters to improve the estimation [Wang et al., 2017], [Yang et al., 2018].

A recent study by Emami et al. [2019] proposes a method using a Neural Network to estimate the queue length, based solely on data from probe vehicles and a known penetration rate. They claim a penetration rate of at least 20% is necessary for decent results.

Finally, Rempe [2019] and Rao et al. [2019] propose methods to identify congested periods on urban intersections based on clustering techniques. Data such as the vehicles' speed, the estimated queue length and the incurred delay are classified into different clusters, each representing a certain level of oversaturation.

#### 3.2.2 Spillover Detection

To improve their method for the estimation of the queue length, Ramezani and Geroliminis [2015] proposed a Bayesian inference method to detect spillovers. The

probability of a spillover is determined by evidence on the estimated red signal time and the time interval between two start waves. This leads to a probability of being in a spillover state, given a certain estimated shockwave profile. Its main drawbacks are the lack of estimations for signal cycles without probe vehicle and the restriction to single-lane approaches.

A study by Christofa et al. [2013] proposes two other methods, a gap-based method and a shockwave-based method, but it analyses the downstream traffic state rather than the upstream state. The gap-based method estimates the distance between the last detected vehicle in the queue and the maximal queue length based on knowledge of the penetration rate. If the position of this vehicle is further than a certain maximum queue length, a spillover warning is given for the upstream intersection. If no probe vehicle is present during a cycle, the probability of spillover is reduced. The second method considers a shockwave approach, where the last probe vehicle to leave the upstream intersection in a certain traffic signal cycle is used to estimate the stop shockwave. Again, if the position of this vehicle is further than a certain threshold, a spillover warning is sent out.

### 3.3 Other Methods

Dynamic traffic models can also be used to approximate and evaluate the traffic state on a certain road. These models differ from the previously mentioned ones as they do not use recent data to estimate the traffic state, but are calibrated on historical data in order to evaluate new signal control strategies or varying demand patterns. An example of such a model is the shockwave profile model (SPM) which analytically estimates the shockwaves resulting from various circumstances [Wu and Liu, 2011]. It takes a different approach than numerical traffic models, such as the Cell Transmission Model (CTM), where the link is split into separate cells and the number of vehicles in each cell is numerically calculated for each time step [Daganzo, 1995]. These numerical models experience problems in urban networks due to the many discontinuities, leading to high-frequent traffic state changes [Rosas-Jaimes et al., 2013]. Using SPM, the saturation level and presence of spillovers can be determined by analysing the predicted shockwaves.

### 3.4 Summary

In this chapter, the available research is elaborated and discussed. The methods are classified based on their data source and their theoretical approach. The review is not limited to spillover detection, but also discusses the more general approach of queue length estimations. The discussed research is summarised in Table 3.1.

### 3. LITERATURE REVIEW

---

Paper	Goal	Description	Data Source
Webster [1958]	Queue length, average delay	Measure cumulative input-output & estimate formulae to derive average delay	Loop detectors
Sharma et al. [2007]	Queue length, average delay	Use vehicle's inductive ID to find point of entry and leaving; FIFO	2 loop detectors per lane
Vigos et al. [2008]	Queue length, average delay	Estimate number of vehicles based on inflow-outflow + extension with Kalman Filter based on flow & occupancy	$\geq 3$ loop detectors per lane
Liu et al. [2009]	Queue length	Shockwaves determined based on breakpoints in occupancy measurements	Loop detectors
Wu et al. [2010]	Spillover	Restricted time-interval within which queues can be caused by red signal	Loop detectors
Geroliminis [2009]	Spillover	Definition of critical occupancy for spillover based on geometric analysis	Loop detectors
Rempe [2019], Rao et al. [2019]	Congestion level	K-means clustering into different congestion levels	FCD, Loop detectors
Comert and Cetin [2009]	Queue length	Given location of last probe vehicle, estimate queue length with given PDF	FCD

### 3.4. Summary

---

Ramezani and Geroliminis [2015]	Queue length	Estimation of shockwaves and traffic signal cycles based on entry and exit of trajectory in the queue	FCD
Wang et al. [2017]	Queue length	Estimation of shockwaves based on speed pattern of probe vehicles	FCD
Emami et al. [2019]	Queue length	NN-model to predict queue length based on vehicle position, speed & penetration rate	FCD
Christofa et al. [2013] Spillover Method 1		Similar reasoning to Comert on downstream link: if downstream queue longer than threshold, spillover danger upstream	FCD
Christofa et al. [2013] Spillover Method 2		Similar reasoning to Liu on downstream link: if downstream queue longer than threshold, spillover danger upstream	FCD
Ramezani and Geroliminis [2015]	Spillover	Bayesian analysis of spillovers based on estimated signal durations	FCD
Wu and Liu [2011]	Traffic state model	SPM: Analytical estimation of shockwaves for state model	-

---

Table 3.1: A summary of the available literature, their aim, working principle and data sources.

### 3.5 Originality of the Proposed Method

In this thesis a novel probabilistic method to detect spillovers based on FCD is proposed. It uses a Hidden Markov Model (HMM) with a logistic regression model to determine the transition probabilities, as elaborated in Chapter 4. This type of models is regularly applied in medicine, land use planning and maintenance management [Jackson et al., 2003], [Sirima and Pokorny, 2014], [Li et al., 2020]. However, the application of Markov models for traffic state estimation is limited. Some techniques use stationary Markov chains, which is a severe oversimplification due to changes in demand and weather conditions [Yeon et al., 2008]. One study was found that proposed a similar technique to the proposed method, applied to freeway traffic using loop detector data and a restricted number of covariates [Noroozi and Hellinga, 2014].

The proposed method is capable of extrapolating the traffic state to states without probe vehicles, even though currently a coarse approximation is made. Moreover, the method can handle multilane approaches and performs well under priorly unknown and varying penetration rates.

# Chapter 4

## Methodology

Previous research has made the first steps towards spillover detection using FCD but has several limitations such as a known penetration rate and the restriction to a single-lane approach. Other limitations inherent to FCD need to be addressed as well. Its penetration rate is limited, which stipulates the need for extrapolating the traffic state for cycles without probe vehicles. Moreover, the FCD's limited accuracy warrants a pseudo-online setting in order to identify the lane travelled by a probe vehicle, which is only known after the vehicle has chosen the continuation of its route. Additionally, significant measurement errors and potential unexpected behaviours cause uncertainty on the observed trajectories. Consequently, a probabilistic method is proposed that attempts to detect spillovers and to measure the saturation level, while taking the aforementioned problems into account.

In this chapter, the theoretical background of the proposed Hidden Markov Model is discussed. First, the considered alternatives are briefly introduced and the choice for this method is explained. Second, an overview of the methods framework is given and its two interlinked stages are discussed in detail. Finally, the metrics to evaluate the model's performance are enumerated. The second method, which is used to compare to the HMM, is a simplification of this method and is not elaborated separately.

### 4.1 Model Selection

In this thesis, several methods were considered, which can be generally divided into two types: deterministic methods and probabilistic methods. For the former type an extension to the research by Wang et al. [2017] was examined, whereas for the latter type multiple options were considered.

The deterministic method builds further on the queue profile estimation technique proposed by Wang et al. [2017]. Their model uses the stop-and-go pattern of the probe vehicles to estimate the shockwave profile on the approach, but it lacks the ability to estimate the traffic state when no probe vehicles are present during a cycle. Therefore, a potential research direction is to complement this method with a traffic

#### 4. METHODOLOGY

---

model such as SPM by [Wu and Liu \[2011\]](#). The main drawbacks of this approach are that real-time information on the traffic demand and an estimation of the fundamental diagram are required. Moreover, the results are expected to be very sensitive to measurement errors and unexpected behaviours in the measurements. The model is consequently deemed invalid for a real-life implementation. The proposed method takes a probabilistic approach, aiming to predict a probability of being in a certain state, rather than a deterministic state classification.

One considered probabilistic method is based on the framework of Bayesian filters for data fusion. A traffic model such as CTM or SPM continuously predicts the traffic state on the approach based on a numerical or analytical estimation of the shockwaves, respectively. Upon the arrival of a probe vehicle on the network, the filter corrects the model's prediction based on the vehicle's characteristics, resulting in a better estimation of the current state and the future states [[Welch and Bishop, 2006](#)].

Another option is to base the method on the framework of Markov models where the traffic state is considered as a time series and a new state distribution is estimated in every time step based on certain transition probabilities. The time interval between discrete time steps will be referred to as a cycle. The transition probabilities, which represent how probable a transition from one state to another is, can either be stationary or non-stationary. The Markovian framework is chosen in this thesis due to its simplicity, its ability to make predictions for cycles without probe vehicles, and its intuitive way of handling transitions between time steps.

## 4.2 General Overview of the Model

The presented method is a Hidden Markov Model (HMM), and is described as a discrete-time finite-state first-order Markov chain with non-homogeneous (non-stationary) transition probabilities and covariates [[Bartolucci et al., 2014](#)]. As schematically shown in Figure 4.1, the model's framework consists of two interlinked stages: a simple Markov model predicts a time series of state distributions and is complemented by a multinomial logistic regression model (MLR) to calculate the transition probabilities based on measurements [[Fink, 2014](#)]. The original method was first proposed by [Goodman \[1974\]](#) and [Muenz and Rubinstein \[1985\]](#), and later extended by [Islam et al. \[2004\]](#), [Bartolucci et al. \[2014\]](#), [Koki et al. \[2019\]](#) and others.

In the first stage of the method, a Markov model predicts a state distribution for each time step, based on the one from the previous time step and a transition probability matrix [[Winston and Goldberg, 2004](#)]. This process is represented by

$$S_t = S_{t-1} \cdot P(t) \tag{4.1}$$

where  $S_t$  represents the state distribution at time  $t$ , and  $P(t)$  the transition probability matrix at time  $t$ .

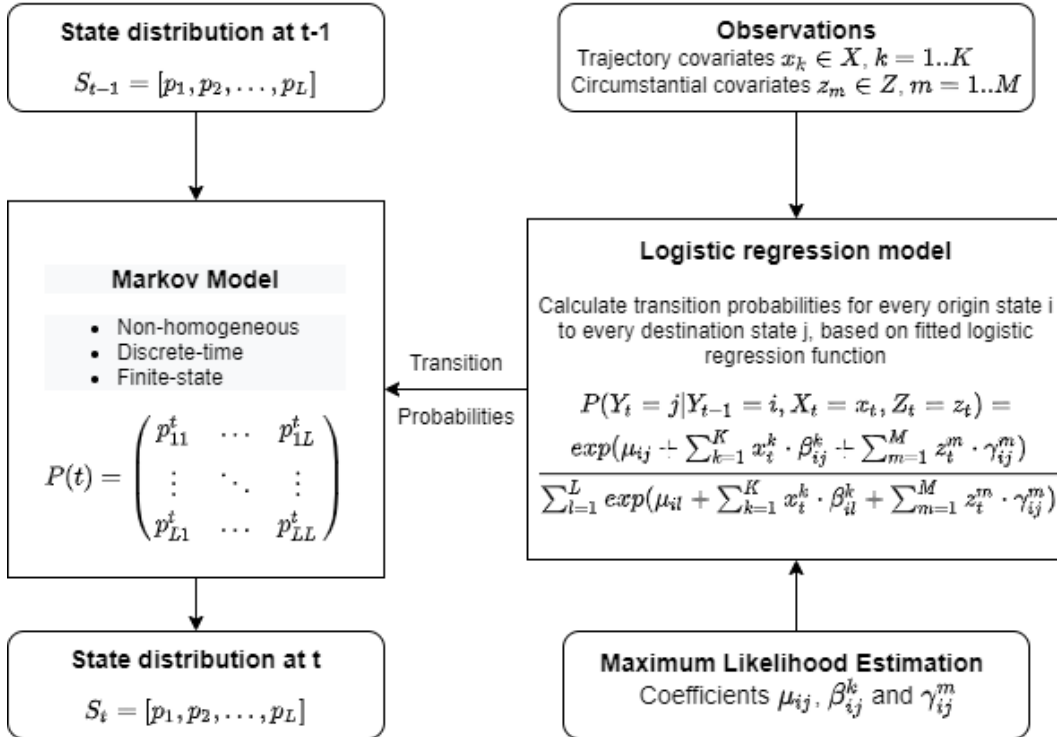


Figure 4.1: Schematic overview of the Hidden Markov Model.

In the second stage of the model, the non-stationary transition probabilities are calculated based on the observations at time  $t$ . In other words, the transition probability  $p_{ij}^t$  represents the probability of being in state  $j$  at time  $t$ , given that the state at time  $t - 1$  was  $i$  and certain characteristics are observed in a probe vehicle's trajectory at time  $t$ . The relationship between these probabilities and the observations is given by a logistic regression model, for which the coefficients are calibrated by a Maximum Likelihood Estimation (MLE) on historical data.

The observed characteristics are split in two types: trajectory variables (trajectory covariates) and circumstantial variables (circumstantial covariates). The former covariates  $X$  enclose information derived from the trajectory such as the travel time, the number of stops, the assessment of the shockwave profile, and others. The latter covariates  $Z$  contain information on the circumstances of the intersection at time  $t$  such as the traffic state at neighbouring intersections and the traffic demand.

### 4.3 Markov Model

In this section, the theoretical framework of the Markov model is elaborated further. Some design choices regarding the state space and the time resolution are also discussed. Moreover, methods using stationary transition probabilities are compared to those with non-stationary ones.

#### 4.3.1 Theoretical Framework of Markov Models

Markov models are stochastic processes, where one aims to estimate the value of a random variable that changes over time [Winston and Goldberg, 2004]. They are applied in a wide range of applications such as birth-death processes, pattern recognition and economics [Novozhilov et al., 2006], [Fink, 2014], [Briggs and Sculpher, 1998]. A Markov model differs from other stochastic processes in that it assumes the Markov Property, which states that the model is memory-less, i.e. the state at time  $t + 1$  only depends on the state at time  $t$ . Simplifying the model to a discrete-time finite-state model, this can be written as:

$$P(Y_t = j | Y_{t-1} = i, \dots, Y_1 = i_1, Y_0 = i_0) = P(Y_t = j | Y_{t-1} = i) = p_{ij}^t \quad (4.2)$$

where  $p_{ij}^t$  is the transition probability from state  $i$  at time  $t - 1$  to state  $j$  at time  $t$  and  $Y$  is the state variable, where each state belongs to the finite state set  $I$  [Winston and Goldberg, 2004]. These transition probabilities can be homogeneous, where they are independent of time, or non-homogeneous, where they change over time. If the number of states is assumed finite and equal to  $L$ , the probabilities can be written as an  $L \times L$ -matrix, the transition probability matrix  $P(t)$ :

$$P(t) = \begin{bmatrix} p_{11}^t & \dots & p_{1L}^t \\ \vdots & \ddots & \vdots \\ p_{L1}^t & \dots & p_{LL}^t \end{bmatrix} \quad (4.3)$$

Obviously, transition probabilities are all non-negative and the sum of the elements on a row of the transition matrix equals 1 since each row indicates the probability of moving from one state to every other state.

Finally, given the state distribution  $S_{t-1}$  in the previous time  $t - 1$ , the new state distribution  $S_t$  at time  $t$  can be found by multiplying this prior distribution with the transition matrix at time  $t$ , as shown in equation (4.1). Of course, when the initial state and the transition matrices are given, this equation can be generalised to  $n$  time steps [Winston and Goldberg, 2004]:

$$S_t = S_0 \cdot P(0) \cdot P(1) \cdot \dots \cdot P(t-1) \quad (4.4)$$

#### 4.3.2 Finite-state Assumption

The proposed Markov model assumes a finite number of states  $L$ , which are collected in the state set  $I$ . The Markov model results in a state distribution  $S_t$ , which is a

$L \times 1$ -vector containing the probability  $p_i$  of being in state  $i$  at time  $t$ .

Alternatively, continuous-state Markov models also exist, where the state variable  $Y$  is a continuous random variable and the transition probabilities are extended to probability distributions [Li, 2010]. These distributions indicate the conditional probability of each new value of the continuous state variable, given the prior state [Perla et al., 2020]. Extending to a continuous state-space entails some additional difficulties. First, the states in the thesis need to be translated to one unambiguous variable, which is not trivial in the researched application as different indicators are used when distinguishing between under- and oversaturation or between oversaturation and spillover. A potential solution is to split the model in an primary Markov model to distinguish spillover from non-spillover states and an underlying Markov model to measure the oversaturation level. This extension is left for further research, and the model is limited to the finite state-space.

#### 4.3.3 Time Resolution

The proposed method uses a discrete-time Markov model, which entails that a transition to a new state can only happen at predefined discrete time steps. Consequently, a new state distribution is predicted at every time step, regardless of the number of probe vehicles that passed the intersection during the cycle.

Alternatively, continuous-time Markov models also exist, where a new state is predicted continuously. This extension would probably provide more accurate predictions due to the immediate inclusion of the latest information, but induces additional complexity for the design. Handling the Markov Property in this setting is more intricate and decaying factors need to be included for the periods where no probe vehicles are available [Privault, 2018]. The initial method therefore limits itself to a discrete-time model.

#### 4.3.4 Transition probabilities

In this section, the definition of the transition probabilities is discussed. First, the homogeneous case is elaborated, followed by the reasons for non-homogeneous transition probabilities.

##### Stationary Markov Model

In a stationary or time-homogeneous Markov model, the transition probabilities are assumed independent of time. This means that the time indices in equation (4.3) can be dropped, and one transition matrix is used for the entire time-domain of the application. The assumption of homogeneity is often made as it severely reduces the complexity of the model, even though realistic processes rarely behave accordingly [Uche, 1990].

Stationary transition probabilities can be approximated by counting the number of

#### 4. METHODOLOGY

---

occurrences  $n_{ij}$  of a certain transition in the training set. The estimated transition probability is thus given by

$$\hat{p}_{ij} = \frac{n_{ij}}{\sum_{j=1}^L n_{ij}} \quad (4.5)$$

The assumption of homogeneity is not valid in the researched application. Looking at the traffic pattern on a typical day, for example, there are several peak periods in the traffic demand, where transitions to spillover states are more likely than during off-peak periods. In the stationary transition probability matrix, these differences are smoothed out, resulting in an overestimation of spillover states during off-peak and an underestimation of these states during peak periods.

A proof of concept using stationary transition probabilities is built as an illustration of the Markov model's validity. As the resulting state distribution converges to a stationary one, the predictions are updated using a neural network which takes the observations of the probe vehicles into account. The working principle and the results of this model are discussed in appendix 7. As expected, the shortcomings of the homogeneity-assumption become apparent in this example.

#### Non-stationary Markov Model

For the aforementioned reasons, it is necessary to adopt an inhomogeneous Markov model, where transition probabilities vary according to time-dependent variables such as the traffic demand, weather conditions and other observations [Bartolucci et al., 2014].

For the purpose of estimating the transition probabilities, a wide variety of methods exist. First, if the covariates are categorical, the transition probability matrix can be duplicated for every combination of categories [Bolano, 1985]. An example for two different levels of demand with a limited number of states is shown in Table 4.1. The duplication of the transition probabilities becomes more difficult when multiple covariates are included or when more fine-meshed levels of the covariates are required, as separate probabilities need to be estimated for every combination of the covariates' levels [Bolano, 1985].

States	Demand	Undersaturation	Oversaturation	Spillover
Undersaturation	Low	0.90	0.07	0.03
Undersaturation	High	0.60	0.25	0.15
Oversaturation	Low	0.50	0.40	0.10
Oversaturation	High	0.20	0.60	0.20
Spillover	Low	0.20	0.50	0.30
Spillover	High	0.10	0.50	0.40

Table 4.1: Example of the transition probability matrix with categorical covariates.

A more suitable approach to calculate the transition probabilities is to find an expression for the relation between the covariates and the transition probabilities. One option is to fit separate MLRs for every transition starting from state  $i$  to every state  $j$  [Sinha et al., 2011]. This method is implemented as it is not required to make assumptions on the covariates' distributions [Withers, 2009]. Moreover, MLRs have a straightforward mathematical formulation, and are familiar.

Similarly, techniques using Bayesian inference are often used in HMMs. They estimate the posterior probability  $p(Y_t|X_t)$  based on prior believes on the relationship between the observations and the states and on the actual observations [Castellano and Scaccia, 2007]. This allows to include the uncertainty on this relationship effectively, but deciding on the prior believe is not trivial [Murphy, 2012]. The decision is made to develop an initial model using the MLR-approach.

## 4.4 Logistic Regression Model

The relation between the transition probabilities of the Markov model and the covariates is modelled by a multinomial logistic regression model. In this section, the theoretical background of the model is discussed, followed by an analysis of the covariates. Furthermore, the methods to train and validate the MLRs are proposed.

### 4.4.1 Theoretical Framework of Multinomial Logistic Regression

MLRs are widely used for classification purposes in machine learning, discrete choice theory and many more [Çokluk, 2010]. They transform a linear regression function into a probability of being in a certain state using a sigmoid-transformation. The general formula of the MLR is thus given by:

$$\log \frac{P(Y = l|x)}{P(Y = L|x)} = \mu_0 + \beta_1^l x_1 + \beta_2^l x_2 + \dots + \beta_k^l x_k \quad (4.6)$$

for  $l = 1, \dots, L$  the different states and  $k = 1, \dots, K$  the covariates with their respective coefficients  $\beta_k^l$ . The class  $L$  is assumed as the reference category in this formulation, which needs to be included in order to normalise the probabilities, resulting in 0-values for all its coefficients [Neath and Johnson, 2010].

For the implementation of the model in the HMM, the MLR can be rewritten as

$$P(Y_t = j|Y_{t-1} = i, X_t = x_t) = \frac{\exp(\mu_{ij} + \sum_{k=1}^K x_t^k \cdot \beta_{ij}^k)}{\sum_{l=1}^L \exp(\mu_{il} + \sum_{k=1}^K x_t^k \cdot \beta_{il}^k)} \quad (4.7)$$

where  $\mu_{ij}$  is the intercept and  $\beta_{ij}^k$  is the coefficient of the  $k$ -th covariate  $x_t^k$  for the transition from state  $i$  to  $j$ . The covariates  $Z$ , that were shown in Figure 4.1, are included in the covariates  $X$  to simplify the notation. This expression thus results in the probability of being in state  $j$  at time  $t$ , given that the state at time  $t - 1$  was  $i$  and the observations  $x_t$  are measured at time  $t$ . Every element in the transition

## 4. METHODOLOGY

---

matrix can consequently be written as equation (4.7). In order to assure that all elements on one row sum to 1, the normalisation, which is the denominator of this equation, is defined as the sum of all elements of that row. A separate MLR needs to be determined for every origin-state  $i$  of the Markov model.

### 4.4.2 Observations

The covariates used in the MLR are obtained from observations at the intersection. Two types of observations are distinguished: trajectory observations and circumstantial observations. The former type is the observation of a probe vehicle, decomposed into its variables such as the travel time, the number of stops, and the average duration of these stops. The latter type comprises of observations of the intersection from other sources such as the traffic demand or the congestion level at downstream intersections. An overview of the included covariates is given in Section 5.2.2.

The trajectory observations are gathered as soon as the probe vehicle passes the intersection since the lane on which the vehicle was travelling needs to be determined. The observations are attributed to the first time step after the time of passage. Due to the limited penetration rate and the stochastic nature of the presence of loop detectors, it regularly happens that multiple observations are made during a cycle, or inversely that no observations are made.

The case where multiple probe vehicles are present during one cycle is handled by averaging the covariates of these trajectory observations. This is suboptimal as the high-frequent changes in urban traffic cause significant differences in the experienced traffic state, even when vehicles are present during the same cycle. If one probe vehicle shows a clear indication of a certain state, and the other shows only mild signs of being in that state, these clear indications are smoothed out. This is not necessarily a problem and might even be desirable as it indicates that only some vehicles during the cycle experienced the state completely.

The case where no probe vehicle is present during a cycle is more problematic as the transition probabilities need to be calculated even though no new information of the trajectories is available. There are two options considered in this research. A first option is to assume that the latest measurements remain the best indicator of the current traffic state, resulting temporarily in an almost stationary transition probability matrix. This could introduce a bias in the state distribution as the transitions occur according to potentially outdated information [Liu, 2016]. A second option is to replace the transition probability matrix by a stationary one for cycles without probe vehicles. When there is low autocorrelation between successive cycles, this might be a safer option as the transitions occur according to historical data, rather than to an earlier observation. Of course, combinations of these options are also possible, where the estimated transition probabilities slowly decay towards historical ones as long as no new observations come in. The first option is chosen in the initial model as the vehicles' characteristics are not expected to change drastically

between successive time steps.

The circumstantial covariates do not encounter these problems, as they generally do not directly rely on the FCD. They can be obtained at every time step from loop detector data, a parallel implementation of the HMM on a downstream intersection, or other data sources which predict the state at these discrete time. If these sources measure their data asynchronously compared to the HMM on the upstream intersection, similar approaches to those for the trajectory covariates can be taken.

#### 4.4.3 Training the Model

The MLR is trained based on a historical time series of the true state, further referred to as the ground truth, and a time series of both trajectory and circumstantial measurements. The dataset with trajectory observations is divided in smaller subsets based on the state in the cycle prior to the observation, resulting in  $L$  subsets.

Next, a MLR can be calibrated for each subset. Separate coefficients  $\beta_{ij}^k$  and the intercepts  $\mu_{ij}$  are estimated for every origin-state  $i$  except for the reference state  $L$ , using a Maximum Likelihood Estimation. This technique determines the set of coefficients that maximises the likelihood that a series of observations was generated by the respective ground truth [Myung, 2003].

In order to evaluate the fit of the MLRs, the estimated coefficients are interpreted by checking whether the sign coincides with the expected influence of the covariate. Moreover, the size of the coefficients can be compared in absolute terms if the covariates are normalised, resulting in the relative importance of the corresponding covariates. Furthermore, the confidence interval of the estimated coefficient can be assessed to evaluate the certainty on it.

The regression models can also be pruned by running the model without one of the variables. If the pruned model achieves a similar accuracy as the full model, the variable has limited explanatory value and can be left out.

### 4.5 Evaluation of Results

In order to evaluate the overall performance of the HMM, two types of metrics are used. Some metrics evaluate the correctness of the most probable state, while others take the probability at which the states are predicted into account.

A first evaluation is based on the confusion matrices and the accuracy. Here, the predicted state distribution for each cycle is brought back to a deterministic one, where the most probable state is chosen as the prevailing state. Next, it is possible to count the number of correctly predicted cycles, as well as the number of falsely classified ones. The accuracy of the model can be defined as the percentage of correctly predicted cycles over the measuring period. This can either be

#### 4. METHODOLOGY

---

done for all states together, leading to an overall accuracy, or for each state separately.

A disadvantage of the accuracy-metric is that it measures the performance of the model only on the deterministic state classification. Consequently it is quite strict, as it might be that two states are almost equally probable according to the state distribution, but the incorrect state has a slightly higher probability. In this situation, the model's performance is equal to that of a model that predicts a low probability for the correct state. In order to account for these distributions, the log loss (cross-entropy loss, LL) is calculated, which compares the true state with the model's predictions [Rusiecki, 2019]. The formula of the log loss is given by:

$$LL(y, p) = -\frac{1}{T} \sum_{t=1}^T \sum_{l=1}^L (y_l^t \cdot \log(p_l^t)), \quad (4.8)$$

where  $L$  is the number of states,  $T$  is the total number of time steps in the validation set,  $p_l^t$  is the predicted probability of being in state  $l$  at time  $t$  and  $y_l^t$  is 1 if the ground truth indicates state  $l$  at time  $t$  [Rusiecki, 2019]. The cross-entropy loss can take any non-negative value, and a lower log loss is considered better.

The HMM's performance is compared to two reference models. The first model, referred to as the null-model ( $M_0$ ), predicts a constant state distribution based on the ratio of the state's occurrences in the training data. The second model ( $M_1$ ) is a MLR with the same covariates as the HMM, but is trained on the full dataset. It classifies the observations in each iteration to a certain state without considering the state in the previous time steps.

### 4.6 Summary

In this chapter the theoretical layout of the proposed model has been explained. This model is a Hidden Markov Models consisting of two interlocked stages, where a state distribution is predicted using a discrete-time finite-state Markov model. Its transition probabilities are non-homogeneous and depend on observations of the probe vehicles as well as on circumstantial information on the intersection. This dependency is modelled with a MLR for every prior state.

To evaluate the model's performance, several metrics are introduced, where the accuracy and the log loss are the most important ones. The performance of the HMM is compared to a null-model that predicts a constant state distribution and a MLR that classifies the states without considering the prior state distribution.

The method is applied to the case study in the next chapter. It mainly handles a practical definition of the ground truth and the covariates. The results of the models is also discussed in that chapter.

# Chapter 5

## Model Implementation

In the previous chapter, a method was proposed to distinguish spillovers and determine a saturation level on urban networks. This method is based on a HMM, where a first-order Markov model is complemented by a MLR that estimates the transition probabilities based on observations on the network. This chapter applies the model to the simulated counterpart of a real-world case study. This simulation allows to evaluate the method under varying circumstances and limits the complexity of the implementation by removing the measurement error and delineating the ground truth clearly. Furthermore, the chapter defines the covariates that can be included in the model. Lastly, the obtained results are evaluated and discussed.

### 5.1 Case Study

As introduced in section 1.2.3, the model is applied to a case study in Deventer, the Netherlands. Below, the layout of the intersection and the assumptions in the simulated counterpart are presented. This microsimulation is built in *VISSIM* and produces equivalent data to the real-life case. Furthermore, the different regimes used to train the model are elaborated.

#### 5.1.1 Network

The case study consists of a network with four successive intersections, which are schematically presented in Figure 5.1 as A026, A023, A020 and A010. Each intersection has multiple incoming and outgoing links that consist of up to four lanes. They connect an arterial road, the N344, with local roads going to the city centre. Due to the abundance of short links between the intersections, spillovers occur regularly and cause significant disturbances to many stakeholders.

The intersections A026 and A023 are selected for a closer analysis which aims to detect spillovers on the lane of the intersection A026 that is labelled *researched lane* in Figure 5.1. It connects to the downstream lanes DL1, DL2 and DL3 of intersection A023, on which the model is implemented as well in order to obtain a

## 5. MODEL IMPLEMENTATION

---

downstream state estimation.

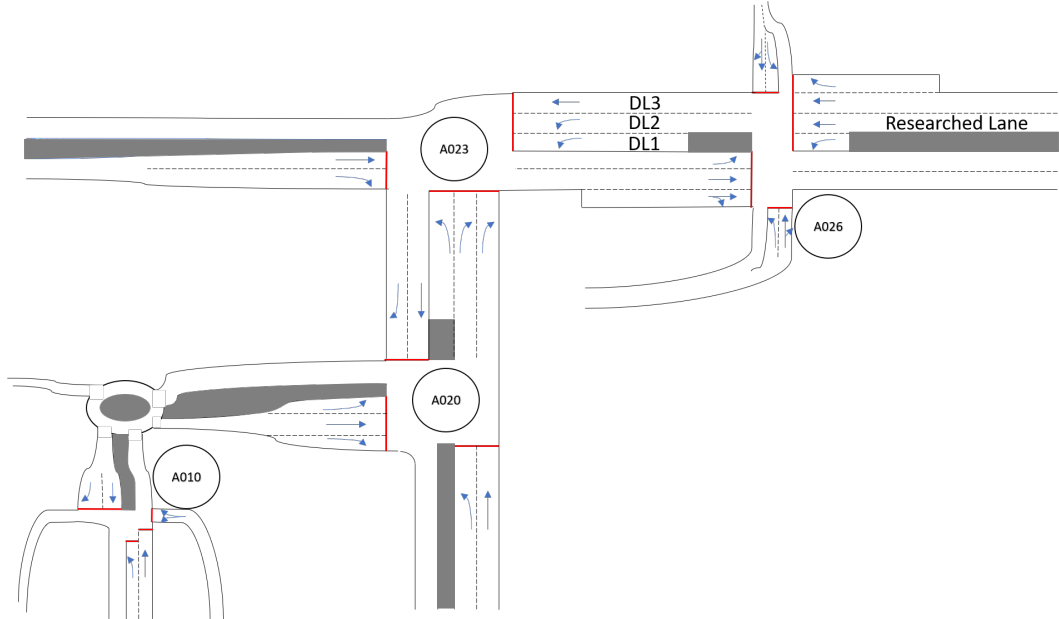


Figure 5.1: Schematic representation of the network. The four intersections are indicated with their respective IDs, the red lines represent the stop line where traffic signals are present, the lane labelled *Researched lane* is examined closer for the development of the tool, while the downstream lanes of this approach are labelled DL1, DL2 and DL3.

The intersections are regulated by an adaptive traffic signals control system which uses the loop detector's presence detections to decide on the signal cycles that would minimise the total delay [Gao et al., 2020]. Consequently, they change dynamically and are hard to estimate without knowledge of the implemented control systems. Since the traffic signal state is available in the historical dataset, an approximation is made where two time periods in the peak and off-peak hours are used as representative signal cycles for the simulation.

### 5.1.2 Simulation

A microsimulation based on the real network is built as this allows to generate the necessary traffic data in a controlled setting. Consequently, the simulation allows to establish a ground truth for every time step, to artificially moderate the traffic states that prevail on the network, and to evaluate the model under different penetration rates.

After carefully replicating the layout of the network in *VISSIM*, several simplifications are made compared to the real-world. The first simplification comprises the

implementation of the traffic signals, which are approximated by fixed ones since the real-world control strategy is not available. This simplification does not have a major effect on the methods if the signal cycles are known, as they can easily be extended to include the variable signal cycles. When the true signal cycles are not known, the methods will not function properly as the covariates' interpretation changes drastically. The second simplification entails the route choice of the drivers, which is based on the average loop detector counts over a 30-day period. Currently, they are assumed stationary over the simulation period, even though they change over time in reality. This does not impact the methods' definitions significantly, but makes the simulation less compliant with reality. Lastly, the traffic inflow rates are imposed on the network. They are initially based on the loop detector counts and are iteratively adapted until the appropriate congestion patterns were found on the researched lanes.

## Simulated Data

The simulated setting provides idealised equivalents of the data sources available in this thesis. The vehicle records are the equivalent of the FCD and contain the accurate locations and driving speed of all vehicles on the network at a 5 Hz resolution. These accurate measurements can be used to determine the lane on which the vehicle travels in real-time. However, as the aim is to approach reality as closely as possible, the pseudo-online setting is maintained. The penetration rate of 100% in the vehicle records is used, however, as it allows for an accurate estimation of the ground truth. Furthermore, the traffic signal state can be obtained for every signal group, which are processed in a similar way to real-life data.

## Simulated Regimes

The traffic state on the two selected intersections is simulated under three different regimes: a low-spillover, medium-spillover and high-spillover regime. In the low-spillover regime there are some runs where no spillovers occur, whereas on average one or two brief spillovers take place. The high-spillover regime consists of multiple spillover periods which are often sustained for longer durations. The medium-spillover regime is somewhere in between the two other regimes. These different regimes are created by adapting the traffic signal cycles at the downstream intersection: shorter green cycles result in more spillovers for the researched lane.

Every regime is simulated for 20 simulation runs of 5 hours with a 2-hour peak period. Fifteen of these runs are reserved for training the model, while five are used for validation purposes. The demand level in each simulation run is similar but not equal as small random perturbations are included in the arrival patterns.

## 5.2 Implementation

The application of the proposed methods to the simulation is discussed in this section. The HMM is introduced in Chapter 4 as a discrete-time, finite-state Markov Model with non-homogeneous transition probabilities. It consists of two stages: a first-order Markov model and a logistic regression model. The implementation of the Markov model entails decisions on the time step and the number of traffic states. The training of the logistic regression model requires the definition of the ground truth and of the included covariates. The second method that only uses the MLR to predict the traffic state, follows identical implementation steps to the second stage of the HMM.

### 5.2.1 The Markov Model

The Markov model predicts a new state distribution with a time step of 1 min. This time step can be chosen according to the desired application. However, an excessively long cycle will result in a high time lag and in overlooking short-lived states. On the other hand, a very short time step is also undesirable as it decreases the number of probe vehicles that pass the intersection per cycle, especially if the time step is lower than the traffic signal cycle.

The model distinguishes five states that can prevail on the intersection. It can be in undersaturation ( $U$ ), which is the lowest level of saturation. Furthermore, three levels of oversaturation ( $O_1$ ,  $O_2$ ,  $O_3$ ) are defined, where in  $O_1$  some vehicles stop more than once, and in  $O_3$  all vehicles stop multiple times while approaching the intersection. Finally, the spillover state ( $Sp$ ) occurs when the first vehicle in the queue has to stand still for a different reason than a red signal.

### 5.2.2 The Logistic Regression Model

The transition probabilities used in the Markov model are determined by a MLR, based on trajectory and circumstantial observations. Its general formula is given by equation (4.7). These MLRs need to be trained separately for every origin-state. The work flow of the conversion from the simulated data to the training of the model looks as follows: (1) the simulated trajectories are allocated to time step  $t$ , which is immediately after they passed the intersection; (2) the ground truth for each time step is determined; (3) the trajectories are decomposed into their covariates, which are normalised between 0 and 1; (4) the trajectories are split into subsets according to the state in the previous cycle; and (5) the coefficients are estimated using the MLE-method defined in the *sklearn*-package in Python.

This section first discusses how a ground truth can be obtained in the simulated setting. Next, the covariates that can be included in the models are defined.

### Ground Truth

In order to train the model, knowledge of the true state present during a certain cycle is primordial as the MLR is a supervised learning technique. Defining this ground truth is straightforward in the simulated setting since the trajectory of every vehicle on the network is available.

The level of oversaturation is defined by the average number of stops of all vehicles assigned to the examined time step. In undersaturation  $U$ , the average number of stops should be lower than 1, as in the limit each vehicle has to stop once. The oversaturation levels  $O_1$ ,  $O_2$  and  $O_3$ , are divided based on an increasing average number of stops, as shown in Table 5.1. Furthermore, spillovers  $Sp$  are classified based on the stop-and-go pattern of the first vehicle on the approach to the intersection, i.e. the vehicle that is closest to the stop line. If this vehicle stands still while the traffic signal is green, a spillover is present. A small time margin is added to this definition as the driver does not react instantly to a green signal.

State	Classification criterion
$U$	$0 \leq n < 1$
$O_1$	$1 \leq n < 2$
$O_2$	$2 \leq n < 3$
$O_3$	$3 \leq n$
$Sp$	Standstill period of first vehicle in the queue coincides with green signal

Table 5.1: Classification of the states in the model, where  $n$  equals the average number of stops of the vehicles during the approach to the intersection.

A major problem with the definition of spillovers is that vehicles are only added to a time step as soon as they leave the intersection. Vehicles are by definition standing still during spillover, and their attributes are consequently assigned to the cycles after the actual spillover. Therefore, these later cycles should also be classified as state  $Sp$ . These additional cycles are further referred to as the spillover's effective duration. Two different definitions of the effective duration are implemented and the resulting models are compared. A first option is to extend spillovers with a fixed time interval of two time steps, as shown in Figure 5.2a. A second option is to make the effective duration dependent of the true spillover duration, as shown in Figure 5.2b. This is plausible, as longer spillovers affect more vehicles and are thus present in more cycles after the spillover. Both definitions are tested and the resulting performance of the models compared, where the second definition showed slightly worse results than the first definition, leading to the implementation of this definition.

Another key issue is that, contrary to the classification of the saturation level

## 5. MODEL IMPLEMENTATION

---

where all vehicles experience the prevailing state up to a certain degree, it is possible that some vehicles assigned to time step in spillover while they did not experience the spillover, as shown in Figure 5.2a where the effective duration starts before the actual spillover is present. This causes the inclusion of non-spillover trajectories in the training set for spillover states, polluting them for the model’s training. To prevent the presence of too many polluting trajectories, cycles where a spillover ends near the end of the cycle are classified as non-spillover and the next cycle is classified as spillover, as shown in Figure 5.2c. A trade-off is made between the inclusion of some strongly affected trajectories and the exclusion of polluting trajectories.

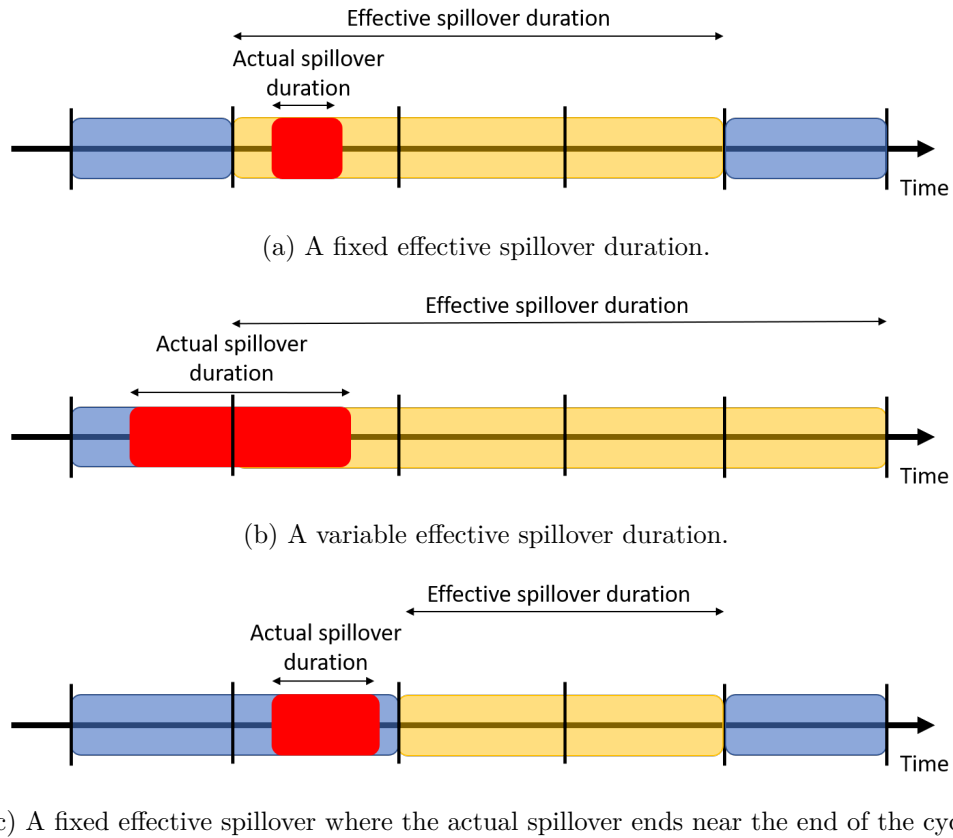


Figure 5.2: Two definitions of the effective spillover duration and the definition of later starts for spillovers that end near the end of the cycle.

In the ideal scenario, the effective duration would start at the same time as the actual spillover and end when the last affected trajectory leaves the intersection. However this requires a continuous-time model and results in long spillover durations as they last until the last vehicle in the queue leaves the intersection.

## Covariates

The observations used as covariates in the MLR are discussed in this section. Generally, the division is made between trajectory and circumstantial covariates, where the former are observed when the probe vehicle passes the intersection, and the latter at every discrete time step. A summary of the considered covariates is given in Table 5.2.

**Travel Time** The travel time on the approach to the intersection is the duration between the probe vehicle's entrance on the approach and the moment when the intersection's stop line is crossed. Obviously, this variable is expected to play a major role in the classification of the saturation level, as longer travel times are the result of a higher saturation level. Moreover, the travel time is hypothesised to be slightly higher in spillover states, but this effect is expected to be less pronounced since spillovers often occur when the saturation level is high.

**Number of Stops** Similarly, the number of stops a vehicle makes during its approach to the intersection is extracted from the observations. This requires a filtering technique to determine when a stop started and how long it lasted. The assumption is made that a vehicle joins a queue as soon as its speed decreases to less than  $5 \frac{km}{h}$  [Ma et al., 2014]. Moreover, stops are only counted if they last more than 2 seconds. The variable is expected to have a comparable effect on the state estimation to the travel time, and is probably highly correlated to that variable. Therefore, the model is tested with and without the number of stops as a variable in order to check whether it has added value. The performance of the models appears similar. Consequently, the variable is not included in the eventual model since it does not contain additional information on the dependent variable.

**Average Duration of Stops** Related to the number of stops, the average stopping duration is a clear indicator of spillovers as these states are characterised by a stop that is longer or shorter than the red cycle time. During long spillovers, early stops or late departures, the vehicles experience a standstill longer than the red cycle, while during short spillovers, the standstill period typically lasts a limited time. The logit model is not well suited for covariates that have a low and a high level to indicate increased probabilities for a certain state [Stoltzfus, 2011]. Consequently, the variable is replaced by the maximal and the minimal duration of stops.

**Maximal Duration of Stops** This covariate explicitly represents the longer stops that occur during long spillovers, early stops and late departures. During these types of spillovers, the duration of stops is expected to be higher than the red cycle time, while during standard operations the stops are less than or equal to the red cycle time. As the start shockwave is faster than the stop wave, the stop duration will be shorter the further the vehicle is away from the intersection. Not every affected vehicle will consequently experience this longer stop.

## 5. MODEL IMPLEMENTATION

---

Covariate	Type	Description	Included?
Travel time	Trajectory	Travel time during the approach	Yes
Number of stops	Trajectory	The number of stops during the approach	No
Average stopping duration	Trajectory	Average duration of the stops during the approach	No
Minimal stopping duration	Trajectory	Shortest stops during the approach	Yes
Maximal stopping duration	Trajectory	Longest stop during the approach	Yes
Time on the intersection	Trajectory	Travel time over the intersection	Yes
Shockwave	Trajectory	Difference between interpolated start wave and the start of the green cycle	Yes
Traffic demand	Circumstantial	Upstream inflow rate towards the intersection	No
Downstream state	Circumstantial	State estimation on the downstream intersection	Yes
Traffic signal timing	Circumstantial	Duration of the green and red signal cycles	No

Table 5.2: Summary of the considered covariates.

**Minimal Duration of Stops** Similarly, the minimal duration of stops explicitly represents the short spillovers. Due to the stops caused by lane-changers and the stochastic arrival pattern of the vehicles, which result in vehicles potentially arriving at the back of the queue and only standing still for a short period, the variable is not a very reliable indicator of spillovers. It is therefore expected to have a limited influence on the transition probabilities.

**Time on the Intersection** Spillovers are caused when a queue from downstream spills back onto the intersection, which blocks the entry of new vehicles. Therefore, it is reasonable to look at the time a vehicle has spent on the intersection after crossing the stop line of the upstream link and before entering the downstream link. If this takes longer than usual, a blockage must be present.

These longer travel times are often only experienced by the blocking vehicles that cause the actual spillover. Vehicles that experienced the spillover on the examined lanes leave the intersection when the blockage has cleared and therefore do not have to wait as long. These irregularities make it more difficult to distinguish spillover cycles from non-spillover cycles based on this covariate only. Nevertheless, the covariate is expected to be an important covariate as it occurs only in spillover situations.

**Shockwave** It is also possible to extract information based on the LWR-model, as proposed in Ramezani and Geroliminis [2015] and Wang et al. [2017]. The definition of this variable is based on the assumption that under normal conditions the vehicle's stop-and-go pattern is dictated by the traffic signals [Rempe, 2019]. Consequently, the start and stop shockwaves travel upstream from the intersection at the time of the signal change, and the vehicles adjust their speed accordingly when they cross a shockwave. In spillover situations, the vehicle's behaviour is no longer dictated by the traffic signals alone. The shockwave that is experienced by the observed trajectory does not coincide with a traffic signal change, as depicted in Figure 5.3 by shockwave 2.

The covariate is thus defined as the time difference between the traffic signal change and the intersection of the shockwave with the stop line. This difference is calculated for every stop that the vehicle had to make during its approach and the maximal value over all stops is selected as the variable's value. In order to account for occasional faster reactions than expected, the variable can be slightly negative, as shown by shockwave 3.

Theoretically, this analysis could be done for both the stop and the start waves. However, the stop wave is much less reliable since it depends on the arrival pattern of the vehicles, resulting in piecewise linear waves that are hard to estimate without an additional data source upstream. Therefore, this shockwave is not considered in this thesis. On the contrary, assuming the start wave to be linear with a fixed slope is a more realistic assumption since it has the fastest wave speed

## 5. MODEL IMPLEMENTATION

---

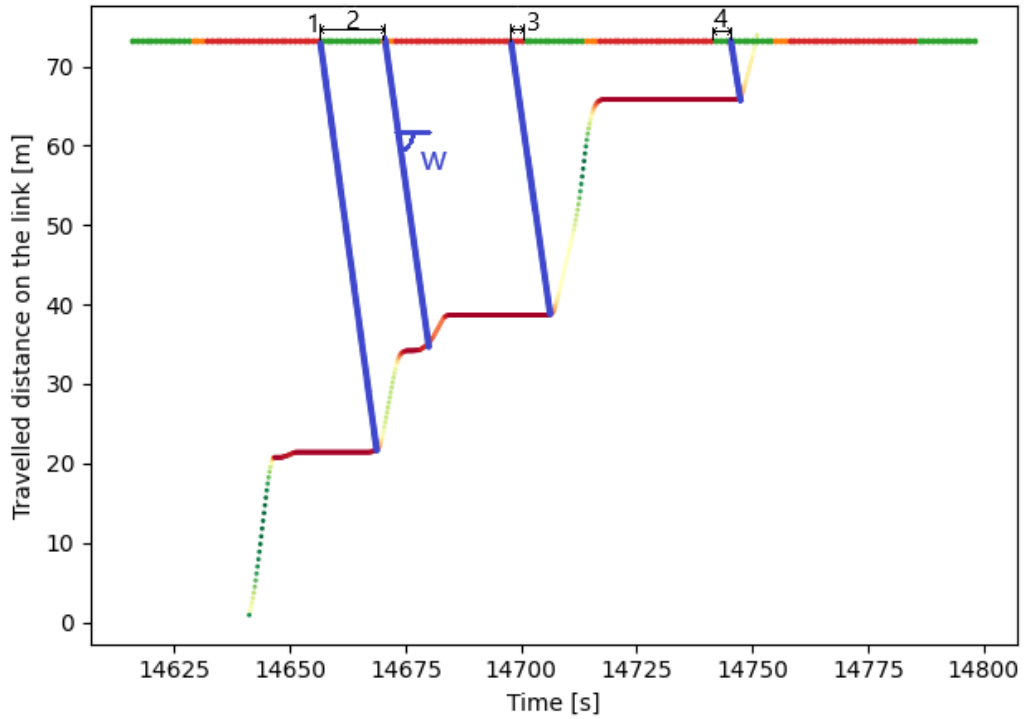


Figure 5.3: Example of a trajectory with the start shockwaves for each of its four stops. Shockwave (1) perfectly coincides with a green signal, (2) does not coincide with a green signal due to a short spillover, (3) is faster than expected and causes a negative deviation from the green signal, (4) is slower than expected and causes a positive deviation from the green signal.

on the link and can consequently not be disturbed by other upstream travelling waves.

In order to estimate the slope of the start shockwave, an empirical fundamental diagram is ideally used. This is not possible in this thesis due to the lack of accurate vehicle length estimates to calculate the fundamental parameters with single loop detectors, as discussed earlier. Therefore, the slope of the shockwave is estimated based on the experienced shockwaves. For every link in the network, multiple sequences of two consecutive trajectories are examined and the difference in time and location of the vehicles' acceleration point is used to find the average start wave. The assumption is made that the shockwave's slope is constant at all times, which is not necessarily true under different circumstances such as rain, nighttime, and changing vehicle mixes [Liu et al., 2020]. Moreover, some drivers might react slower or faster than average to the changing traffic signal, causing small deviations in the shockwave's slope.

Under high oversaturation the preliminary data analysis of the covariate shows a high difference between the shockwave's intersection with the stop line and the

time of the signal change. Three reasons can be found for this. A first reason is that as the queue becomes longer the drivers' reactions accumulate and the shockwave becomes less reliable. A second reason is that further away from the intersection the layout of the road changes, resulting in different shockwave speeds. A third reason is that in congested traffic lane-changing vehicles are more likely to cause short queues when waiting for a sufficient gap to change to the neighbouring lane. Consequently, the shockwave is less reliable when it is caused by a stop further away from the stop line. Therefore, a non-linear combination of the covariate with the distance of the concerned stop is proposed, reducing the value of the covariate when the stop is further away from the stop line. It is however also important that stops close to the intersection are not over-prioritised since they rely heavily on the reaction time of one or two vehicles. The weight function that resulted in the best performance of the model is a quadratic function with a maximum in the middle of the link. The equation of this smoothing factor is thus given by

$$\sigma = \begin{cases} \frac{-1.4}{g^2} \cdot x^2 + \frac{1.1}{g} \cdot x + 0.8, & \text{if } x \leq g \\ 0.5, & \text{if } x > g \end{cases} \quad (5.1)$$

where  $\sigma$  is the smoothing factor that is multiplied with the initial variable,  $g$  is the length of the link and  $x$  is the position of the stop.

**Traffic Demand** At times of high demand, the transition probabilities towards oversaturated and spillover states are higher than when there is low demand. This variable is therefore expected to play an important role in the proposed model. Measuring the traffic demand is not possible when only FCD is available, except when an exact penetration rate is known [Sunderrajan et al., 2016]. Therefore, other data sources such as loop detectors should be present if one wants to include this covariate. Alternatively, if historical data on the traffic flow per hour is available, either through temporary counting methods or through a well-calibrated traffic assignment model, the variable could take a value strictly depending on the time of day. This option is obviously less suited for days where the demand varies in comparison to a regular day.

**Downstream State** Spillovers are caused by the queues on a downstream link spilling back onto the intersection. Consequently, the traffic state on these downstream links should play an important role in the prediction of spillovers. For example, when all downstream links experience low saturation levels, it is highly unlikely that the upstream link is in a spillover state. The other way around, when there is high congestion on at least one of the downstream links, the probability of spillover on the upstream links increases.

The downstream state is expressed as a general score that comprises the state distribution on the downstream links that might have a direct or indirect effect on the upstream link. The calculation of this score consists of two steps: the determination of a score per lane and the aggregation of these scores to a general congestion level.

## 5. MODEL IMPLEMENTATION

---

The score per lane is calculated as the weighted sum of the estimated state distributions:

$$C_{lane} = \alpha_1 p_1 + \alpha_2 p_2 + \alpha_3 p_3 + \alpha_4 p_4 + \alpha_5 p_5 \quad (5.2)$$

where  $\alpha_l$  represents the influence of the different states on traffic spillback. For instance,  $\alpha_0$  represents the influence of undersaturation on the upstream intersection and has therefore a low value, whereas  $\alpha_3$  and  $\alpha_4$  have higher weights as they represent high saturation levels and spillover, respectively.

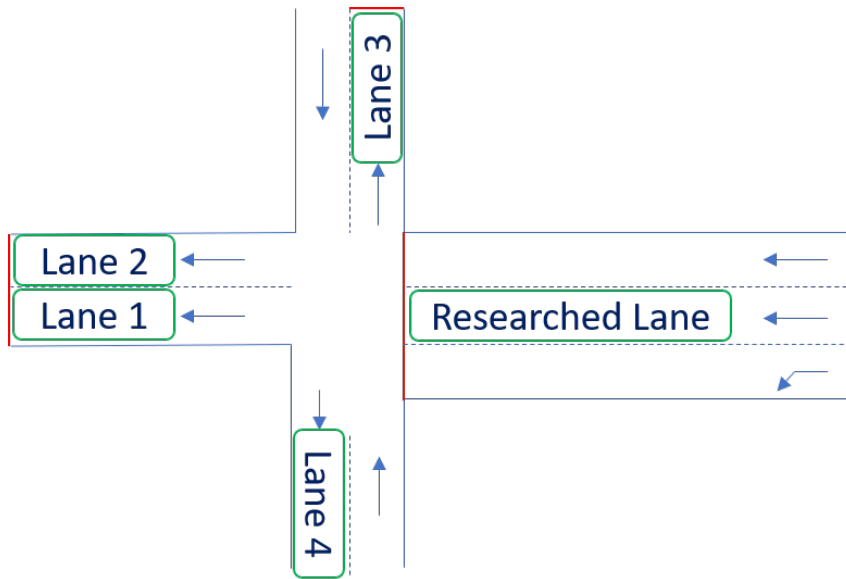


Figure 5.4: Example of a simplified intersection, where lane 1 is a directly connected downstream lane with respect to the researched lane, and lane 2, 3 and 4 are indirectly connected downstream lanes.

Next, the scores per lane are aggregated over all downstream lanes. Here, a distinction is made between lanes that directly connect to the lane on which a state estimation is being made, and lanes that are only connected after a lane change or a turn, as illustrated in Figure 5.4. The former types is expected to have a higher importance in the score estimation, whereas the latter lanes influence the state only indirectly and consequently have a lower weight. These weights  $\gamma_{lane}$  can be calibrated beforehand, or can be guesstimated. The score is determined by

$$X_{downstream} = \sum_{lane \in downstream\ lanes} \gamma_{lane} C_{lane} \quad (5.3)$$

An important limitation of this covariate is that it requires the state distribution on the downstream links. If there are no intersections downstream on which the

proposed spillover detection model can run simultaneously, the score cannot be calculated in this way and other data sources are required.

**Traffic Signal Timing** In the simulated setting, the traffic signal cycles are assumed fixed, i.e. every signal cycle has exactly the same duration. Nowadays, many traffic signals in reality are actuated, which means that they change according to the detection of vehicles on the approach [Eom and Kim, 2020]. A signal control scheme is used to indicate the minimal green cycles and the priority rules when multiple vehicle detections occur on different approaches at the same time [Eom and Kim, 2020].

The traffic signals are expected to play a major role in the interpretation of certain variables such as the average duration of stops and the travel time. Therefore, this variable could be included in a non-linear transformation of these variables, for instance by taking the ratio of the maximal stop duration and the duration of the current red cycle. As fixed cycles are currently implemented in the simulation, the variable is not included in the presented model.

### Summary

The previous section discussed the implementation of the HMM on the simulated network. This requires first the definition of the time resolution, which is chosen to be 1 min. Next, the five different states are defined: undersaturation  $U$ , three levels of oversaturation  $O_1$ ,  $O_2$  and  $O_3$ , and a spillover state  $Sp$ .

Determining the ground truth is rather straightforward for the simulated case as all vehicles on the network can be analysed. However, the pseudo-online setting warrants the extension of the actual spillovers to an effective spillover duration in order to include the directly affected vehicles.

Lastly, the covariates included in the MLRs can be defined. The included variables comprise of four trajectory variables and one circumstantial variable. Other variables can be imagined, but are not included due to constraints of the MLR or because they do not make sense in the simulated setting.

The HMM is compared to a MLR without inclusion of the prior state. This MLR is trained similarly to the HMM, except for that it is not necessary to split the training data in smaller subsets. The outcomes of this model indicate the probability of being in a certain state rather than the probability of transitioning from one state to another.

## 5.3 Results

After implementing the model as discussed above, the model's performance can be analysed. Below, the estimated coefficients of the MLRs in the HMM are examined.

## 5. MODEL IMPLEMENTATION

---

This allows to find whether the covariates behave according to the expectations discussed in the previous section. Next, it is possible to compare the performance of the HMM to the two reference models under different regimes and with different penetration rates for the FCD.

### 5.3.1 Validation of the Full Model's Logistic Regression Functions

The coefficients of the MLR for each origin-state can be interpreted: the sign of the coefficients is an indicator to assess the direction of the variable's effect, whereas their size indicates the relative importance of the respective variables in the model. The coefficients are defined relative to the reference category, which is chosen to be the origin-state of the model, as it is the most common transition in the subset. For example, the transition from  $O_3$  to  $O_3$  is chosen as the reference category for the dataset where the previous time step was in  $O_3$ . The coefficients for this dataset are shown in Table 5.3.

A first covariate that plays an important role in the model is the travel time over the link. As expected, the saturation level is mostly dominated by this covariate. Transitions to lower saturation levels can only occur if the travel time on the approach is low. The difference between  $O_3$  and  $Sp$  is much less pronounced, as both states have similar travel times. The coefficient suggests that higher travel times are an indicator of spillover, but its effect is rather limited.

A second interesting covariate is the time spent on the intersection. The highly positive coefficient for spillovers indicates that it is much more likely that a spillover occurs when the time on the intersection increases. This is to be expected as the travel time on the intersection are almost constant in non-spillover cycles.

Next, the downstream state also shows a high variable importance. It should be noted, however, that even though the scores for the downstream state are theoretically bounded between 0 and 1, the values are highly skewed towards the lower boundary. Still, it can be considered an important factor for both spillover detection and the level of oversaturation.

The minimal and maximal duration of stops have a limited influence on the transition probability to  $Sp$ . The directions of the influence is according to expectations as a lower minimal duration and a higher maximal duration result in higher spillover probabilities. The coefficients for the transitions to lower saturation levels indicate that they are more likely when the maximal stop is short and the minimum stop is high, i.e. when the traffic signals cycles are respected better.

Deviations from the start wave induced by the traffic signal appear to influence the transition probability to  $Sp$  only marginally. Large deviations are often present in  $O_3$ , despite the addition of the smoothing term for the distance to the intersection. It is hypothesised that a more restrictive smoothing factor should be implemented.

The coefficients for the other MLRs can be found in Appendix 7. In general, the same patterns as described above can be seen. The probabilities for moving from a low saturation state to  $Sp$  are in general lower than when the prior state is  $O_3$  since the coefficients are more negative in the former models.

Some important notes are required in order to correctly interpret these results, however. The sample size for certain subsets is rather limited. Especially the  $O_2$ -state is chosen too narrowly, resulting in potential overfitting on the trajectories that occur in the few  $O_2$ -cycles. This can be seen, for example, in the positive effect of the maximal stopping duration on the transitions from  $O_3$  to  $O_2$ , which is contrary to the expectations and the coefficients of the other transitions. This can easily be resolved by changing the classification of the ground truth such that the average number of stops for  $O_2$  spans between 2 and 6 stops, for example. State  $O_3$  is currently chosen too widely, which results in the very negative coefficients of the travel time for lower saturated states.

Furthermore the size of the coefficients cannot be compared between MLRs of different origin-states since the covariates are normalised before splitting it in subsets. The travel time, for instance, will therefore be bounded by 0 and 0.1 in the dataset for origin-state  $U$ , whereas it is bounded by 0.05 and 1 in the dataset for origin-state  $O_3$ . This can be resolved by normalising after splitting in subsets, but as this requires a separate normalisation for every trained MLR, this is not included.

### 5.3.2 Comparison of the Models

In this section, the performance of three different models are compared and discussed. The first model is the null-model  $M_0$ , which predicts a stationary state distribution equal to the states' ratios of occurrence in the training data. The second model is the logistic regression model  $M_1$ , which predicts the state based on the aforementioned covariates without including the state distribution at the previous time step. The final model  $M_2$  consists of the HMM that predicts a time series of state distributions based on the transition probabilities predicted by the five MLRs.

The models are trained on the joint dataset with the three different spillover-regimes with low, medium, and high levels of spillover, respectively. They are compared in this section for the artificial situation where one probe vehicle is available in every cycle. Consequently, the models do not have to extrapolate the state for cycles without probe vehicles. The influence of the penetration rate is discussed in Section 5.3.3.

The models are evaluated based on multiple metrics. The state classification is evaluated as a deterministic state to determine the overall accuracy and the accuracy of the spillover detections. Furthermore, the state distribution is evaluated as well: a

## 5. MODEL IMPLEMENTATION

---

Variable	Coefficient	Odd Ratio
Logistic Function from $O_3$ to U		
Intercept	-3.339	0.035
Travel Time	-16.551	<0.001
Min Stop Duration	3.664	39.017
Max Stop Duration	-4.822	0.008
Time on Intersection	2.863	17.514
Shockwave	-8.232	<0.001
Downstream State	0.067	1.069
Logistic Function from $O_3$ to $O_1$		
Intercept	0.208	1.231
Travel Time	-23.273	<0.001
Min Stop Duration	2.652	14.182
Max Stop Duration	-2.107	0.122
Time on Intersection	2.116	8.298
Shockwave	-14.762	<0.001
Downstream State	-3.610	0.027
Logistic Function from $O_3$ to $O_2$		
Intercept	1.464	4.323
Travel Time	-28.289	<0.001
Min Stop Duration	0.642	1.900
Max Stop Duration	5.659	286.862
Time on Intersection	0.310	1.363
Shockwave	-9.439	<0.001
Downstream State	-5.712	0.003
Logistic Function from $O_3$ to $O_3$ : Reference Category	0	1.000
Logistic Function from $O_3$ to $Sp$		
Intercept	-6.164	0.002
Travel Time	0.831	2.296
Min Stop Duration	-0.468	0.626
Max Stop Duration	0.444	1.559
Time on Intersection	10.506	>1,000.000
Shockwave	0.578	1.782
Downstream State	12.724	>1,000.000

Table 5.3: Resulting coefficients and odd-ratios of the logistic regression model from state  $O_3$  to all other states.

model that predicts a probability of being in spillover of 40% during actual spillovers is a better model than one that predicts a probability of 10%. This is measured through the log loss, both globally over all states and specifically for spillovers.

### Null-model $M_0$

The null-model predicts a stationary state distribution, based on the ratio of the state's occurrence in the training data. If the proposed models perform worse than this model, they do not have any predictive capabilities and are not capable of assessing the traffic state on the intersection. Its performance indicators are presented in Table 5.4. The accuracy is equal to the ratio of the most common state  $U$  since this state is predicted as the most probable one in every time step.

A [%]	LL	$A_{Sp}$ [%]	$LL_{Sp}$ [%]
30.38	1.500	0.00	0.305

Table 5.4: Accuracy (A) and log loss (LL) of  $M_0$

### Logistic Regression Model $M_1$

In Figure 5.5 the resulting state distributions are shown for the three different regimes. The low-spillover regime is represented twice, once for a period where some spillovers are present and once where no spillovers occur. The bar below the graph represents the corresponding ground truth. Visually, the pattern of spillovers is predicted accurately during all regimes. Even in the low spillover regimes, the result shows a clear increase in the probability of spillovers, although they are often not predicted as the most probable state. Longer and more severe spillovers in high spillover regimes result in better predictions, often with a spillover probability of over 90%. Due to the definition of the spillover states, which includes some cycles after the actual spillover, the estimation is regularly higher early on in the spillover duration but decreases quickly.

It is clear that the behaviour of the predictions is quite erratic as the previous state is not taken into account when predicting the current state. For spillover states, this can be a realistic behaviour, as they occur suddenly and only last for a limited number of time steps. For non-spillover states, the transitions are expected to follow a smoother pattern as the number of stops that a probe vehicle makes cannot drastically change in one time step. Moreover, the exclusion of a prior state estimate occasionally results in time steps that are very badly estimated when an extraordinary trajectory is observed, e.g. at time 1950 in figure 5.6a.

The model shows an overall accuracy of 70.23%. States in spillover are however only correctly classified in 54.15% of the total spillover-cycles. This is mainly due

## 5. MODEL IMPLEMENTATION

---

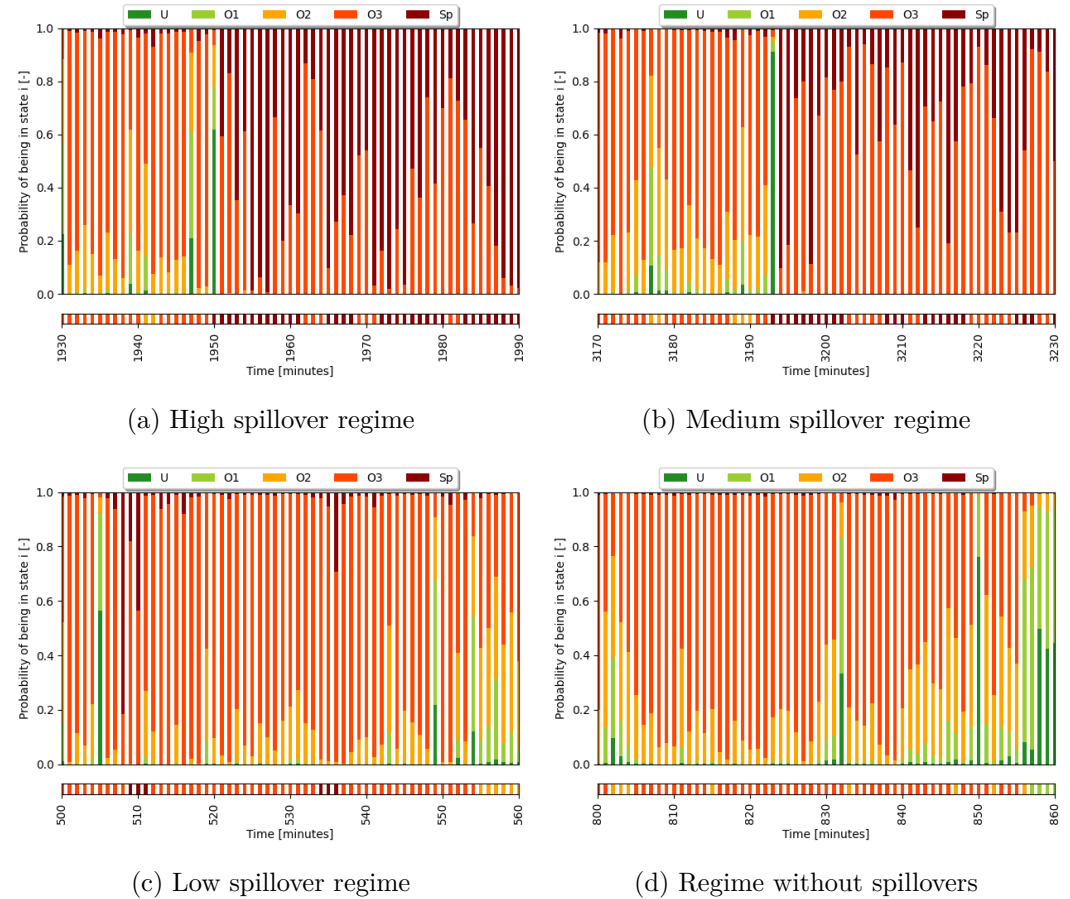


Figure 5.5: State distribution during peak-periods in the four regimes predicted by  $M_1$  with one vehicle per cycle. Each bar represents the state distribution at every time step, while the strips underneath the plot represent the ground truth for the corresponding time step. The surges in the spillover probability correctly coincide with spillover time steps.

to the regimes with limited spillovers, where they can clearly be distinguished from non-spillover cycles, but do not reach the highest probability. Moreover, the false detection rate of spillovers is on average 15.82%, which indicates the number of predicted spillover cycles that were actually non-spillover cycles. They mostly occur shortly before or after a true spillovers since the fixed definition of the effective spillover duration underestimates the spillover-duration in some cases. The log loss of the model is 0.679, which is considerably lower than the null-model, indicating that the estimations of the model coincide relatively well with the true state. When only considering the spillover detection, the model reaches a log loss of 0.122, which is better than  $M_0$  as well.

### Hidden Markov Model $M_2$

Model  $M_2$  is also run for one vehicle per cycle, resulting in the state distributions shown in Figure 5.6 for the same periods as before. Visually, the main peaks in the spillover probabilities coincide with the actual spillover periods in the ground truth. Contrary to  $M_1$ , the predictions now follow a much smoother pattern due to the inclusion of the previous state. Nevertheless, when a spillover occurs the model correctly identifies it relatively quickly, depending on the probe vehicles it measures. The duration of the spillovers appears to be slightly overestimated by the model, as it fades out too gradually.

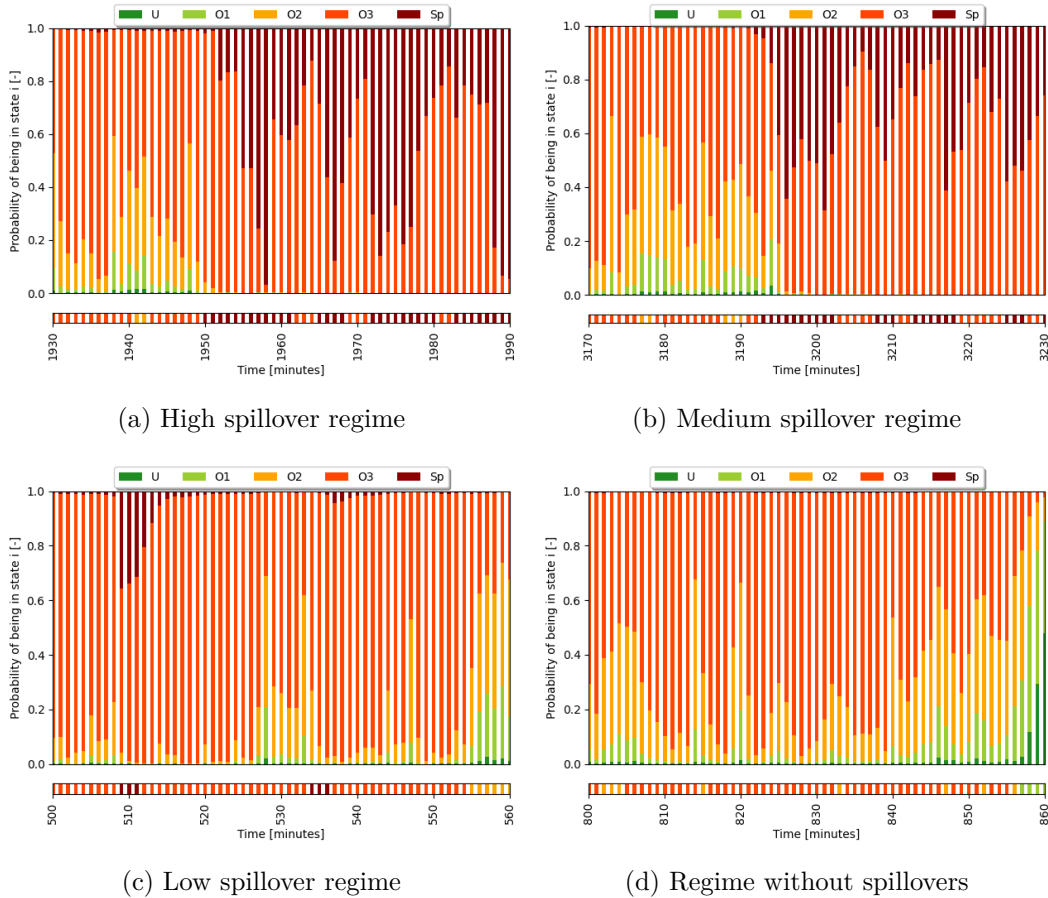


Figure 5.6: State distribution during peak-periods in the four regimes predicted by  $M_2$  with one vehicle per cycle. Each bar represents the state distribution at every time step, while the strip underneath the plot represents the ground truth for the corresponding time step. The surges in the spillover probability correctly coincide with spillover time steps and change more smoothly compared to  $M_1$ .

In Figure 5.7, the prediction over the 5-hour period can be seen for a medium-regime. This shows that the other states during off-peak periods are also predicted with high

## 5. MODEL IMPLEMENTATION

---

accuracy. The model is consequently usable for an overall traffic state estimation rather than only for spillover detection.

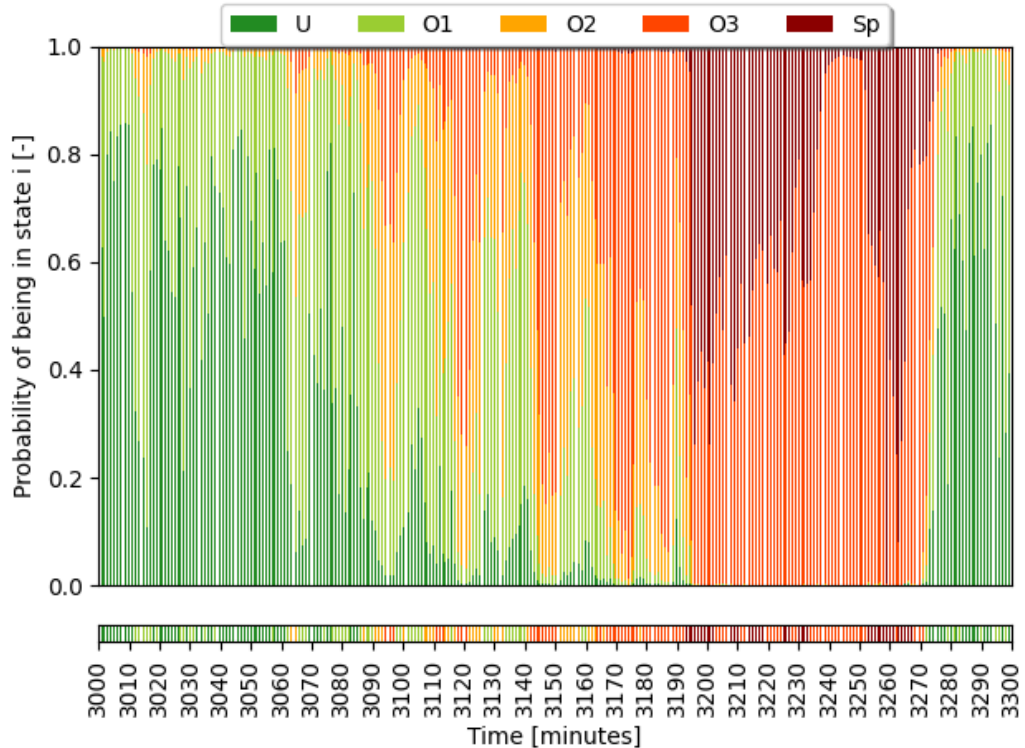


Figure 5.7: The state distribution of the 5-hour period in medium regime by  $M_2$  with one vehicle per cycle. Each bar represents the state distribution at every time step, while the strip underneath the plot represents the ground truth for the corresponding time step. The traffic state is correctly approximated for all states.

The model obtains an overall accuracy of 72.87%, and 48.09% of the spillover cycles are predicted as the most probable state. The number of correctly identified spillovers is thus lower than in  $M_1$  due to  $M_2$ 's more conservative predictions. However, the false detection rate of spillovers is slightly better at only 13.40%. This model thus predicts spillovers less frequently, but is more reliable than  $M_1$ . The overall log loss is 0.626, while the log loss for spillovers is 0.125. The model is consequently slightly better than  $M_1$  at predicting the smooth transitioning between saturation levels, but slightly worse at predicting the radical changes to spillover states.

### 5.3.3 Comparison of Penetration Rates

Next, the influence of the penetration rate on the models is discussed. Expectations are that  $M_1$  performs worse under low penetration rates, as there are multiple cycles where no probe vehicles are present and the model predicts almost constant

probabilities.  $M_2$  extrapolates the traffic state to those cycles using the previously estimated transition probabilities.

In Figure 5.8, the performance metrics for the models  $M_1$  and  $M_2$  are shown under varying penetration rates. Visually, the predictive capabilities of the models improve when more probe vehicles are present. This is an expected result as the models in that case need to extrapolate less. However, the metrics stagnate when the penetration rate increases further. This is also to be expected, as less cycles lack observations when the penetration rate increases. The additional probe vehicles will bring nuance to the other observations during the same cycles, but this does not improve the state estimation drastically.

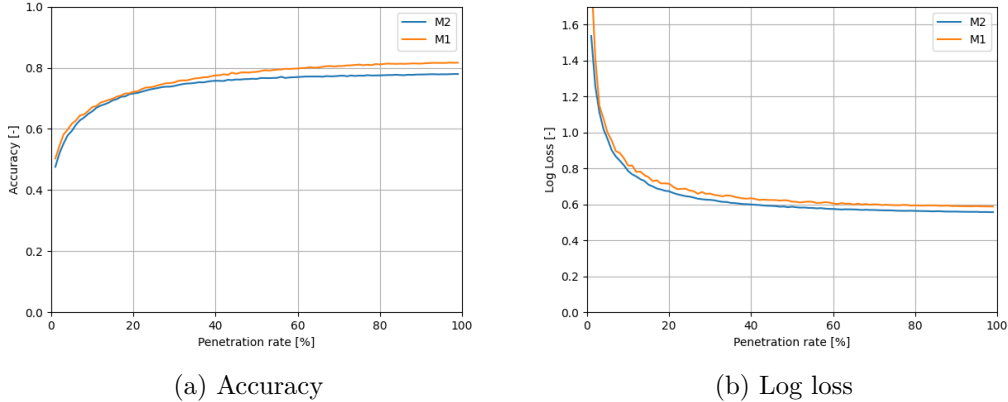


Figure 5.8: Comparison of the  $M_1$  (orange)- and  $M_2$  (blue)-model's accuracy and log loss.

$M_1$  and  $M_2$  have a comparable overall accuracy for low penetration rates. At higher penetration rates,  $M_1$  performs better as it makes less conservative predictions. The overall log loss is consistently lower for  $M_2$ , which indicates that it predicts the state closer to the ground truth. The same analysis can be done for the performance of the spillover detection. This shows a consistently better performance of  $M_1$ . This supports the conclusion that even though both models are able to detect spillovers, the addition of the Markov model results in state distributions that are too conservative and predict the sudden spillovers worse than  $M_1$ . However, the spillover states can be correctly identified when comparing the spillover probabilities over the time-period for both models.

At penetration rates lower than 2%, it is better to use the constant predictions of  $M_0$  than the predictions of the other two models. On the other hand, the marginal gain in performance decreases drastically when a penetration rate of about 10% is reached. In trade-off with the added costs for increasing the penetration rate, it can be decided that the current penetration rate of 10% is sufficient for the road

## 5. MODEL IMPLEMENTATION

---

authorities.

Furthermore, the resulting state distributions for the two models can also be visually compared for the lower penetration rates. The main advantage of the HMM becomes clear in Figure 5.9. In  $M_1$ , the state estimation remains almost stationary for cycles where no probe vehicles are available, resulting in the plateaux in Figure 5.9b. The changes in the state distribution only occur as a result of the changing downstream state variable. Due to the inclusion of the Markov model, the state estimation of  $M_2$  changes with the predicted transition probabilities in the previous cycle. This results in much smoother transitions between cycles, as long as the last probe vehicle showed the correct characteristics to change in the direction of the true state.

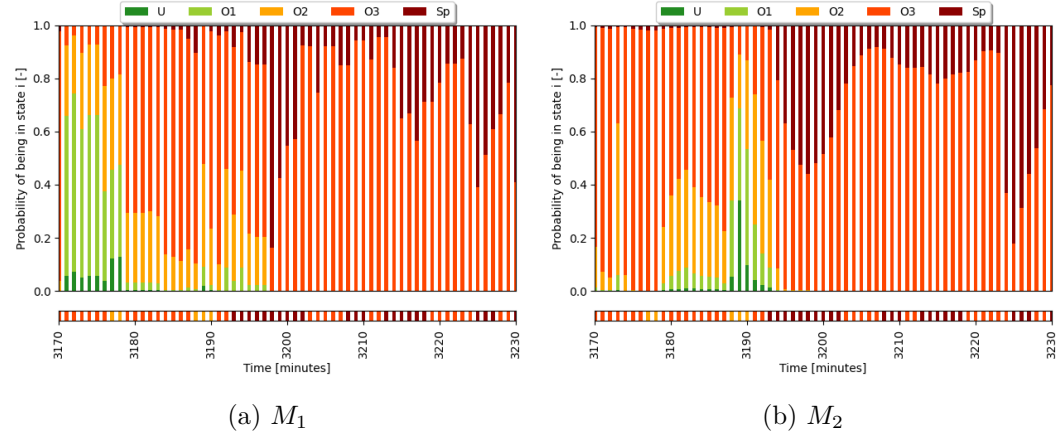


Figure 5.9: State estimation at 5% penetration rate for  $M_1$  (left) and  $M_2$  (right). Each bar represents the state distribution at every time step, while the strip underneath the plot represents the ground truth for the corresponding time step.

### 5.3.4 Overview of the Results

Finally, the results of the different models are summarised in Table 5.5. They show that even though  $M_1$  achieves a higher overall accuracy, its log loss is higher, which indicates that the state estimation is less reliable: even though more cycles are correctly classified, others are predicted to be less likely than with  $M_2$ . Only considering the spillovers,  $M_1$  obtains better results for both the accuracy and the log loss, as it is able to make stronger predictions.  $M_2$  underestimates the probability of spillover due to their short-lived nature, but is still able to clearly distinguish them from non-spillover cycles.

The previous analysis remains valid for all levels of the penetration rate.  $M_1$  consistently outperforms on spillover detection and accuracy measures, whereas  $M_2$  is better at estimating the overall traffic state. For the case with one vehicle per

$\rho$ [%]	$M_1$					$M_2$			
	A [%]	LL	$A_{Sp}$ [%]	$LL_{Sp}$	A [%]	LL	$A_{Sp}$ [%]	$LL_{Sp}$	
1	50.32	1.879	0.370	0.181	47.60	1.537	0.228	0.200	
5	61.69	0.998	0.442	0.148	59.31	0.963	0.313	0.156	
10	67.18	0.816	0.475	0.135	65.76	0.786	0.369	0.143	
20	72.15	0.715	0.520	0.124	71.61	0.673	0.416	0.132	
50	78.66	0.616	0.533	0.118	76.34	0.587	0.446	0.126	
100	81.67	0.589	0.541	0.115	77.96	0.557	0.457	0.125	
1 per cycle	70.23	0.679	0.543	0.122	72.87	0.620	0.483	0.125	

Table 5.5: Overview of the resulting accuracy (A) and log loss (LL) of  $M_1$  and  $M_2$  for different penetration rates  $\rho$ .

cycle,  $M_1$  shows a slightly worse performance than  $M_2$  in terms of overall accuracy. The other metrics for this case are in line with the findings for varying penetration rates. A reason for this strange result could not be found.

## 5.4 Summary

In this chapter the proposed method is applied to a case study, where four spillover-prone intersections are examined. Limitations of the FCD and the lack of a ground truth to train the model require the approximation of this network in a microsimulation for the validation of the model. This simulation reflects the real intersections, even though some simplifications and adaptations are made in order to include the desired amount of spillovers and level of oversaturation. A 5-hour period with one peak in demand is simulated under one of three regimes with a low, medium and high amount of spillovers respectively.

Next, the practical implementation of the model is elaborated. This mainly entails the definition of the ground truth and a discussion on the covariates to be included in the model. Five states are distinguished: undersaturation, three levels of oversaturation and spillover. The saturation level is distinguished based on the average number of stops in a cycle, whereas spillovers are found by examining the stop-and-go pattern of the first vehicle in the queue. The included covariates in the MLR consist of the observations of trajectories and of the intersection.

Finally, the results obtained by the Hidden Markov Model under different penetration rates are presented and compared to two reference models: a static random model and a MLR without inclusion of the prior state. Overall, the proposed HMM reaches promising results when evaluating the traffic state over the entire period. Moreover, spillovers are clearly distinguishable from non-spillover cycles. However, the MLR predicts them with a higher probability, while the HMM is more conser-

## 5. MODEL IMPLEMENTATION

---

vative. This results in a slightly worse accuracy of the latter model, but a better log loss, indicating that the smooth transitions estimate the real traffic state better. The MLR shows a more erratic behaviour, which causes some major errors in the state prediction, while the HMM is more robust.

# Chapter 6

## Discussion

In the previous chapters, a Hidden Markov Model  $M_2$  was proposed and implemented on a real-life network in a simulated setting. It was compared to a Multinomial Logistic Regression model  $M_1$  that predicts the state distribution without knowledge of the prior state. Both models led to promising results where the five states - undersaturation, three levels of oversaturation, and spillover - were often predicted correctly.  $M_2$  reached a comparable performance to  $M_1$ , but showed to be more conservative in its spillover detections. On the other hand,  $M_2$  smooths out unexpected measurements better, and is consequently more robust.

In this chapter, the main assumptions and limitations that need to be taken into account when using the models are discussed, followed by an overview of possible improvements. Next, the application of the model to a real-life setting is elaborated. The main difficulty is that a ground truth needs to be determined in order to train the MLRs and that the accuracy of the FCD is rather limited.

### 6.1 Assumptions and Limitations

The proposed models make several assumptions that are not always fully respected. Below, the assumptions that are inherent to the MLR are enumerated explicitly and their validity in the proposed application are questioned. Next, the assumptions that are inherent to the Markov model are elaborated for  $M_2$ . Furthermore, the main limitations that became apparent when validating the model are clarified. Finally, additional steps or alternative approaches in the methodology are proposed and discussed.

#### 6.1.1 Assumptions of the Multinomial Logistic Regression Models

Contrary to many other classification techniques, the MLR does not assume that the variables are distributed according to a certain distribution [Withers, 2009]. This allows to use the variables without pre-preprocessing steps or transformations. Moreover, it does not restrict the model to linear combinations of the covariates

## 6. DISCUSSION

---

[Withers, 2009]. However, the MLR is based on four main assumptions for the included independent variables: (1) the independence of observations, (2) the presence of a linear relationship to the logit-transformation of the dependent variable, (3) the absence of multicollinearity and (4) the lack of strongly influential outliers [Stoltzfus, 2011].

The first assumption states that the training trajectories should be independent from each other, and thus do not come from repeated measurements [Romano and Kromrey, 2009]. This assumption is slightly violated as the model is trained using multiple trajectories affected by the same spillover, even though they experienced the spillover differently. One solution would be to include only one trajectory per spillover but this resulted in a worse performance of the model due to small number of remaining trajectories.

Furthermore, due to the definition of spillovers in the ground truth which includes a fixed number of cycles after the spillover, certain trajectories can be included in spillover cycles even though the probe vehicle did not experience a spillover, thereby polluting the dataset. A solution to this problem is to redefine the ground truth such that only vehicles that were actually affected by the spillover are considered as spillover-trajectories. In the simulated environment, this is not trivial as it requires to find the exact length of the queue that was caused by the spillover. In a real-life setting, this is even more difficult as not all vehicles are available.

Consequently, the assumption of independence of observations is violated, and even though some solutions are proposed, they are not implemented due to a lack of better results or time-constraints. The influence of this effect is difficult to estimate, but can in some cases lead to a high bias in the resulting predictions as the coefficients are overfitted on the limited number spillover events [Romano and Kromrey, 2009].

The second assumption states that there is a linear relationship of each dependent variable to the logit-transformation of the outcome [Stoltzfus, 2011]. This assumption was visually checked by looking for an S-curved relationship between the independent variables and the log-odds of the coinciding ground truth, which turned out to be the case for most variables. Only for the average stop duration, having both low values and high values as an indicator of spillovers, the relation is not linear. This variable was therefore not included in the model.

The third assumption states that the variables should be uncorrelated in order to prevent multicollinearity. If this assumption is not sufficiently met, the estimated coefficients will be unreliable [Stoltzfus, 2011]. In order to check whether the assumption is respected, the Pearson Correlation between the independent variables and the Variance-Inflation-Factor are calculated [Kim, 2019]. Both values indicate a high correlation between the travel time on the link and the number of stops. Running the model without the latter variable resulted in a similar performance, showing that the variable did not contribute significantly to the model.

The fourth assumption states that the number of strongly influential outliers in the variables should be limited [Stoltzfus, 2011]. This was again checked visually by examining the density distributions and the boxplots of the variables, but even though there were some outliers, they were not excluded in the analysis. It is hypothesised that these outliers contain important information as the number of spillovers in the dataset is limited.

An important note when analysing the aforementioned assumptions is that the complete dataset is split in multiple smaller subsets based on the previous state for  $M_2$ . As analysing the variables for every subset separately would be too time-consuming and working with different variables sets in different models would be impractical, the analysis above is done for the combined set. In the smaller subsets, some of the aforementioned assumptions where not a strongly present.

### 6.1.2 Assumptions of the Markov Model

The Markov model's most important assumption is the Markov property which states that the state distribution at time  $t$  only depends on the previous state distribution a time  $t - 1$ . This assumption can be relaxed by higher-order Markov models where state distributions of the previous cycles are included when estimating the transition probabilities by, for instance, including them as latent variables [Berchtold and Raftery, 2002]. However, it is unclear whether this would result in significant improvements as the output of the current model shows that the inclusion of the previous state results in the overestimation of the spillover duration and too conservative guesses for the spillover probability. It might however further improve the estimation of the non-spillover states, as they do not change drastically from cycle to cycle.

### 6.1.3 Limitations of the Model

Even though the results are promising, the two models have some limitations, mainly with regards to the time setting and the training data. Also,  $M_2$  seems to predict spillover states too conservatively, whereas  $M_1$  is too erratic for the non-spillover states.

A first limitation is that the models only take into account a probe vehicle as soon as it passes the intersection, since the lane on which it drove needs to be identified. However, the vehicles might, in the worst case, spend up to 12 minutes on the link before reaching the intersection, resulting in a major time lag. The vehicle might contain valuable information that is currently only included in the state estimation at the time of passing. An obvious solution would be to include the partial trajectory of the vehicle earlier. This requires knowledge on the lane on which the vehicle drives at that time. This is not possible with the FCD's current accuracy.

## 6. DISCUSSION

---

Moreover, as the ground truth-definition currently uses the same effective spillover duration, regardless of the actual spillover duration, only the immediate effects on the trajectories are measured by the model. A vehicle that was in the back of the queue during the actual spillover might still experience the spillover slightly. When it passes the intersection after the effective spillover duration, these effects are included in the observations, leading to a potential overestimation of the spillover duration. This issue can be solved in two ways. One option is to take into account the time of the stop relative to the crossing time. The shockwaves and the stopping durations of these earlier stops should be considered as less important than the more recent ones. This will cause the predictions to better fit the current ground truth definition, but is not the most realistic approach. A better option is to change this ground truth definition in order to include all vehicles that experienced the effect of the spillover as spillover-trajectories. This would result in longer spillover durations with trajectory measurements that decay slowly towards oversaturated states. Therefore, it is expected that  $M_2$  will perform better with this new definition, whereas  $M_1$  will have difficulties distinguishing the spillover states in later time steps.

Related to this, the model currently only allows for a discrete-state ground truth definition, whereas continuous states could allow to show more intricacies between the states. However, this is not trivial to implement. The traffic state needs to be determined by one continuous dependent variable to distinguish between different saturation levels and spillovers. As a physical variable that does this could not be imagined, it is possible to determine these continuous states using clustering techniques, as proposed by [Rao et al. \[2019\]](#). Furthermore, a continuous dependent variable requires a different technique for calculating the transition probabilities, as the MLR only allows for a discrete dependent variable [\[Stoltzfus, 2011\]](#).

Another limitation of the models is that they are meant to estimate the state of the current cycle based on the latest information in this cycle. Currently, the HMM does not make predictions for future states, even though this is more interesting for the control mechanism so as to prevent spillovers. However, it can be assumed that the trajectory information only shows the characteristics of spillovers after they happen. On the other hand, when other detections such as the traffic demand are included, it might be possible to find prior indications that precede the spillover. When the flow rate to the downstream link exceeds the capacity of this link, spillover probability increases for the following time steps. The current implementation of the method is capable of making predictions, similar to how it handles cycles without probe vehicles, but this is expected to be a very coarse prediction for multiple time steps in the future.

Next,  $M_2$  showed less pronounced spillover estimations compared to  $M_1$ . This is to be expected, as shown in the following example where a trajectory with clear characteristics of a spillover passes and the state distribution in the previous time step was given by

$$S_{t-1} = [0.05, 0.05, 0.10, 0.70, 0.10]^T \quad (6.1)$$

$M_1$  will disregard the previous state and only base its predictions on the characteristics of the vehicle, resulting in a high probability for spillover, e.g.

$$S_t = [0.01, 0.02, 0.07, 0.20, 0.70]^T \quad (6.2)$$

The full model will take into account that there is a small chance that the true state in the previous time step was  $O_1$  or  $O_2$ , which have low probabilities for transitioning to spillover, resulting in a less distinct distribution given by

$$S_t = S_{t-1} \cdot P(t) \text{ where } P(t) = \begin{bmatrix} 0.30 & 0.40 & 0.15 & 0.10 & 0.05 \\ 0.10 & 0.20 & 0.40 & 0.20 & 0.10 \\ 0.05 & 0.05 & 0.10 & 0.40 & 0.40 \\ 0.02 & 0.03 & 0.15 & 0.20 & 0.60 \\ 0.01 & 0.01 & 0.03 & 0.05 & 0.90 \end{bmatrix} \quad (6.3)$$

$$= [0.02, 0.03, 0.08, 0.67, 0.20]^T \quad (6.4)$$

This is considerably lower than the state distribution in equation (6.2), and the spillover is not classified as the most probable state. This is not necessarily a problem as spillover cycles can be clearly distinguished from non-spillover cycles in the predicted probabilities by looking at the difference in probability compared to the average probability of spillover.

This more conservative approach due to the Markov's smoothing effect might even be preferred by the control mechanism as it results in less erratic changes and thus in smoother adaptations of the control strategy. Moreover, when the method is implemented in a real-world setting, the measurement error is more substantial and  $M_1$  will have difficulties to achieve its current performance.  $M_2$  is expected to be more robust and handle this error more adequately.

An additional limitation is that MLRs need a rather extensive dataset in order to be trained accurately, especially as the data is divided into five subsets for  $M_2$  [Riveros, 2020]. In the simulation, this is not a major problem as more simulation runs can be used to increase the number of available samples. In the real-world setting, where spillovers do not occur often, it may be necessary to use additional techniques such as the jackknife or bootstrap approaches [Riveros, 2020]. Other models such as the naive Bayes-classifier can handle the lower data availability better as it converges faster to its asymptotic error, while the MLR converges slower but performs better once converged [Ng and Jordan, 2002]. This is not further investigated in this thesis.

Finally, the current model includes only linear combinations of the covariates, whereas interaction terms can be added. This can for example be the number of stops per demand level, which would be an indication of how efficient the intersection is working. As mentioned before, the traffic signal cycles can also be used in a non-linear transformation with the stop duration in order to account for adaptive traffic control systems.

## 6.2 Application to a Real-life Setting

So far, the methods have been tested on a simulated counterpart of the real network. The prime reason is that a ground truth needs to be defined and that the FCD possesses a significant measurement error. These problems and their potential solutions are discussed in this section.

### 6.2.1 Ground Truth

As the MLR is a supervised learning method, it requires the definition of a ground truth for every time step. In the simulated setting, this can be obtained through the analysis of all vehicles on the network. Finding the ground truth is much less trivial in a real setting, especially when no other data sources are available. There are three main strategies to solve this: (1) using loop detector data, (2) classifying the states visually and (3) constructing an accurate microsimulation.

A first option is to use one of the methods based on loop detector data discussed in Chapter 3. In order to estimate the average number of stops for all vehicles that pass between time  $t - 1$  and time  $t$ , methods proposed by Liu et al. [2009] and Sharma et al. [2007] can be used. They use the changing occupancy measurement at the loop detector's location to estimate the shockwave profiles. Similarly, spillovers can be detected using the methods proposed by Geroliminis [2009] and Wu et al. [2010]. Apart from the obvious limitation that loop detectors need to be present at the researched intersection, these methods also have limited accuracy due to the unreliability of the data source in congested traffic conditions [Yulianto, 2018]. Moreover, the required estimations of the different threshold parameters, such as the critical occupancy, vary when the conditions on the network change. With an unreliable ground truth, the training trajectories cannot be correctly classified and the resulting model is expected to be unreliable.

A second option is to visually classify the states. Especially spillovers can be spotted quite easily using video images of the intersection and checking for blocking vehicles on the intersection during green signals. The level of oversaturation can be obtained similarly, but this might require changing the definition of the oversaturation-level to a metric that is more easily measurable, such as the maximal queue length. The visual detection can happen manually, but with the recent advancements in image processing, a tool can potentially be developed to classify it automatically. In case permanent cameras can be installed, this method might even replace the proposed methods if it proves reliable.

A third option is to build an accurate micro-simulation of the intersection on which the model is trained, as was done in this thesis. Building an accurate simulation requires appropriate knowledge and takes time. Moreover, the real situation can only be approximated, leading to potential errors in the state estimation when applying it to the real intersection.

In further research, it should also be checked how the coefficients change when applied to different intersections. If similar intersections show similar regression coefficients, one model can be trained for a certain type of intersections, where covariates correct for small differences in the layout, such as the length of the approach. Additional efforts can be directed towards the initial training of the model, as it can next be applied to every intersection that falls into one of the trained categories.

### 6.2.2 Attributes

The simulated trajectories reflect the exact location of the vehicles, whereas FCD is typically prone to measurement errors. Therefore, some additional steps are required to obtain the characteristics of the vehicle and the HMM may need to be extended to account for this measurement error.

To assess covariates such as the number of stops and the stopping duration, the trajectories need to be filtered in order to clearly distinguish standstill and moving periods. The main problem occurs when the traffic signal is green for a very short period or when short spillovers occur since they result in limited advancements of the queuing vehicles. The filter should be able to distinguish these small position changes from a longer standstill period, as they are one of the main indicators of spillovers.

Additionally, the measurement of the travel time attributes is rather straightforward using FCD [Cvetek et al., 2021]. Trying to determine the travel time over the intersection might be not as trivial since this requires a relatively accurate location measurement. Consequently, the definition of this covariate might have to be extended such that it can be measured more easily.

Furthermore, the shockwave profile can be obtained similarly to the proposed method for the simulated data. However, these shockwaves might differ at different times due to the influence of weather conditions and others. This can be handled in two ways: either the use of a coarse estimation of the average shockwave speed as is currently implemented, or the use of different shockwave speeds based on weather forecasts.

Lastly, not all trajectories are equally reliable for the state estimation due to the differences in accuracy or unwarranted behaviour. To tackle this problem, it is proposed to include a reliability index where a higher reliability results in stronger decisions for the new transition probabilities. This measure could include the Horizontal Dilution of Precision (HDOP), which is a metric that indicates the possible horizontal accuracy of the measurement [Liu et al., 2018]. Furthermore, unwarranted behaviour such as stopping to pick up a passenger or delays caused by a crossing pedestrian needs to be smoothed out. This is currently partly handled by the Markov model in  $M_2$ , but still a step in the wrong direction will be made if such a trajectory passes. Therefore, a metric that indicates the likelihood of being a vehicle with such

## 6. DISCUSSION

---

behaviour should also be included in the reliability index. This can, for example, be based on the layout of the intersection, i.e. when the location of a stop can be related to a bus stop or a pedestrian crossing.

The introduction of the measurement error might warrant the extension of the MLR to an measurement error model. In the current implementation, the covariates are assumed to be free of error, which leads to a potential bias in the estimated coefficients [Mwalili et al., 2005]. On the one hand, several extensions to the MLR exist to adjust for the bias in the approximated coefficients by taking into account measurement errors [Stefanski and Carroll, 1985], [Liu and Liang, 1991]. Other research proposes Bayesian methods to handle the measurement error [Dellaportas and Stephens, 1995],[Welch and Bishop, 2006]. Further research is required in order to assess the importance of the measurement error and compare the different solutions.

### 6.3 Validity of Floating Car Data

The aim of this research was to assess the validity of FCD for spillover detection. Based on the obtained results, it appears to be capable of replacing loop detectors, even without significant improvements in the penetration rate. Nevertheless, further research is needed for the implementation of the model in a real-life setting.

If only used for spillover detection, the method  $M_1$ , using only the MLR, can possibly reach the desired results, as it correctly predicts the sudden changes to spillover. However, it also behaves more erratically and is strongly influenced by unexpected trajectories as it does not take the previous cycles into account. When a prediction of the saturation level needs to be estimated as well, or when the measurement error proves significant, the extension to a HMM is warranted, as it allows for a smoother sequence of states, and is more robust. Moreover, it is also capable of correctly identifying spillovers.

It is difficult to compare the model's performance with models based on loop detectors from literature, as they use different simulated case studies and different evaluation methods. In further research, a comparative study is required to allow for a formal decision on the benefits of the proposed methods over the existing ones.

### 6.4 Summary

In this chapter, the main assumptions and shortcomings of the proposed models are discussed and solutions are elaborated. The main problems concern the data gathering and ground truth definition, which is currently too coarse for a well-defined model. Other limitations include the conservative state predictions by the HMM and the high data requirements of the MLR models.

Furthermore, the methods need to be implemented in a real-life setting and compared

#### 6.4. Summary

---

to traditional methods before firm conclusions on their performance can be made. This entails additional difficulties in order to deal with measurement errors and to find the ground truth.



# Chapter 7

## Conclusion

The aim of this thesis was to assess the validity of floating car data for the purpose of spillover detection. This detection is necessary for the adequate control of signalised intersections. Current practice is mainly based on data from loop detectors, which are expensive to install and maintain. FCD is a cheaper method, but currently lacks a high penetration rate. The proposed method aims to solve this through a probabilistic model that interpolates the traffic state when no probe vehicles are present on the intersection.

After a thorough analysis of the problem, it appeared that there are four different types of spillovers with vastly different characteristics. Even though a blockage is present during green time in all these situations, the moment of occurrence relative to the traffic signals changes the shockwave profiles considerably. Moreover, the analysis of the available data showed that the main problems of the FCD are its limited penetration rate and the lack of accurate position measurements.

The proposed method follows the structure of a Hidden Markov Model, where a first-order Markov chain is used to update the state distribution at discrete time steps. It aims to predict the probability of being in one of five states: undersaturation, three levels of oversaturation, and spillover. This Markov model is complemented by a logistic regression model that uses several covariates to calculate the transition probability from one cycle to another. The covariates included can be obtained from information on a passing probe vehicle and on the surroundings of the intersection. The method is compared to a reference model that consists of a multinomial logistic regression model that predicts the state distribution based on the same covariates as the HMM but does not take the previous state into account.

Due to the aforementioned inaccuracy of the FCD and the need for a ground truth definition, it was decided to build a microsimulation in *VISSIM* to validate the model. This simulation is based on a case study of a real-life network in Deventer, the Netherlands. It consists of several successive intersections with multilane approaches to each intersection.

## 7. CONCLUSION

---

Even though the simulation simplifies the setting, the models obtain promising results. Both the HMM- and the MLR-models are able to distinguish spillover cycles from non-spillover cycles. While the latter model achieves a slightly higher accuracy than the former one, it is behaves erratically and is less suited for distinguishing the saturation level. The HMM also obtains satisfactory results, is more robust and is consequently expected to be better suited for the real-life implementation of the model.

In conclusion, FCD provides a good opportunity for traffic management at urban intersections in the future, where it can reduce the need for loop detectors. However, further steps are required to test how the model performs in the real world and whether higher performance levels can be reached than with the current methods.

## Future Research

An important next step is to implement the proposed method in a real-life setting. This encompasses additional challenges with regards to finding a ground truth and the addition of a measurement error. Moreover, the model needs to be tested on different intersections to find out how influential the intersection layout is.

Furthermore, extensions to the model are possible, such as the continuous-time or continuous-state definitions of the Markov models. The former has the advantage that it handles the probe vehicle's information as soon as it comes in, but the implementation is not trivial due to the introduction of a decaying factor for longer periods without probe vehicles. The latter extension allows for a more detailed state division, but requires more sophisticated models to determine the transition density functions.

Comparable models such as Bayesian classification techniques can further increase the reliability as they require less data for adequate training. Moreover, the extension to measurement error models might be necessary for the implementation in a real-world setting. The research presented in this thesis provides a good basis for these further developments.

# Bibliography

- G. Abu-Lebdeh and R. F. Benekohal. Design and evaluation of dynamic traffic management strategies for congested conditions. Technical Report 2, 2003. URL [www.elsevier.com/locate/tra](http://www.elsevier.com/locate/tra).
- A. S. A. Al-Sobky and R. M. Mousa. Traffic density determination and its applications using smartphone. *Alexandria Engineering Journal*, 55(1):513–523, 3 2016. ISSN 11100168. doi: 10.1016/j.aej.2015.12.010.
- F. Bartolucci, A. Farcomeni, and F. Pennoni. Latent Markov models: A review of a general framework for the analysis of longitudinal data with covariates. *Test*, 23(3):433–465, 8 2014. ISSN 11330686. doi: 10.1007/s11749-014-0381-7. URL <https://link.springer.com/article/10.1007/s11749-014-0381-7>.
- A. Berchtold and A. E. Raftery. The Mixture Transition Distribution Model for High-Order Markov Chains and Non-Gaussian Time Series. Technical Report 3, 2002. URL [www.stat.washington.edu/raftery](http://www.stat.washington.edu/raftery).
- D. Bolano. Handling Covariates in Markovian Models with a Mixture Transition Distribution Based Approach. 1985. doi: 10.3390/sym12040558. URL [www.mdpi.com/journal/symmetry](http://www.mdpi.com/journal/symmetry).
- A. Briggs and M. Sculpher. An introduction to Markov modelling for economic evaluation. *PharmacoEconomics*, 13(4):397–409, 1998. ISSN 11707690. doi: 10.2165/00019053-199813040-00003. URL <https://pubmed.ncbi.nlm.nih.gov/10178664/>.
- E. Brockfeld, S. Lorkowski, P. Mieth, and P. Wagner. Benefits and Limits of Recent Floating Car Data Technology - An Evaluation Study. Technical report, 2007.
- M. Campestrini and P. Mock. European vehicle market statistics. *International Council on Clean Transportation*, pages 1–50, 2011. URL <http://eupocketbook.theicct.orghttp://scholar.google.com/scholar?hl=en&btnG=Search&q=intitle:European+Vehicle+Market+Statistics#4%5Cnhttp://scholar.google.com/scholar?hl=en&btnG=Search&q=intitle:European+vehicle+market+statistics#4>.
- R. Castellano and L. Scaccia. Bayesian inference for Hidden Markov Model. Technical report, 2007. URL <https://www.researchgate.net/publication/23535157>.

## BIBLIOGRAPHY

---

- E. Christofa, J. Argote, and A. Skabardonis. Arterial queue spillback detection and signal control based on connected vehicle technology. *Transportation Research Record*, (2356):61–70, 2013. ISSN 03611981. doi: 10.3141/2356-08. URL <chrome-extension://dagcmkpagjlhakfdhnbgmjdpkdklff/enhanced-reader.html?openApp&pdf=https%3A%2F%2Fjournals.sagepub.com%2Fdoi%2Fpdf%2F10.3141%2F2356-08>.
- S. Cohen and Z. Christoforou. Travel time estimation between loop detectors and Fcd: A compatibility study on the Lille Network, France. In *Transportation Research Procedia*, volume 10, pages 245–255. Elsevier, 1 2015. doi: 10.1016/j.trpro.2015.09.074.
- B. Coifman and S. B. Kim. Speed estimation and length based vehicle classification from freeway single-loop detectors. *Transportation Research Part C: Emerging Technologies*, 17(4):349–364, 8 2009. ISSN 0968090X. doi: 10.1016/j.trc.2009.01.004.
- O. Çokluk. Logistic Regression: Concept and Application. Technical report, 2010.
- G. Comert and M. Cetin. Queue length estimation from probe vehicle location and the impacts of sample size. *European Journal of Operational Research*, 197(1):196–202, 8 2009. ISSN 03772217. doi: 10.1016/j.ejor.2008.06.024.
- D. Cvjetek, M. Muštra, N. Jelušić, and L. Tišljarić. A survey of methods and technologies for congestion estimation based on multisource data fusion, 3 2021. ISSN 20763417.
- C. F. Daganzo. The cell transmission model, part II: Network traffic. *Transportation Research Part B*, 29(2):79–93, 1995. ISSN 01912615. doi: 10.1016/0191-2615(94)00022-R.
- P. Dellaportas and D. A. Stephens. Bayesian Analysis of Errors-in-Variables Regression Models. Technical Report 3, 1995. URL <https://about.jstor.org/terms>.
- A. Emami, M. Sarvi, and S. Asadi Bagloee. A neural network algorithm for queue length estimation based on the concept of k-leader connected vehicles. *Journal of Modern Transportation*, 27(4):341–354, 2019. ISSN 21960577. doi: 10.1007/s40534-019-00200-y. URL <https://doi.org/10.1007/s40534-019-00200-y>.
- M. Eom and B.-I. Kim. The traffic signal control problem for intersections: a review. *European Transport Research Review*, 2020. doi: 10.1186/s12544-020-00440-8. URL <https://doi.org/10.1186/s12544-020-00440-8>.
- E. Fekpe, D. Gopalakrishna, and D. Middleton. Highway Performance Monitoring System Traffic Data for High Volume Routes : Best Practices and Guidelines. Technical report, Office of Highway Policy Information, Federal Highway Administration, U.S. Department of Transportation, Washington D.C., 2004.

## BIBLIOGRAPHY

---

- G. A. Fink. *Markov Models for Pattern Recognition*. Springer London, 2014. doi: 10.1007/978-1-4471-6308-4.
- FLIR. The Evolution of Intersections—From Inductive Loops to Artificial Intelligence | FLIR Systems, 2020. URL <https://www.flir.com/discover/traffic/urban/the-evolution-of-intersections-from-inductive-loops-to-artificial-intelligence/>.
- K. Gao, S. Huang, J. Xie, N. N. Xiong, and R. Du. A review of research on intersection control based on connected vehicles and data-driven intelligent approaches, 6 2020. ISSN 20799292.
- N. Geroliminis. Queue spillovers in city street networks with signal-controlled intersections. *Transportation Research Board 89th Annual Meeting*, pages 10–34, 2009.
- L. A. Goodman. Exploratory latent structure analysis using both identifiable and unidentifiable models, 1974. ISSN 00063444. URL <http://www.statmodel.com/bmuthen/ED231e/RelatedArticles/Goodman.pdf>.
- H. Greenberg. An Analysis of Traffic Flow. 1958. URL <https://www.jstor.org/stable/167595?seq=1>.
- B. D. Greenshields, J. R. Bibbins, W. S. Channing, and H. H. Miller. A Study of Traffic Capacity. *Highway Research Board Proceedings*, 14, 1935.
- J. Guerrero-Ibáñez, S. Zeadally, and J. Contreras-Castillo. Sensor technologies for intelligent transportation systems. *Sensors (Switzerland)*, 18(4):1–24, 2018. ISSN 14248220. doi: 10.3390/s18041212.
- S. P. Hoogendoorn. *Traffic Flow Theory and Simulation Lecture material*. 2010.
- M. Houbraken, S. Logghe, M. Schreuder, P. Audenaert, D. Colle, and M. Pickavet. Automated Incident Detection Using Real-Time Floating Car Data. *Journal of Advanced Transportation*, 2017, 2017. ISSN 20423195. doi: 10.1155/2017/8241545.
- H. Immers and S. Logghe. Course H 111 Verkeerskunde Basis Traffic Flow Theory. Technical report, 2002.
- M. A. Islam, S. Arabia, and R. I. Chowdhury. A Three State Markov Model for Analyzing Covariate Dependence. *International Journal of Statistical Sciences*, 3 (i):241–249, 2004.
- C. H. Jackson, L. D. Sharples, S. G. Thompson, S. W. Duffy, and E. Couto. Multistate Markov models for disease progression with classification error. Technical report, 2003.
- J. H. Kim. Multicollinearity and misleading statistical results. *Korean Journal of Anesthesiology*, 72(6):558–569, 12 2019. ISSN 20057563. doi: 10.4097/kja.19087. URL <http://ekja.orgpISSN2005-6419\global\>

## BIBLIOGRAPHY

---

```
let\T1\textbullet\protect\unhbox\voidb@x{\def{\MessageBreakfor}
symbol`textbullet'}\edefT1{TS1}\xdef\T1/lmr/m/n/10.95{\T1/lmr/
m/n/10.95}\begingroup\escapechar`m@ne\let\MT@subst@\T1/lmr/m/n/
10.95\def{\@par}\T1\textbullet\textbulletISSN2005-7563https:
//doi.org/10.4097/kja.19087.
```

- L. A. Klein, M. K. Mills, and D. R. Gibson. Traffic Detector Handbook: Third Edition—Volume I. Technical Report October, 2006. URL <https://www.fhwa.dot.gov/publications/research/operations/its/06108/01.cfm> http://www.fhwa.dot.gov/publications/research/operations/its/06108/01.cfm#ind.
- V. L. Knoop and W. Daamen. Automatic fitting procedure for the fundamental diagram. *Transportmetrica B*, 5(2):133–148, 4 2017. ISSN 21680582. doi: 10.1080/21680566.2016.1256239. URL <https://www.tandfonline.com/action/journalInformation?journalCode=ttrb20http://dx.doi.org/10.1080/21680566.2016.1256239>.
- C. Koki, L. Meligkotsidou, and I. Vrontos. Forecasting under model uncertainty: Non-homogeneous hidden Markov models with Pólya-Gamma data augmentation. Technical report, 2019.
- K. Li, M. Feng, A. Biswas, H. Su, Y. Niu, and J. Cao. Driving factors and future prediction of land use and cover change based on satellite remote sensing data by the LCM model: A case study from gansu province, China. *Sensors (Switzerland)*, 20(10), 2020. ISSN 14248220. doi: 10.3390/s20102757. URL [/pmc/articles/PMC7285483/](https://pmc/articles/PMC7285483/) pmc/articles/PMC7285483/?report=abstracthttps://www.ncbi.nlm.nih.gov/pmc/articles/PMC7285483/.
- Q. L. Li. *Constructive computation in stochastic models with applications: The RG-factorization*. Springer, 2010. ISBN 9783642114915. doi: 10.1007/978-3-642-11492-2.
- M. Lighthill and G. Whitham. On Kinematic Waves. II. A Theory of Traffic Flow on Long Crowded Roads. 1955. URL [https://www-jstor-org.kuleuven.ezproxy.kuleuven.be/stable/99769?sid=primo&seq=1#metadata\\_info\\_tab\\_contents](https://www-jstor-org.kuleuven.ezproxy.kuleuven.be/stable/99769?sid=primo&seq=1#metadata_info_tab_contents).
- D. Liu, L. Chen, Y. Wang, J. Lu, and S. Huang. How much can we trust GPS wildlife tracking? An assessment in semi-freeranging Crested Ibis Nipponia nippon. *PeerJ*, 2018(7):e5320, 7 2018. ISSN 21678359. doi: 10.7717/peerj.5320. URL <https://peerj.com/articles/5320>.
- H. X. Liu, X. Wu, W. Ma, and H. Hu. Real-time queue length estimation for congested signalized intersections. *Transportation Research Part C: Emerging Technologies*, 17(4):412–427, 2009. ISSN 0968090X. doi: 10.1016/j.trc.2009.02.003. URL [http://dx.doi.org/10.1016/j.trc.2009.02.003](https://dx.doi.org/10.1016/j.trc.2009.02.003).

- M. Liu, M. Chiaki, Y. Oeda, and T. Sumi. Modelling fundamental diagrams according to different water film depths from the perspective of the dynamic hydraulic pressure. *Scientific Reports*, 10(1):1–18, 12 2020. ISSN 20452322. doi: 10.1038/s41598-020-63381-1. URL <https://doi.org/10.1038/s41598-020-63381-1>.
- X. Liu. Methods for handling missing data. In *Methods and Applications of Longitudinal Data Analysis*, pages 441–473. Elsevier, 1 2016. doi: 10.1016/b978-0-12-801342-7.00014-9.
- X. Liu and K. iang. Adjustment for non-differential misclassification error in the generalized linear model. *Statistics in Medicine*, 10(8):1197–1211, 8 1991. ISSN 10970258. doi: 10.1002/sim.4780100804. URL <https://onlinelibrary-wiley-com.kuleuven.e-bronnen.be/doi/full/10.1002/sim.4780100804><https://onlinelibrary-wiley-com.kuleuven.e-bronnen.be/doi/abs/10.1002/sim.4780100804><https://onlinelibrary-wiley-com.kuleuven.e-bronnen.be/doi/10.1002/sim.4780100804>.
- D. Ma, D. Wang, Y. Bie, S. Jin, and Z. Mei. Identification of spillovers in urban street networks based on upstream fixed traffic data. *KSCE Journal of Civil Engineering*, 18(5):1539–1547, 2014. ISSN 19763808. doi: 10.1007/s12205-014-0534-y.
- K. Merry and P. Bettinger. Smartphone GPS accuracy study in an urban environment. *PLoS ONE*, 14(7), 7 2019. ISSN 19326203. doi: 10.1371/journal.pone.0219890. URL <https://www.ncbi.nlm.nih.gov/pmc/articles/PMC6638960/>.
- L. R. Muenz and L. V. Rubinstein. Markov Models for Covariate Dependence of Binary Sequences. *Biometrics*, 41(1):91, 3 1985. ISSN 0006341X. doi: 10.2307/2530646.
- K. P. Murphy. *Machine Learning: A Probabilistic Perspective*. MIT Press, 2012. ISBN 0262304325. URL [https://books.google.be/books?id=RC43AgAAQBAJ&dq=Murphy,+K.+P.+%282012%29.+Machine+Learning:+A+Probabilistic+Perspective.+The+MIT+Press&lr=&hl=nl&source=gbs\\_navlinks\\_s](https://books.google.be/books?id=RC43AgAAQBAJ&dq=Murphy,+K.+P.+%282012%29.+Machine+Learning:+A+Probabilistic+Perspective.+The+MIT+Press&lr=&hl=nl&source=gbs_navlinks_s).
- S. M. Mwalili, E. Lesaffre, and D. Declerck. A Bayesian ordinal logistic regression model to correct for interobserver measurement error in a geographical oral health study. *Journal of the Royal Statistical Society. Series C: Applied Statistics*, 54(1):77–93, 1 2005. ISSN 00359254. doi: 10.1111/j.1467-9876.2005.00471.x. URL <http://www.blackwellpublishing.com/rss>.
- I. J. Myung. Tutorial on maximum likelihood estimation. *Journal of Mathematical Psychology*, 47(1):90–100, 2 2003. ISSN 00222496. doi: 10.1016/S0022-2496(02)00028-7.
- R. C. Neath and M. S. Johnson. Discrimination and classification. In *International Encyclopedia of Education*, pages 135–141. Elsevier Ltd, 1 2010. ISBN 9780080448947. doi: 10.1016/B978-0-08-044894-7.01312-9.

## BIBLIOGRAPHY

---

- A. Y. Ng and M. I. Jordan. On Discriminative vs. Generative classifiers: A comparison of logistic regression and naive Bayes. Technical report, 2002. URL <http://ai.stanford.edu/~ang/papers/nips01-discriminativegenerative.pdf>.
- R. Noroozi and B. Hellinga. Real-Time Prediction of Near-Future Traffic States on Freeways Using a Markov Model. *Transportation Research Record: Journal of the Transportation Research Board*, 2421(1):115–124, 2014. ISSN 0361-1981. doi: 10.3141/2421-13.
- A. S. Novozhilov, G. P. Karev, and E. V. Koonin. Biological applications of the theory of birth-and-death processes, 3 2006. ISSN 14675463. URL <https://academic.oup.com/bib/article/7/1/70/263777>.
- B. J. Park, T. Kim, I. Yang, J. Heo, and B. Son. A method for measuring accurate traffic density by aerial photography. *Journal of Advanced Transportation*, 49(4): 568–580, 6 2015. ISSN 20423195. doi: 10.1002/atr.1288.
- J. Perla, T. J. Sargent, and J. Stachurski. Continuous State Markov Chains. Technical report, 2020.
- N. Privault. Continuous-Time Markov Chains. In *Understanding Markov Chains*, chapter 9, pages 211–263. Springer, Singapore, 2018. ISBN 10.1007/9789811. doi: 10.1007/978-981-13-0659-4\\_\\_9. URL [https://doi.org/10.1007/978-981-13-0659-4\\_9](https://doi.org/10.1007/978-981-13-0659-4_9).
- M. Ramezani and N. Geroliminis. Queue Profile Estimation in Congested Urban Networks with Probe Data. *Computer-Aided Civil and Infrastructure Engineering*, 30(6):414–432, 6 2015. ISSN 14678667. doi: 10.1111/mice.12095.
- W. Rao, J. Xia, W. Lyu, and Z. Lu. Interval data-based k-means clustering method for traffic state identification at urban intersections. *IET Intelligent Transport Systems*, 13(7):1106–1115, 2019. ISSN 1751956X. doi: 10.1049/iet-its.2018.5379.
- F. Rempe. Traffic Speed Estimation and Prediction Using Floating Car Data. 2019.
- J. Riveros. Low sample size and regression: A Monte Carlo approach. *Journal of Applied Economic Sciences*, 2020. doi: 10.14505/jaes.v15.1(67).02. URL <http://cesmaa.org/Extras/JAES>.
- J. L. Romano and J. D. Kromrey. What are the consequences if the assumption of independent observations is violated in reliability generalization meta-analysis studies? *Educational and Psychological Measurement*, 69(3):404–428, 9 2009. ISSN 15523888. doi: 10.1177/0013164408323237. URL <http://epm.sagepub.com>.
- S. Y. R. Rompis. Traffic Flow Model and Shockwave Analysis. *Jurnal Sipil Statik*, 6 (1):13–20, 2018. ISSN 2337-6732.

- O. Rosas-Jaimes, M. A. M. Martinez, and J. C. L. Rivera. Use of the Cell Transmission Model in Urban Networks with Flow Discontinuities. 2013. URL [https://www.researchgate.net/publication/281038626\\_Use\\_of\\_the\\_Cell\\_Transmission\\_Model\\_in\\_Urban\\_Networks\\_with\\_Flow\\_Discontinuities](https://www.researchgate.net/publication/281038626_Use_of_the_Cell_Transmission_Model_in_Urban_Networks_with_Flow_Discontinuities).
- A. Rusiecki. Trimmed categorical cross-entropy for deep learning with label noise. *Electronics Letters*, 55(6):319–320, 3 2019. ISSN 00135194. doi: 10.1049/el.2018.7980. URL <http://yann.lecun.com/exdb/mnist/>.
- A. Sharma, D. M. Bullock, and J. A. Bonneson. Input-output and hybrid techniques for real-time prediction of delay and maximum queue length at signalized intersections. *Transportation Research Record*, (2035):69–80, 2007. ISSN 03611981. doi: 10.3141/2035-08.
- H. K. Sharma and B. L. Swami. MOE-Analysis for Oversaturated Flow with Interrupted Facility and Heterogeneous Traffic for Urban Roads. *International Journal of Transportation Science and Technology*, 1(3):287–296, 9 2012. ISSN 20460449. doi: 10.1260/2046-0430.1.3.287.
- H. K. Sharma and B. L. Swami. Congestion characteristics of interrupted flow for urban roads with heterogeneous traffic structure. *MATEC Web of Conferences*, 81, 2016. ISSN 2261236X. doi: 10.1051/matecconf/20168101001.
- H. D. Sherali. Springer Optimization and Its Applications VOLUME 84. Technical report, 2014. URL <http://www.springer.com/series/7393>.
- a. N. C. Sinha, A. A. Islam, and K. S. Ahamed. Logistic regression models for higher order transition probabilities of Markov chain for analyzing the occurrences of daily rainfall data. *Journal of Modern Applied Statistical Methods*, 10(1):337–348, 2011. ISSN 15389472. doi: 10.22237/jmasm/1304224200.
- P. Sirima and P. Pokorny. Hidden markov models with covariates for analysis of defective industrial machine parts. *Journal of Mathematics and Statistics*, 10(3): 322–330, 2014. ISSN 15493644. doi: 10.3844/jmssp.2014.322.330.
- A. Skabardonis and N. Geroliminis. Real-Time Monitoring and Control on Signalized Arterials. *Journal of Intelligent Transportation Systems*, 12(2):64–74, 2008. ISSN 1547-2442. doi: 10.1080/15472450802023337. URL <https://www.tandfonline.com/action/journalInformation?journalCode=gits20>.
- S. L. Skszek. Report on Non-Traditional Traffic Counting Methods. page 505, 2001.
- Staat van Deventer. Inwoneraantal - Deventer - Staat van Deventer, 2021. URL [https://www.staatvandeeventer.nl/](https://www.staatvandeventer.nl/).
- L. A. Stefanski and R. J. Carroll. Covariate Measurement Error in Logistic Regression. *The Annals of Statistics*, 13(4):1335–1351, 1985. URL [www.jstor.org/stable/2241358](http://www.jstor.org/stable/2241358).

## BIBLIOGRAPHY

---

- J. C. Stoltzfus. Logistic Regression: A Brief Primer. *Academic Emergency Medicine*, 18(10):1099–1104, 10 2011. ISSN 10696563. doi: 10.1111/j.1553-2712.2011.01185.x. URL <http://doi.wiley.com/10.1111/j.1553-2712.2011.01185.x>.
- A. Sunderrajan, V. Vaisagh, W. Cai, and A. Knoll. Traffic State Estimation Using Floating Car Data. *Procedia Computer Science*, 80:2008–2018, 2016.
- N. Talpe. Floating Car Data, 2016.
- V. Thamizh and A. . G. Dhivya. Measurement of Occupancy of Heterogeneous Traffic Using Simulation Technique. 2009. doi: 10.3182/20090902-3-US-2007.0070.
- K. Torp and H. Lahrmann. Floating Car Data For Traffic Monitoring. Technical report, 2003. URL [www.cs.aau.dk/~torp/www.plan.aau.dk/~lahrmann](http://www.cs.aau.dk/~torp/www.plan.aau.dk/~lahrmann).
- P. I. Uche. Non-homogeneity and transition probabilities of a markov chain. *International Journal of Mathematical Education in Science and Technology*, 21(2):295–301, 1990. ISSN 14645211. doi: 10.1080/0020739900210217.
- R. T. Underwood. Speed, Volume, and Density Relationships. 1961.
- G. van der Brugt. © IT&T KWC 10 Jaar & Management Dashboard Verkeersproces. 2000.
- Vialis. V-Log protocol en definities. Technical report, 2020. URL [www.vialis.nl](http://www.vialis.nl).
- G. Vigos, M. Papageorgiou, and Y. Wang. Real-time estimation of vehicle-count within signalized links. *Transportation Research Part C: Emerging Technologies*, 16(1):18–35, 2008. ISSN 0968090X. doi: 10.1016/j.trc.2007.06.002.
- Z. Wang, Q. Cai, B. Wu, L. Zheng, and Y. Wang. Shockwave-based queue estimation approach for undersaturated and oversaturated signalized intersections using multi-source detection data. *Journal of Intelligent Transportation Systems: Technology, Planning, and Operations*, 21(3):167–178, 2017. ISSN 15472442. doi: 10.1080/15472450.2016.1254046. URL <https://doi.org/10.1080/15472450.2016.1254046>.
- F. V. Webster. Traffic signal settings. *Road Research Technical Paper, No.39, Road Research Laboratory, London*, page 44, 1958.
- G. Welch and G. Bishop. An Introduction to the Kalman Filter. *In Practice*, 7(1):1–16, 2006. ISSN 10069313. doi: 10.1.1.117.6808. URL <http://citeseerx.ist.psu.edu/viewdoc/download?doi=10.1.1.79.6578&rep=rep1&type=pdf>.
- W. L. Winston and J. B. Goldberg. *Operations Research: Applications and Algorithms*. Hinrichs, Curt, 4 edition, 2004. ISBN 978-0-534-42358-2.
- S. D. Withers. Data Analysis, Categorical. In *International Encyclopedia of Human Geography*, pages 159–165. Elsevier, 1 2009. doi: 10.1016/b978-0-08-102295-5.10364-6.

## BIBLIOGRAPHY

---

- N. Wu and S. Giuliani. Capacity and Delay Estimation at Signalized Intersections under Unsaturated Flow Condition Based on Cycle Overflow Probability. In *Transportation Research Procedia*, volume 15, pages 63–74. Elsevier B.V., 1 2016. doi: 10.1016/j.trpro.2016.06.006.
- X. Wu and H. X. Liu. A shockwave profile model for traffic flow on congested urban arterials. *Transportation Research Part B: Methodological*, 45(10):1768–1786, 2011. ISSN 01912615. doi: 10.1016/j.trb.2011.07.013. URL <http://dx.doi.org/10.1016/j.trb.2011.07.013>.
- X. Wu, H. X. Liu, and D. Gettman. Identification of oversaturated intersections using high-resolution traffic signal data. *Transportation Research Part C: Emerging Technologies*, 18(4):626–638, 2010. ISSN 0968090X. doi: 10.1016/j.trc.2010.01.003. URL <http://dx.doi.org/10.1016/j.trc.2010.01.003>.
- H. Xu, J. Chen, and J. Xu. Integration of Model-Based Signal Control and Queue Spillover Control for Urban Oversaturated Signalized Intersection. *Mathematical Problems in Engineering*, 2019, 2019. ISSN 15635147. doi: 10.1155/2019/3149275.
- K. . Yang, M. Menendez, and K. Yang. Queue estimation in a connected vehicle environment A convex approach Queue Estimation in a Connected Vehicle Environment: A Convex Approach. 2018. doi: 10.3929/ethz-b-000279557. URL <https://doi.org/10.3929/ethz-b-000279557>.
- J. Yeon, L. Elefteriadou, and S. Lawphongpanich. Travel time estimation on a freeway using Discrete Time Markov Chains. *Transportation Research Part B: Methodological*, 42(4):325–338, 2008. ISSN 01912615. doi: 10.1016/j.trb.2007.08.005.
- B. Yulianto. Detector technology for demand responsive traffic signal control under mixed traffic conditions. In *AIP Conference Proceedings 1977*, volume 2112, page 40139, 2018. ISBN 9780735416871. doi: 10.1063/1.5042991. URL <https://doi.org/10.1063/1.5043014><https://doi.org/10.1063/1.5033803>.



# **Appendices**



# The Lighthill-Whitham-Richard Model

The wave-like behaviour of traffic is described mathematically by the Lighthill-Whitham-Richard (LWR) Model [Lighthill and Whitham, 1955]. They proposed a first-order model that inserts the formulation of the fundamental diagram  $Q_e(k)$  in the continuity equation, resulting in the following equation [Immers and Logge, 2002]:

$$\frac{\delta k(x, t)}{\delta t} + \frac{Q_e(k(x, t))}{\delta k} \cdot \frac{\delta k(x, t)}{\delta x} = 0 \quad (1)$$

The solution to this partial differential equation is given by

$$k(x, t) = F(x - ct, t) \text{ where } c = \frac{dQ_e}{dk} \text{ and } F \text{ an arbitrary function} \quad (2)$$

In other words, small disturbances of an initial density  $k_0$  in the traffic state are propagating through the traffic with speed  $c$  [Hoogendoorn, 2010]. Assuming a triangular fundamental diagram, these waves, typically referred to as kinematic waves, propagate downstream with speed  $u_f$  when  $k_0$  coincides with a state on the free-flow branch and propagate upstream with speed  $w$  when  $k_0$  coincides with a state on the congested branch [Hoogendoorn, 2010].

In urban traffic, these small discontinuities are rare as the state is often dominated by sudden changes in the traffic state due to a changing traffic signal, for example [Rempe, 2019]. Instead of kinematic waves, these changes cause shockwaves, which represent the boundary between two areas with different traffic conditions. Considering the conservation of vehicles at the shockwave's location, the wave speed  $\omega$  can be determined by

$$\omega_{12} = \frac{q_1 - q_2}{k_1 - k_2} \quad (3)$$

where  $q_1$  and  $k_1$  are the flow and density of the upstream state and  $q_2$  and  $k_2$  the flow and density of the downstream state [Hoogendoorn, 2010]. The shockwave speeds can also be read from the fundamental diagram as the slope of the line between the upstream and downstream states in the flow-density diagram.

# Proof of Concept

In chapter 4, the Markov model is introduced as a stochastic method to predict the traffic states on signalised intersections. In order to illustrate this approach, a simplified discrete-time finite-state Markov chain is built. Contrary to the proposed Hidden Markov Model, the proof of concept uses stationary transition probabilities based on the counted occurrences of the states in the training dataset. This model is supplemented by a neural network that takes the measured trajectories into account.

## Methodology

When only a stationary Markov chain is used, the state distributions converge to stationary probabilities after  $n$  time steps. Moreover, the model does not update when new information arrives. Therefore, the state distribution is adapted by a neural network when a new trajectory passes the intersection. If no probe vehicles pass the intersection, the state distribution is equal to the outcome of the Markov chain. The structure of the model is visualised in Figure 1.

The neural network consists of an input layer with four nodes, namely the predicted distribution of the Markov Chain and the trajectory observations on the travel time, the number of stops, and the average duration of these stops. Next, the best results were obtained with two hidden layers and an output layer activated by sigmoid-activation function. The network results in a new state distribution that replaces the previous distribution of the Markov Chain.

## Case study

To illustrate the working principle of this model, it was implemented for severely simplified case study where two successive intersections with single-lane approaches are simulated. The aim of the model is to classify the cycles in an under- or oversaturated state. The demand on the network is calibrated such that a medium demand is present, resulting in a balanced set of cycles, where both undersaturated and

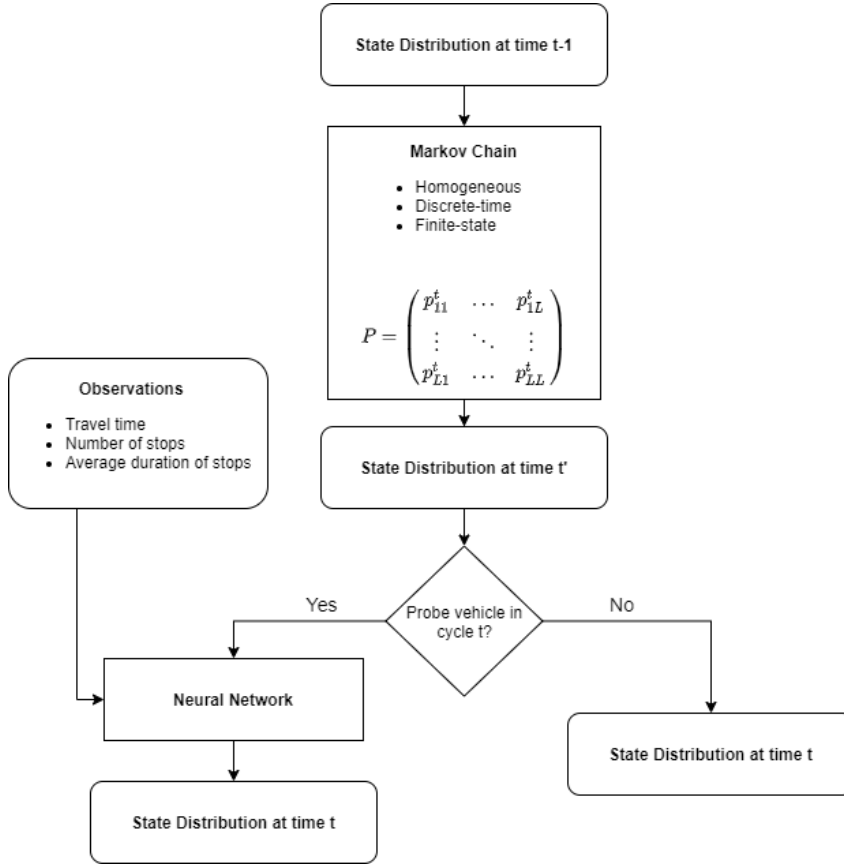


Figure 1: Framework of the Proof of Concept.

oversaturated states occur equally often.

The obtained results are presented in the confusion matrix in Table 1, which leads to the conclusion that 82% of the cycles are correctly classified when the penetration rate is 10%. Moreover, the wrongly classified cycles predict a state distribution with more or less equal state probabilities but where the wrong value was eventually chosen.

Predicted State	Real State	
	Undersaturated	Oversaturated
Undersaturated	234	42
Oversaturated	52	272
Accuracy [%]	81.82	86.62

Table 1: Confusion matrix resulting from the proof of concept.

## PROOF OF CONCEPT

---

The main problem with this technique is that the Markov chain estimates the transition probabilities based on the occurrences in the training set, aggregated over all demand levels. This means that the Markov model makes a very coarse prediction that always needs to be corrected by the neural network. The neural network pulls the model's predictions back in the right direction, but in the next time steps it keeps transitioning back in the wrong direction when no new probe vehicles are present. This is not expected to yield satisfying results when more complex situations are implemented.

# The Coefficients of the Logistic Regression Models

## The Logistic Regression Model from State $U$

Variable	Coefficient	Odd Ratio
Logistic Function from U to U: Reference Category	0	1.000
Logistic Function from U to $O_1$		
Intercept	-1.226	0.293
Travel Time	11.945	>1,000.000
Min Stop Duration	-8.634	<0.001
Max Stop Duration	22.021	>1000.000
Time on Intersection	-9.263	<0.001
Shockwave	-2.433	0.088
Downstream State	-1.554	0.211
Logistic Function from U to $O_2$		
Intercept	-6.301	0.002
Travel Time	12.303	>1,000.000
Min Stop Duration	-9.556	<0.001
Max Stop Duration	21.535	>1,000.000
Time on Intersection	-4.173	0.015
Shockwave	2.764	15.863
Downstream State	2.733	15.383
Logistic Function from U to $O_3$		
Intercept	-8.328	0.000
Travel Time	16.116	>1,000.000
Min Stop Duration	-9.159	<0.001
Max Stop Duration	20.119	>1,000.000
Time on Intersection	-1.704	0.182
Shockwave	7.712	>1,000.000
Downstream State	2.515	12.367
Logistic Function from U to $Sp$		
Intercept	-9.070	<0.001
Travel Time	16.146	>1,000.000
Min Stop Duration	-8.318	<0.001
Max Stop Duration	28.499	>1,000.000
Time on Intersection	-3.826	0.022
Shockwave	4.762	116.980
Downstream State	10.270	>1,000.000

Table 2: Resulting coefficients and odd-ratios of the logistic regression model from state  $U$  to all other states.

## The Logistic Regression Model from State $O_1$

Variable	Coefficient	Odd Ratio
Logistic Function from $O_1$ to U:		
Intercept	0.676	1.966
Travel Time	-10.863	<0.001
Min Stop Duration	5.953	384.906
Max Stop Duration	-19.847	<0.001
Time on Intersection	6.320	555.573
Shockwave	3.030	20.697
Downstream State	-4.534	0.011
Logistic Function from $O_1$ to $O_1$ : Reference Category	0	1.000
Logistic Function from $O_1$ to $O_2$		
Intercept	-5.018	0.007
Travel Time	37.917	>1,000.000
Min Stop Duration	-1.300	0.273
Max Stop Duration	5.814	334.956
Time on Intersection	-0.694	0.500
Shockwave	12.863	>1,000.000
Downstream State	-0.129	0.879
Logistic Function from $O_1$ to $O_3$		
Intercept	-6.310	0.002
Travel Time	14.924	>1,000.000
Min Stop Duration	-0.145	0.865
Max Stop Duration	-0.343	0.710
Time on Intersection	1.782	5.942
Shockwave	11.003	>1,000.000
Downstream State	-1.464	0.231
Logistic Function from $O_1$ to $Sp$		
-> DOES NOT OCCUR IN THE TRAINING DATA		

Table 3: Resulting coefficients and odd-ratios of the logistic regression model from state  $O_1$  to all other states.

## The Logistic Regression Model from State $O_2$

Variable	Coefficient	Odd Ratio
Logistic Function from $O_2$ to U:		
Intercept	-1.347	0.260
Travel Time	-5.579	0.004
Min Stop Duration	2.501	12.195
Max Stop Duration	-13.329	<0.001
Time on Intersection	0.744	2.104
Shockwave	-4.295	0.014
Downstream State	-1.193	0.303
Logistic Function from $O_2$ to $O_1$		
Intercept	2.149	8.576
Travel Time	-21.149	<0.001
Min Stop Duration	1.533	4.632
Max Stop Duration	-3.438	0.032
Time on Intersection	0.427	1.533
Shockwave	-14.899	<0.001
Downstream State	-2.621	13.749
Logistic Function from $O_2$ to $O_2$ : Reference Category	0	1.000
Logistic Function from $O_2$ to $O_3$		
Intercept	-4.431	0.012
Travel Time	26.745	>1,000.000
Min Stop Duration	-0.244	0.783
Max Stop Duration	-1.938	0.144
Time on Intersection	1.000	2.718
Shockwave	14.924	>1,000.000
Downstream State	2.100	8.166
Logistic Function from $O_2$ to $Sp$		
Intercept	-5.352	0.005
Travel Time	0.216	1.241
Min Stop Duration	1.461	4.310
Max Stop Duration	-4.365	0.013
Time on Intersection	1.199	3.317
Shockwave	-1.127	0.324
Downstream State	1.793	6.007

Table 4: Resulting coefficients and odd-ratios of the logistic regression model from state  $O_2$  to all other states.

## The Logistic Regression Model from State $O_3$

Variable	Coefficient	Odd Ratio
<hr/>		
Logistic Function from $O_3$ to U		
Intercept	-3.339	0.035
Travel Time	-16.551	<0.001
Min Stop Duration	3.664	39.017
Max Stop Duration	-4.822	0.008
Time on Intersection	2.863	17.514
Shockwave	-8.232	<0.001
Downstream State	0.067	1.069
<hr/>		
Logistic Function from $O_3$ to $O_1$		
Intercept	0.208	1.231
Travel Time	-23.273	<0.001
Min Stop Duration	2.652	14.182
Max Stop Duration	-2.107	0.122
Time on Intersection	2.116	8.298
Shockwave	-14.762	<0.001
Downstream State	-3.610	0.027
<hr/>		
Logistic Function from $O_3$ to $O_2$		
Intercept	1.464	4.323
Travel Time	-28.289	<0.001
Min Stop Duration	0.642	1.900
Max Stop Duration	5.659	286.862
Time on Intersection	0.310	1.363
Shockwave	-9.439	<0.001
Downstream State	-5.712	0.003
Logistic Function from $O_3$ to $O_3$ : Reference Category	0	1.000
<hr/>		
Logistic Function from $O_3$ to $Sp$		
Intercept	-6.164	0.002
Travel Time	0.831	2.296
Min Stop Duration	-0.468	0.626
Max Stop Duration	0.444	1.559
Time on Intersection	10.506	>1,000.000
Shockwave	0.578	1.782
Downstream State	12.724	>1,000.000

Table 5: Resulting coefficients and odd-ratios of the logistic regression model from state  $O_3$  to all other states.

## The Logistic Regression Model from State $Sp$

Variable	Coefficient	Odd Ratio
<hr/>		
Logistic Function from $Sp$ to U		
Intercept	-3.076	0.046
Travel Time	-3.038	0.048
Min Stop Duration	1.383	3.987
Max Stop Duration	-2.423	0.089
Time on Intersection	-3.299	0.037
Shockwave	-3.639	0.26
Downstream State	-3.849	0.021
<hr/>		
Logistic Function from $Sp$ to $O_1$		
Intercept	-2.364	0.096
Travel Time	-3.206	0.041
Min Stop Duration	1.984	7.272
Max Stop Duration	-1.928	0.145
Time on Intersection	-3.067	0.047
Shockwave	-4.057	0.017
Downstream State	-5.236	0.005
<hr/>		
Logistic Function from $Sp$ to $O_2$		
Intercept	-3.319	0.036
Travel Time	-2.760	0.063
Min Stop Duration	1.549	4.707
Max Stop Duration	-1.680	0.186
Time on Intersection	-3.293	0.037
Shockwave	-3.669	0.026
Downstream State	-3.906	0.020
<hr/>		
Logistic Function from $Sp$ to $O_3$		
Intercept	0.603	1.828
Travel Time	-0.187	0.829
Min Stop Duration	-0.946	0.388
Max Stop Duration	-0.283	0.754
Time on Intersection	-5.707	0.003
Shockwave	-1.303	0.272
Downstream State	-3.429	0.032
<hr/>		
Logistic Function from $Sp$ to $Sp$ : Reference Category	0	1.000

Table 6: Resulting coefficients and odd-ratios of the logistic regression model from state  $Sp$  to all other states.